



Surface modification of E-glass fibers with radio frequency plasma polymerization and its effect on fatigue resistance of composites  
by Dongrui Fang

A thesis submitted in partial fulfillment of the requirements for the degree of Master of Science in  
Chemical Engineering  
Montana State University  
© Copyright by Dongrui Fang (1996)

**Abstract:**

Today the steady increase in the consumption of reinforced composite materials indicates their value as competitive engineering materials, and they are successfully replacing more conventional materials in many applications. In the wind energy industry, glass fiber reinforced composite materials have been used to make wind turbine blades which require long service life under severe loading and unloading environments. Thus, the fatigue resistance of wind turbine blades is an important design consideration. In this study, a plasma reactor system was developed and plasma polymerization was used to modify the surface of E-glass fibers in an attempt to improve the fatigue resistance of composites.

An inductively coupled radio frequency glow discharge reactor was designed and constructed “in house” for the experiments. E-glass fiber strands and fabric cloth were used as the substrates. Ethylene and methane gases were used as the monomers. The effects of different reaction parameters, such as the discharge power, the reaction time, the gas flow rate and system pressures, were explored. The characteristics of plasma polymerized films were analyzed using x-ray photoelectron spectroscopy (XPS) and scanning electron microscopy (SEM). The mechanical properties of treated fiber strands and fabric cloth were tested by Jinhua Bian at Montana State University.

Plasma treatment of glass fibers is an effective method for modifying the fiber surface properties and allows for the most flexibility. The ethylene or methane plasma polymerized films on the glass fibers could not be washed off with acetone, and no degradation was observed after keeping the treated fibers in- the air for one week. For ethylene or methane plasma treated fiber strands and fabric, a better coating was obtained at higher discharge power and longer reaction time. However, the plasma deposition and plasma etching would reach an equilibrium state and no further plasma deposition could be observed after the equilibrium discharge power and reaction time level.

SURFACE MODIFICATION OF E-GLASS FIBERS WITH RADIO FREQUENCY  
PLASMA POLYMERIZATION AND ITS EFFECT ON FATIGUE  
RESISTANCE OF COMPOSITES

by  
Dongrui Fang

A thesis submitted in partial fulfillment  
of the requirements for the degree

of  
Master of Science  
in  
Chemical Engineering

MONTANA STATE UNIVERSITY-BOZEMAN  
Bozeman, Montana

April 1996

N378  
F214

APPROVAL

of a thesis submitted by

Dongrui Fang

This thesis has been read by each member of the thesis committee and has been found to be satisfactory regarding content, English usage, format, citations, bibliographic style, and consistency, and is ready for submission to the College of Graduate Studies.

4/17/96  
Date

*Kenneth L. Johnson*  
Chairperson, Graduate Committee

Approved for the Major Department

4-17-96  
Date

*John T. Sears*  
Head, Major Department

Approved for the College of Graduate Studies

5/5/96  
Date

*R. L. Brown*  
Graduate Dean

## STATEMENT OF PERMISSION TO USE

In presenting this thesis in partial fulfillment of the requirements for a master's degree at Montana State University-Bozeman, I agree that the Library shall make it available to borrowers under rules of the Library.

If I have indicated my intention to copyright this thesis by including a copyright notice page, copying is allowable only for scholarly purposes, consistent with "fair use" as prescribed in the U.S. Copyright Law. Requests for permission for extended quotation from or reproduction of this thesis in whole or in parts may be granted only by the copyright holder.

Signature *Langston*

Date 04/17/96

## ACKNOWLEDGMENTS

I wish to express my deepest gratitude to Dr. Bonnie Tyler for her supervision, advice and support through the course of this research. I would also like to thank Dr. John T. Sears and Dr. John Mandell for their kind guidance and serving on my committee.

Thanks are extended to James Anderson and Nancy Equall of the Imaging and Chemical Analysis Laboratory at Montana State University for their assistance with XPS and SEM work, and Dr. Recep Avci for his help during this study.

I would also like to thank Jinhua Bian for doing all the mechanical tests, and the staff of the Chemical Engineering Department at MSU for their help and friendship. Lyman Fellows deserves special appreciation for his repeated willingness to help me in the maintenance of the equipment.

Finally, I would like to take this opportunity to thank Erika Johnston at the University of Washington for her valuable suggestions and help in the tuning-up of the system. I would also like to thank Sandia National Laboratories, National Renewable Energy Laboratory and Department of Energy (EPSCoR Program) for their technical and financial support of this study.

## TABLE OF CONTENTS

	Page
LIST OF TABLES.....	vii
LIST OF FIGURES.....	viii
ABSTRACT.....	xi
1. INTRODUCTION.....	1
Motivation and Objectives.....	3
2. LITERATURE SURVEY.....	6
Glass Fibers.....	6
Silane Coupling Agents.....	7
Plasma Polymerization.....	10
What Is a Plasma.....	11
Plasma Process Parameters.....	14
Frequency Of Exciting Potential.....	16
Excitation Power.....	17
Monomer Flow Rate.....	18
System Pressure.....	19
Geometrical Factors Of Reactor.....	20
Temperature Of Deposition Site.....	22
Polymer Deposition Rate.....	22
Flow Rate.....	24
Discharge Power.....	25
W/FM Parameter.....	25
Plasma Etching.....	26
Plasma Etching and Its Advantages.....	28
Oxygen Plasma Etching.....	30
Plasma Etching and Plasma Polymerization.....	33
Glow Discharge Reactors.....	34
RF Reactors and Matching Networks.....	36
Thin Film Analysis Techniques.....	38
X-Ray Photoelectron Spectroscopy.....	38
Principles of the Technique.....	39
Instrumentation.....	42
Scanning Electron Microscopy.....	46
Principles of the Technique.....	48
Instrumentation.....	51

TABLE OF CONTENTS—Continued

	Page
3. EXPERIMENTAL, MATERIALS AND METHODS.....	54
Reaction System.....	54
Gas Lines and Controllers.....	54
Plasma Reactor.....	56
RF Generator and Matching Network.....	56
Pressure Controllers.....	57
Traps and Pumps.....	57
Materials.....	58
Experimental Procedure.....	59
Sample Preparation.....	59
Plasma Polymerization.....	60
Analytical Methods.....	61
X-Ray Photoelectron Spectroscopy.....	61
Scanning Electron Microscopy.....	62
4. RESULTS AND DISCUSSION.....	63
Analytical Results.....	63
Solution Cleaning of Fiber Strands.....	64
XPS Analysis.....	64
SEM Analysis.....	68
Oxygen Etch of Fiber Strands.....	69
XPS Analysis.....	70
SEM Analysis.....	72
Fiber Strands Coated by Ethylene Monomer.....	77
XPS Analysis.....	78
SEM Analysis.....	82
Fiber Strands Coated by Methane Monomer.....	88
XPS Analysis.....	88
SEM Analysis.....	90
Oxygen Etch of Fabric Cloth.....	94
XPS Analysis.....	94
SEM Analysis.....	96
Fabric Cloth Coated by Ethylene Monomer.....	101
XPS Analysis.....	101
SEM Analysis.....	104
Mechanical Test Results.....	108
5. CONCLUSIONS AND RECOMMENDATIONS.....	111
Conclusions.....	111
Recommendations.....	114
REFERENCES CITED.....	116

## LIST OF TABLES

Table	Page
1. Compositions of E-glass Fibers.....	7
2. Dow Corning Silane Coupling Agents.....	9
3. Elemental Surface Concentration (%) Obtained by XPS Analysis of Uncleaned and Base/Acid Cleaned Strands.....	65
4. Elemental Surface Concentration (%) Obtained by XPS Analysis of Oxygen Plasma Etched Fiber Strands.....	71
5. Elemental Surface Concentration (%) Obtained by XPS Analysis of Ethylene Plasma Coated Fiber Strands.....	79
6. The XPS Analysis Results to Examine the Degradation and Stability of Ethylene Plasma Treated Strands.....	81
7. The XPS Analysis Results to Examine the Uniformity of Ethylene Plasma Coatings on Fiber Strands.....	81
8. Elemental Surface Concentration (%) Obtained by XPS Analysis of Methane Plasma Coated Fiber Strands.....	89
9. Elemental Surface Concentration (%) Obtained by XPS Analysis of As-Received and Oxygen Plasma Etched Fabric Cloth.....	95
10. Elemental Surface Concentration (%) Obtained by XPS Analysis of Ethylene Plasma Coated Fabric.....	103
11. The Static Strength and Fatigue Cycle Numbers Obtained by Mechanical Tests of As-Received and Plasma Treated Fiber Strands.....	109

## LIST OF FIGURES

Figure	Page
1. Illustration of plasma.....	12
2. Schematic representation of the dependence of polymer deposition rate on flow rate of a starting material when a constant discharge power is used.....	24
3. Schematic representation of the dependence of polymer deposition rate on discharge power when a constant flow rate is employed.....	25
4. The principle and implementation of plasma ashing.....	27
5. System components used in a glow discharge reactor.....	35
6. The physical basis of XPS.....	40
7. Schematic diagram of an XPS instrument.....	43
8. Signals from specimen in an SEM instrument.....	49
9. Schematic drawing of an SEM instrument.....	51
10. Schematic diagram of the reaction system.....	55
11. XPS survey spectra of uncleaned fiber strands.....	66
12. XPS survey spectra of fiber strands cleaned by base/acid solutions for 9 hrs, respectively.....	67
13. SEM micrographs of glass fibers as received (top), and as cleaned by base/acid solutions for 9 hrs, respectively (bottom).....	68
14. XPS survey spectra of oxygen plasma etched fiber strands at 5 sccm, 0.24 torr and 80 w for 30 min.....	73

LIST OF FIGURES—Continued

Figure	Page
15. XPS C1s binding energy curve for oxygen plasma etched fiber strands.....	74
16. XPS O1s binding energy curve for oxygen plasma etched fiber strands.....	75
17. SEM micrographs of the different spots of oxygen plasma etched fiber strands at 5 sccm, 0.24 torr and 80 w for 30 min.....	76
18. Structure deduced on the basis of crosslink density calculations and functional group concentrations for an ethylene plasma polymer.....	78
19. XPS survey spectra of fiber strands coated by ethylene monomer at 5 sccm, 0.18 torr and 60 w for 15 min.....	83
20. XPS C1s binding energy curve for fiber strands coated by ethylene monomer.....	84
21. SEM micrographs of fiber strands cleaned by base/acid solutions and coated by ethylene monomer at 20 w (top) and 60 w (bottom).....	85
22. High magnification SEM micrographs of the different spots of fiber strands cleaned by base/acid solutions and coated by ethylene monomer at 40 w.....	86
23. SEM micrographs of fiber strands etched by oxygen plasma and coated by ethylene monomer at 20 w (top) and 60 w (bottom).....	87
24. XPS survey spectra of fiber strands coated by methane monomer at 5 sccm, 0.22 torr and 100 w for 20 min.....	91
25. XPS C1s binding energy curve for fiber strands coated by methane monomer.....	92
26. SEM micrographs of fiber strands etched by oxygen plasma and coated by methane monomer for 15 min. (top) and 30 min. (bottom).....	93

LIST OF FIGURES—Continued

Figure	Page
27. XPS survey spectra of oxygen plasma etched fabric cloth at 10 sccm, 0.36 torr and 120 w for 60 min.....	97
28. XPS C1s binding energy curve for oxygen plasma etched fabric cloth.....	98
29. XPS O1s binding energy curve for oxygen plasma etched fabric cloth.....	99
30. SEM micrographs of fabric cloth as received (top), and as etched by oxygen plasma at 10 sccm, 0.36 torr and 120 w for 60 min. (bottom).....	100
31. Pictures of as-received (top) and ethylene plasma treated fabric cloth (bottom).....	102
32. XPS survey spectra of fabric cloth coated by ethylene monomer at 10 sccm, 0.27 torr and 120 w for 30 min.....	105
33. XPS C1s binding energy curve for ethylene plasma coated fabric cloth.....	106
34. SEM micrographs of the different spots of fabric cloth coated by ethylene monomer at 10 sccm, 0.27 torr and 120 w for 30 min.....	107

## ABSTRACT

Today the steady increase in the consumption of reinforced composite materials indicates their value as competitive engineering materials, and they are successfully replacing more conventional materials in many applications. In the wind energy industry, glass fiber reinforced composite materials have been used to make wind turbine blades which require long service life under severe loading and unloading environments. Thus, the fatigue resistance of wind turbine blades is an important design consideration. In this study, a plasma reactor system was developed and plasma polymerization was used to modify the surface of E-glass fibers in an attempt to improve the fatigue resistance of composites.

An inductively coupled radio frequency glow discharge reactor was designed and constructed "in house" for the experiments. E-glass fiber strands and fabric cloth were used as the substrates. Ethylene and methane gases were used as the monomers. The effects of different reaction parameters, such as the discharge power, the reaction time, the gas flow rate and system pressures, were explored. The characteristics of plasma polymerized films were analyzed using x-ray photoelectron spectroscopy (XPS) and scanning electron microscopy (SEM). The mechanical properties of treated fiber strands and fabric cloth were tested by Jinhua Bian at Montana State University.

Plasma treatment of glass fibers is an effective method for modifying the fiber surface properties and allows for the most flexibility. The ethylene or methane plasma polymerized films on the glass fibers could not be washed off with acetone, and no degradation was observed after keeping the treated fibers in the air for one week. For ethylene or methane plasma treated fiber strands and fabric, a better coating was obtained at higher discharge power and longer reaction time. However, the plasma deposition and plasma etching would reach an equilibrium state and no further plasma deposition could be observed after the equilibrium discharge power and reaction time level.

## CHAPTER 1

## INTRODUCTION

When an organic vapor is injected into a glow discharge of an inert gas or when a glow discharge of a pure organic vapor is created, the deposition of polymeric films onto an exposed surface is often observed. Polymer formation that occurs in such a process is generally referred to as plasma polymerization or glow discharge polymerization [1].

Although the recognition of thin film formation by plasma polymerization can be traced back to 1874, and of chemical reactions in electrical discharges to 1868, systematic investigation of plasma polymerization began only in the 1960s [2]. Once some of the advantageous features of plasma coating were recognized, much applied research on the use of the process was done.

Applications of plasma polymer films may conveniently be divided into two classes [3]. Firstly, alteration of the surface properties of a substrate may be the goal. An example of such applications includes modification of a polymer surface for the purpose of increasing (or decreasing) adhesion at the interface. Secondly, the

application may capitalize on the bulk properties of a thin, flawless, and /or highly adherent film. An example would be the use of the transport properties of such films as in membranes for gas separation or water purification.

Since the reactant gases are more reactive in the plasma state than the neutral state, plasma deposition can be carried out at much lower temperatures than those of chemical vapor deposition process. Plasma polymer films also have one or more of the following characteristics:

—Thin films can be easily formed with thicknesses of 500 Å to 1  $\mu\text{m}$ .

—Flawless, uniform and highly crosslinked smooth films can be easily made by this process.

—Such films are often highly coherent and adherent to a variety of substrates including polymer, glass, and metal surfaces.

—Multilayer films or films with a gradation of chemical or physical characteristics are easily made by this process.

However, plasma polymerization process also has some disadvantages, such as, films are not always stoichiometric because of the complexity of the reaction and are often contaminated with by-products and incidental species. Films can be often deposited on the internal electrodes and the

walls of the reactor. The process can also create internal tensile and compressive stresses in the films.

### Motivation and Objectives

Fiber reinforced composite materials are now an important class of engineering materials. They offer outstanding mechanical properties, unique flexibility in design capabilities, and ease of fabrication. Additional advantages include light weight, corrosion resistance, impact resistance, and excellent fatigue strength. In the wind energy industry, glass fiber reinforced composite materials have been used to make wind turbine blades utilizing their high strength to weight ratio and less expensive properties. The fatigue resistance of wind turbine blades is an important design consideration since these blades can experience as many as  $10^8$  to  $10^9$  significant fatigue loading cycles in their ten to thirty year lifetime [4]. In this research, a plasma reactor system was developed and plasma polymerization was used to modify the surface of E-glass fibers in an attempt to improve the fatigue resistance of composites.

Surface modification by plasma treatment has been employed to increase the adhesion and compatibility of dissimilar phases used in composites, but treatment to the surface of E-glass fibers to improve the fatigue resistance

has not been done previously and is studied in this research for the first time. Some published applications of plasma treatment include modification of the surface of polyamide fibers and weaves to increase adhesion to the epoxy matrix in a composite [5,6]. The adhesion of epoxy resins to films of polyethylene, poly(tetrafluoroethylene), and poly(vinyl chloride) has been improved by coating with acetylene plasma polymer [7]. It was found that plasma polymerization at low flow rates yielded the best results and that the plasma polymer coating led to both increased surface polarity and increased roughness.

Extensive research has been directed towards developing filament surface treatments to improve composite interfacial properties. The primary goal of those efforts has been to improve filament wettability, with chemical bond formation as a secondary objective. Filament wetting by the matrix resin is the essential first step in forming an interfacial bond. Good wetting is also required to attain the molecular level contact necessary to form chemical bonds. This approach was illustrated by the development of coupling agents for glass filaments [8] and oxidative surface treatments for graphite filaments [9,10,11]. Another method was used to improve the dry shear properties of the graphite epoxy composites by oxygen etching and polymerization with methylmethacrylate monomer [12].

The main purpose of this study is to develop a plasma treating system and use it to modify the surface of E-glass fiber strands and fabric cloth with plasma polymerization in an attempt to improve the fatigue resistance of composites. The different effects of plasma polymerization parameters (discharge power, reaction time, gas flow rate and system pressure) on the surface properties of coated fibers are studied. X-ray photoelectron spectroscopy and scanning electron microscopy are used to analyze the characteristics of thin films. The mechanical properties of treated glass fibers are tested by Jinhua Bian who is a graduate student at Montana State University.

## CHAPTER 2

## LITERATURE SURVEY

Glass Fibers

A great majority of materials are stronger and/or sometimes stiffer in the fibrous form than as a bulk material. A high fiber aspect ratio (length : diameter ratio) permits very effective transfer of load via matrix materials to the fibers, thus taking advantage of their excellent properties. Therefore, fibers are very effective and attractive reinforcement materials.

The most important reinforcement fiber is E-glass because of its relative low cost. However, boron, graphite, and the aramid polymer fibers are most exceptional because of their high stiffness value. The need for high-temperature reinforcing fibers has led to the development of ceramic fibers.

The first glass developed specifically for production of continuous fibers was a lime-alumina-borosilicate glass designed primarily for electrical applications [13]. Designated E glass, this glass was found adaptable and

highly effective in a great variety of processes and products ranging from decorative to structural applications and it has become known as the standard textile glass. By far the major portion of all continuous filament glass produced today is E glass.

E-glass fiber does not have a single composition but may vary in composition within the range given in Table 1 [13]. Changes within the indicated ranges do not significantly influence its electrical or mechanical properties.

Table 1. Compositions of E-glass Fibers

Material	Range (% by weight)
Silicon Oxide	52-56
Aluminum Oxide	12-16
Calcium Oxide	16-25
Magnesium Oxide	0-6
Boron Oxide	8-13
Sodium Oxide	0-3
Ferrous Oxide	0.05-0.4
Titanium Oxide	0-0.4
Miscellaneous	0-0.5

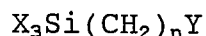
### Silane Coupling Agents

The chemical treatments applied during the forming of glass fibers are called sizes [14]. These are of two general types: temporary sizes and compatible sizes (also called coupling agents).

The temporary sizes are applied to minimize the degradation of strength resulting from abrasion of fibers to one another and to bind the fibers together for easy handling in forming woven glass fiber products. These sizes must be removed and replaced by coupling agents before the fibers can be impregnated with resin.

The most common coupling agents are organofunctional silanes. The function of silane coupling agents is to provide a stable bond between two otherwise nonbonding surfaces and to reduce the destructive effects of water and other environmental forces on this bond. In reinforced and filled plastics, the improved bond between the fibrous or particulate inorganic component and the organic matrix polymer results in greater composite strength and longer service life.

Silane coupling agents are a family of organosilicon monomers which are characterized by the formula [14]:



where  $n = 0-3$

Y = organofunctional group that is compatible with polymer matrix

X = hydrolyzable group on silicon converted to silanol group on hydrolysis.

The group Y may be very simple, for example chlorine, or may contain several chemical functional groups. The silanol functional group establishes hydrogen bonds with the glass



### Plasma Polymerization

Glow discharge polymerization or plasma polymerization, like so many topics in science, is incompletely understood. It has its own sub-language of special terms, with names that are often misleading, and with meanings which can not be assumed to be constant from book to book. In some papers, plasma polymerization is used to describe a special kind of polymer formation mechanism in glow discharge, and glow discharge polymerization is used to refer to plasma polymerization in the wider meaning. In this study, no emphasis is put on the mechanism of glow discharge polymerization, so these two terms are used synonymously just like most applied scientists do, which plasma physicists may get into semantic discussions and arguments.

Another misleading terminology is "polymerization". Although the phenomenon of polymer formation in a glow discharge is referred to as glow discharge polymerization, the term of "polymerization" may not represent the actual process of forming a polymer. The conventional meaning of polymerization is that the molecular units (monomers) are linked together by the polymerization process. Therefore, the resultant polymer is conventionally named by "poly + (the monomer)". For instance, the polymer formed by the polymerization of ethylene is named polyethylene. In this

meaning, polymerization refers to molecular polymerization, i.e., the process of linking molecules of a monomer. In a strict sense, polymerization in the conventional context does not represent the process of polymer formation that occurs in a glow discharge which may be characterized as elemental or atomic polymerization, although molecular polymerization may play a role, depending on the chemical structure of a monomer and also on the conditions of the glow discharge [16].

In plasma deposition, reactive intermediates are formed in the gas phase which can result in the formation of non-volatile species that deposit on surfaces exposed to the plasma. Plasma deposition is a general term used to describe deposition of thin films from plasma sources; when dealing with organic species a term commonly used is plasma polymerization. Plasma polymerization can be carried out with a wide range of reactants including some which are not generally considered to be monomers, such as methane. This is possible due to the conversion of the initial reactant to polymer-forming intermediates in the discharge.

#### What Is a Plasma

A plasma is a partially ionized gas consisting of equal numbers of positive and negative particles, a variety of neutral species including atoms, molecules, free radicals,

and photons [17]. We can consider a simple plasma consisting of positive ions and negative electrons in a sea of neutral atoms as shown in Figure 1 [18]. Ion-electron pairs are continuously created by ionization and destroyed by recombination, and since these processes are always pairwise, the space occupied remains charge neutral. The electron impact process which leads to ionization is also likely to cause excitation and the subsequent relaxation of the atom leading to photon emission, which is another common feature of the plasma. For instance, an oxygen plasma appears a light blue to the eye.

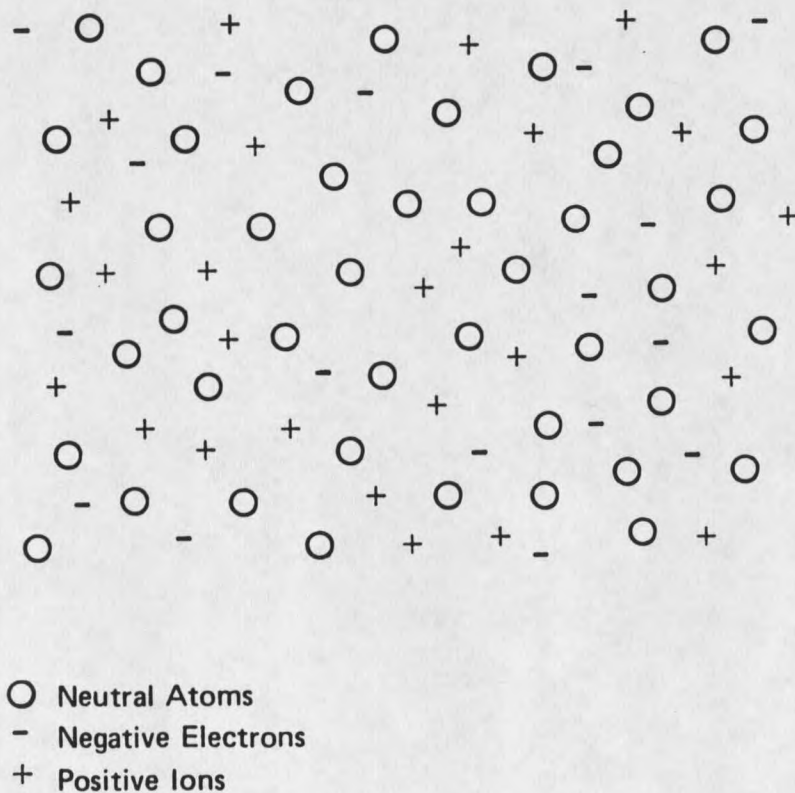


Figure 1. Illustration of plasma

The plasma is formed by exposing the gaseous monomer at low pressure to an electric field. Energy is transferred by the electric field to free electrons which collide with molecules, electrodes and other surfaces. Inelastic electron collisions with molecules generate more electrons as well as ions, free radicals, and molecules in excited states. Although the degree of ionization is low, typically about  $10^{-5}$  -  $10^{-7}$ , charged particles can play an important role in determining both the deposition rate and the chemical structure of the plasma polymer film. All fragments are very reactive with surfaces exposed to the plasma and with other fragments. Ion and neutral molecule temperatures remain near that of the reactor vessel ( $<500^{\circ}\text{K}$ ), hence the designation of low-temperature plasma or cold plasma. Electrons, because of their high mobility, are rapidly accelerated by the applied field and have temperatures one to two orders of magnitude higher than the plasma gas molecules. The electron temperatures are usually over  $20,000^{\circ}\text{K}$  [19].

The complexity of the chemistry which can take place in the glow discharge volume is increased when one considers the processes which may proceed at a surface above which a discharge is initiated and maintained. As such, plasma polymerization involves reactions between plasma species, between plasma and surface species and between surface species. Plasma-surface interactions are at least as important as interactions amongst plasma species in

determining the chemical and physical properties of a plasma polymer film. The general type of plasma-surface processes which may accompany exposure of a surface to fluxes of ions, reactive intermediates, low energy electrons and photons include: the deposition of material from the gas phase onto the surface; the etching of surface material via the production of volatile products and/or the alteration of the surface region by exposure to electronically excited neutrals, ions, electrons and photons emanating from the discharge above it.

#### Plasma Process Parameters

Characteristic polymer deposition by glow discharge polymerization occurs onto surfaces exposed to the glow. Some deposition of polymers occurs on surfaces in nonglow regions, but the deposition rate is orders of magnitude smaller. The surface on which a polymer deposits could be an electrode surface, a wall surface, or a substrate surface suspended in the glow region. Another important factor is that glow discharge polymerization is highly system dependent, which means it also depends on the reactor geometries, e.g., dimensions of reactor vessel and of electrodes, internal or external electrodes or coils, location of monomer inlet with respect to exciting electrodes or coils, location of plasma polymer deposition

with respect to monomer inlet and to exciting electrodes, etc. Therefore, other plasma process parameters such as monomer flow rate, system pressure, and discharge power, etc., representing a set of coating conditions to define the polymerization process carried out in a reactor system may not generally apply to that occurred in another reactor system having different configurations and sizes. This arises often because of the process not being compared at a comparable level of conditions and/or parameters. The system dependence of experimental parameters becomes more complicated in a flow system where plasma polymerization is normally carried out. As the reactor design varies from laboratory to laboratory, interlaboratory comparison of results is generally not straightforward. Consequently, plasma process parameters serve as empirical means of describing operational conditions of glow discharge polymerization in a particular system, but they should not be taken beyond this limitation [20].

The plasma process parameters include [20]: frequency of exciting potential, excitation power, monomer flow rate, system pressure, geometrical factors of reactor, and temperature of deposition site, etc. One thing we should remember is that all parameters influence glow discharge polymerization in an interrelated manner. Any single factor cannot be taken as an independent variable of the process.

Frequency of Exciting Potential Electric power sources with frequencies in the zero (dc) to gigahertz (microwave) range can be used for glow discharge polymerization. The use of a low frequency electric power source (up to about the audio frequency range) requires internal electrodes. With higher frequencies, external electrodes or coils also can be used [20].

The use of internal electrodes has the advantage that any frequency can be used, but polymer deposition often occurs onto the electrode surface under low frequency range. In order to restrict the glow to the space between the electrodes in the low pressure range, it is necessary to employ magnetic enhancement. With a high frequency (radio frequency range) power source, the glow tends to stray away from the space between the electrodes, and polymer deposition onto a substrate surface placed in between the electrodes increases. The microwave apparatus usually generates a plasma of fairly even intensity over a large area, as required for deposition of uniform thin films. In one paper [21], researchers used two different apparatus in which both rf and microwave deposition were carried out. It was demonstrated that the rate of plasma polymer deposition was five times greater using microwave (>100 MHz) than rf (<30 MHz), using identical power levels. In general it has been found that, with a.c. discharges on electrodes, the best results are obtained at higher frequencies. As the

frequency of the discharge is increased, more energy is transferred to the gas and less to the electrodes.

Excitation Power The excitation power or discharge power to describe glow discharge polymerization is a system-dependent parameter, not simply the power input into the system. In essence, the absolute value of discharge power itself cannot be considered as an independent variable of the operation, since a certain level of discharge power (e.g., 60 W) in a given set of discharge conditions for one starting material (e.g., ethylene) could not even initiate a glow discharge with another starting material (e.g., n-hexane) under otherwise identical conditions. In other words, a relative level of discharge power which varies according to the characteristics of starting materials is needed to describe the discharge power for glow discharge polymerization [20].

It is known that the discharge power necessary for glow discharge polymerization depends on both the molecular weight and chemical structure of the compounds. The best first-order approach to dealing with this situation is to use the parameter given by  $W/FM$ , where  $W$  is the power input,  $F$  the flow rate given in cubic centimeters (STP) per minute, and  $M$  the molecular weight of the starting material [22]. The parameter  $W/FM$  represents the power input per unit mass of the starting material. With this parameter, plasma

polymerization of various organic compounds can be compared at a more-or-less comparable level.

Although the composite parameter can be used as a comparable parameter to define the conditions of plasma polymerization occurred in two different reactor systems, it can only be applied in a relative sense. The absolute value of the parameter does not provide a meaningful basis for the comparison simply because it includes no parameter that accounts for the geometrical factor of and flow pattern within the reactor system. However, it is still a useful parameter to describe glow discharge polymerization of different starting materials in a polymerization reactor.

Monomer Flow Rate The flow rate describes the total number of gas molecules coming into a system per unit time, when it is expressed by the volume of gas in the standard state, e.g.,  $\text{cm}^3$  (STP)/min, which is the most commonly used unit for the flow rate. In steady-state flow, the monomer feed rate is equal to the pumping-out rate.

The flow rate in most cases of glow discharge polymerization simply refers to the feeding-in rate of the starting materials into the total vacuum system, and it does not necessarily mean the rate at which the starting material is fed to the region of the system where polymerization occurs since the flow rate is measured in the non-plasma

state and no knowledge of the plasma gas phase is generally available [20].

Another important factor to be considered in conjunction with flow rate is that the plasma polymerization predominantly occurs in the glow region; however, the volume of glow is not always the same as the volume of the reactor. Flow rate is usually measured and presented as the feed-in rate into the reactor volume, but not into the glow volume. For instance, in a bell-jar-type reactor the glow volume is only a few percent of the reactor volume. Therefore, the bypass ration of flow, which may be roughly proportional to the ratio of the reactor volume to the glow volume, should be taken into consideration. However, the bypass ratio itself is a variable under conditions of plasma polymerization, since effective plasma polymerization acts as a pump and sucks the monomer into the glow region from the surrounding volume [20].

System Pressure Two pressures in the reactor should be considered: the pressure before the glow discharge is initiated and the pressure in the steady state glow discharge [20].

The system pressure before glow discharge is a function of the flow rate and the pump (and trap) pumping rate for that particular monomer. At a given flow rate, the higher the pumping rate, the lower is the value of system

pressure. The pumping rate of a system is dependent on the nature of the gas and is particularly important when a liquid nitrogen trap or a turbomolecular pump is employed in a vacuum system. These are excellent pumps for most organic vapors and some gases; however, they offer virtually no pumping action for hydrogen, which is the main product gas when hydrogen-containing compounds are used as the starting material [20].

The pressure in the steady state glow discharge is different from the pressure before the glow discharge because a portion of the monomer is removed by the process of plasma polymerization (decreasing the pressure), but by-product gas is generated (increasing the pressure) if more than one mole of by-product gas is generated per mole of monomer or if the by-product gas is pumped less efficiently by the pump and trap. Consequently, the system pressure with the glow discharge on is largely determined by the pumping efficiency of the product gas, the efficiency of the polymerization, and the production rate of gases. In addition, a generally unrecognized factor affecting the pressure in the steady state glow discharge is the fact that the plasma will generally be at a slightly higher temperature than room temperature [23].

Geometrical Factors of Reactor Reactor design can be divided into bell-jar systems and tubular-flow systems. The

effects of location, at which plasma polymer is deposited within the reactor, is relative to the coil or plates giving rise to the electric field and relative to the monomer inlet. Plasma polymer properties tend to be fairly uniform in a capacitively coupled discharge using flat plate electrodes, and such an arrangement is favored for industrial processes. The effects of location tend to be much more pronounced for inductively coupled, cylindrical reactors [22].

The location where the starting material is introduced is very important for polymer deposition. The importance of flow pattern with respect to the location of energy input and of polymer deposition can be visualized in an example of glow discharge polymerization in a straight tube reactor with an external coil placed in the middle portion of the tube. In such a system, the volume of glow discharge is generally much larger than the volume of the portion of tube which is directly under the coil. Consequently, polymer deposition can occur at the downstream and upstream sides of the coil. This factor is less obvious in a system with internal electrodes.

In glow discharge polymerization which utilizes internal electrodes, either the substrate is placed directly on an electrode surface or in the space between the electrodes. With external electrodes or a coil, the location of substrate can be chosen in a variety of ways. Since the

polymer properties and the deposition rate are dependent on the location within a reactor, this is an extremely important factor in practical applications.

The effect of reactor design has raised considerable interest among researchers in the recent past[24,25]. There are lots of factors to consider when designing a reactor and all the geometrical factors of reactor are important to the properties of plasma polymerization. A generalized conclusion would be that reactor design should be considered relative to the desired application.

Temperature of Deposition Site It is known that substrate temperature has a negative effect on the polymerization rate since the reaction occurs through the adsorption of the radicals on the activated surface. The effect of substrate temperature on the polymerization kinetics and polymer structures has been reported for rf glow discharges fed with fluorocarbon monomers [26,27]. It was noted that increasing the substrate temperature resulted in decreasing the fluorine content of plasma polymerized films, thus the film structure became more crosslinked.

#### Polymer Deposition Rate

Polymer deposition rate is highly dependent on the chemical structure of the monomer, although some other

factors, such as plasma process parameters, also influence the polymer deposition rate.

In plasma polymerization of hydrocarbons, triple bond and/or aromatic structure (group I), double bond and/or cyclic structure (group II), and saturated structure (group III) are three functions which determine the rate of polymer formation and the properties of plasma polymers [28]. Group I compounds form polymers by utilizing the opening of triple bonds or aromatic structures with the least evolution of hydrogen. Group II compounds form polymers via both the opening of double bonds or cyclic structures and hydrogen abstraction. Production of hydrogen is considerably higher than formed by group I compounds. Group III compounds polymerize primarily by plasma polymerization based on hydrogen abstraction. Consequently, hydrogen production is much higher than in those for group II compounds [28].

The discharge power necessary for glow discharge polymerization of hydrocarbons is also dependent on the types of compound. Groups I and II compounds require approximately the same energy input. However, the dependence on flow rate is nearly zero for group I compounds, but an appreciable increase in the required energy input is observed for group II compounds for increasing flow. Group III compounds require the highest energy input and their dependence on flow rate is much greater than that for group II compounds.

Flow Rate The polymer deposition rate usually increases linearly with the flow rate of a starting material under ideal conditions where the conversion ratio of starting material to polymer is high or remains at a constant level. However, the change of flow rate is often associated with changes in flow pattern (affecting the bypass ratio of the flow) and/or the efficiency of discharge power input. Therefore, the apparent dependence of the polymer deposition rate on flow rate is often characterized by a decrease of the polymer deposition rate after passing a maximum or a narrow plateau, as shown in Figure 2 [28].

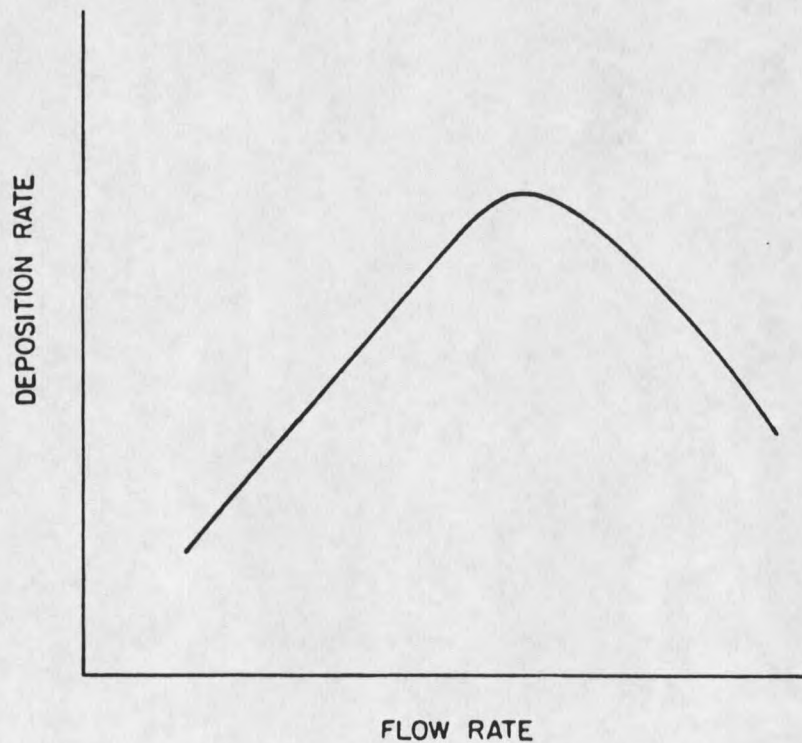


Figure 2. Schematic representation of the dependence of polymer deposition rate on flow rate of a starting material when a constant discharge power is used.

Discharge Power When a constant flow rate is employed, the polymer deposition rate generally increases with discharge power in more or less linear fashion in a certain range of discharge power, and reaches a plateau, as shown in Figure 3 [28]. Further increase of discharge power often decreases the polymer deposition rate.

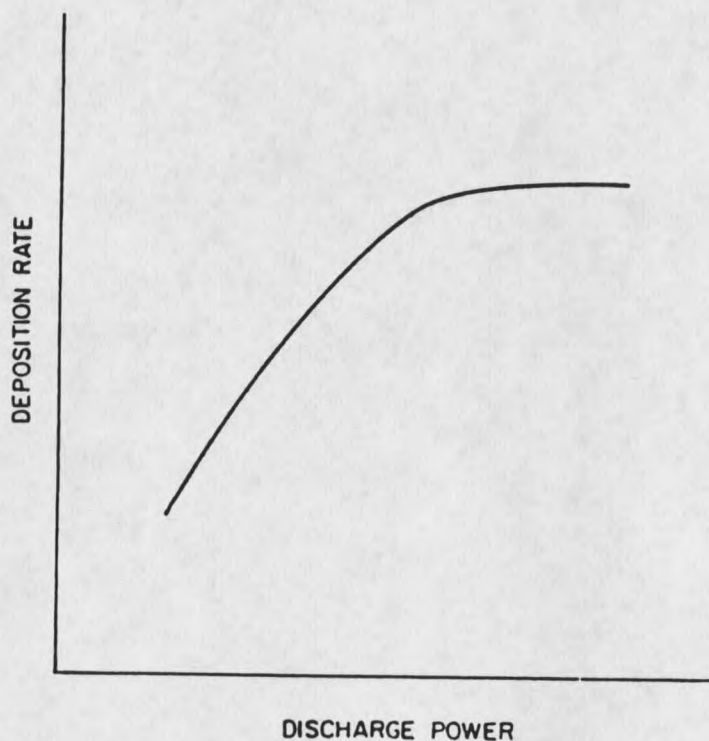


Figure 3. Schematic representation of the dependence of polymer deposition rate on discharge power when a constant flow rate is employed.

W/FM Parameter As mentioned earlier, the effect of flow rate or discharge power cannot be determined independently since glow discharge polymerization is

dependent on the combined parameter of  $W/FM$ . As long as the  $W/FM$  value remains above a critical level where energy input is sufficient for polymerization, the major effect of increasing the flow rate is to increase the feed-in rate, which increases the polymer deposition rate. However, if the  $W/FM$  level drops to a certain level as  $F$  increases at a constant  $W$ , where the discharge power is not sufficient to polymerize all starting materials coming into the reaction system, the polymer deposition rate decreases despite the fact that more starting materials are supplied to the reaction system. Consequently, according to the  $W/FM$  parameter, the discharge power  $W$  must be increased as the flow rate of starting materials increases and/or as the molecular weight of the starting materials increases [28].

### Plasma Etching

Since the late 1960s, plasma treatment of polymers has been applied to fields as apparently diverse as textiles and medicine, hazardous waste handling, and electronics. Most of these applications involve the use of low pressure, low temperature plasmas and can be classified into one of three categories. These are cleaning, pattern definition, and film modification.

The idea of plasma etching seems to have first been applied to semiconductor processing during the 1960s as

plasma ashing, also known as plasma stripping [29]. As shown in Figure 4, this is a technique for the removal of photoresist materials which, being organic, consist essentially of carbon and hydrogen. Solid carbon is converted to gaseous carbon monoxide and carbon dioxide by oxidation in an oxygen glow discharge. These gases, together with other volatile products of the reaction, such as water vapor, are then pumped away by the vacuum system. The purpose of the glow discharge is to convert molecular oxygen, which does not react with photoresist materials at room temperature, into active oxygen atoms which do react readily.

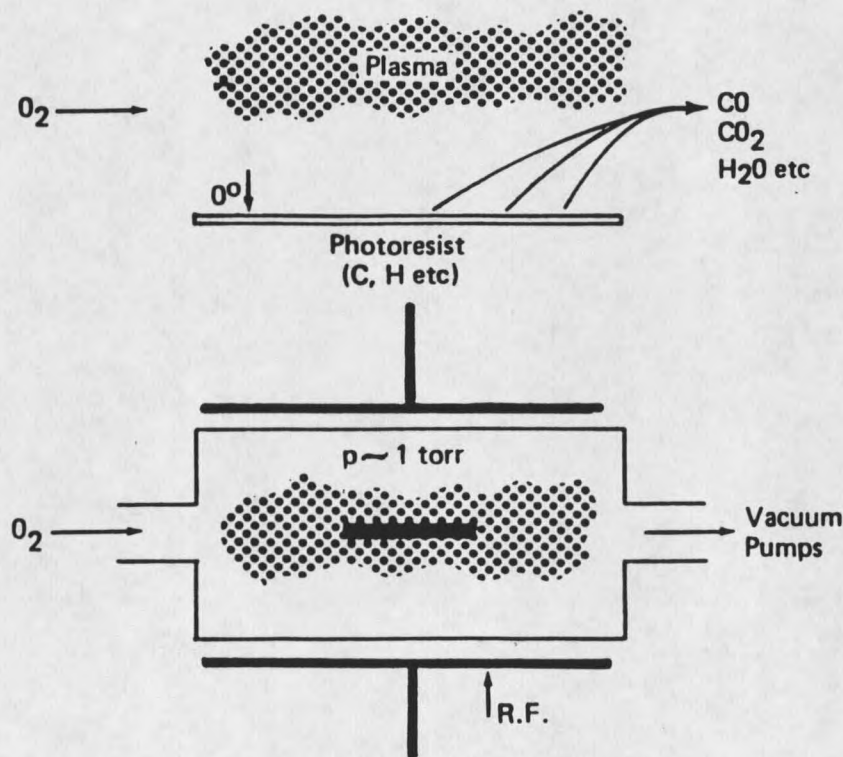


Figure 4. The principle and implementation of plasma ashing

Today, state-of-the-art integrated circuit manufacture depends on the mass replication of tightly controlled, micron-sized features in a variety of materials. Plasma etching has become central to this process because it is the only current technology that can do this job efficiently and with high yield. The plasma etching technique is quite new and not well understood at present, but this does not seem to be hindering its implementation. Only the etching of silicon materials in fluorine-based gases has been the subject of any reasonably well-defined experiments, and even in that materials system there are many unresolved questions, apparent anomalies, and disagreements on interpretation [29]. As the use of polymers increases, and as the plasma technology matures, a better understanding of the polymer etching processes will allow new degrees of freedom in materials engineering, and more development is required to expand the versatility of the process and exploit its potential.

#### Plasma Etching and Its Advantages

In the plasma ashing, since carbon can be etched by the formation of volatile oxides, it is a short logical step to look for etching processes for other materials by the formation of volatile reaction products in a glow discharge. This is the process of plasma etching, which exists today in

a variety of forms and under a variety of names, such as plasma etching, plasma assisted etching, reactive sputter etching, reactive ion etching, etc. These all nevertheless rely on the same basic principle.

Plasma etching is the practice of etching or gasifying substrate material in a plasma. In contrast to physical sputtering, where involatile materials can be ejected across the reactor, plasma etching relies on the chemical combination of the solid surface to be etched, with an active gaseous species produced in a discharge. Involatile products would accumulate on the surface, and passivate it against further reaction.

Plasma etching was explored as a cheaper alternative to wet solvent chemical processes for integrated circuit manufacture in the late 1960s and early 1970s [30]. There are certainly safety considerations, too: silicon nitride can be etched, using wet chemicals, by hot phosphoric acid at 160°C, not too pleasant for the operator; the equivalent plasma etching process involves  $CF_4$ , virtually inert, inside a process chamber. The wet chemical processes were complicated and indirect. At first, the advantages of plasma etching technology seemed to lie in unique processing sequences, substitution of safe nontoxic gases for corrosive liquids, easily discharged waste products and simple automation. By the late 1970s, however, it was widely recognized that plasma etching offered the possibility of

producing fine resolution in small ( $\sim 1 \mu\text{m}$ ) devices, achieved by etching in a directional manner (e.g., anisotropic etching).

There is another path in the genesis of the plasma etching process. Chemical gas phase reactions sometimes occur spontaneously, and can usually be accelerated by heating. There is a range of gas etching techniques that do not involve a glow discharge, but instead rely on heating to activate the process. However, these processes require a high substrate temperature. In semiconductor processing one usually likes to keep wafers cool so as not to disturb diffusion profiles or melt metallization. Plasma etching clearly has an advantage in this respect. It is inherently more controllable, since temperature-controlled chemical reactions tend to have a rate dependence varying exponentially with the temperature [30].

### Oxygen Plasma Etching

Oxygen is other of two elements (i.e., F and O) that tend to be evolved from either the starting material or substrate material, causing significant ablation of organic materials. Consequently, oxygen gas is generally a good starting material for plasma etching.

Oxygen plasmas were used to etch resists both isotropically and anisotropically [31]. Isotropic resist

stripping with O atoms is one of the oldest plasma applications, while anisotropic pattern transfer was developed to permit micron- and submicron pattern transfer. Oxygen chemical treatment was also used to remove epoxy smears from holes in multilayer printed circuit boards and to alter the adhesion of substances to organic surfaces by changing their wettability or by roughening them.

At moderate pressure and high frequency, a glow discharge in pure oxygen produces oxygen atoms. These atoms attack organic materials to form CO, CO<sub>2</sub> and H<sub>2</sub>O as the final end products. Etching rates in pure oxygen plasmas are proportional to oxygen atom concentration [31,32]. Inert gas additions can help stabilize oxygen plasmas. Chemical etching in oxygen plasmas is heavily influenced by the structure and substitutional groups on the polymer, and by physical variables such as temperature.

For hydrocarbon polymer etching using oxygen plasmas, atomic oxygen can add to unsaturated groups to form a radical site on the carbon atom adjacent to the site of the addition. Addition of oxygen atoms to double bonds can also lead to excited intermediates which may react to form epoxides or isomerize to carbonyl compound. Or, oxygen atoms can react with aromatic rings to form phenols in an addition reaction without forming free radicals [33]. This may explain, in part, the greater resistance of aromatic polymers to etching in oxygen plasmas compared with

nonaromatic polymers. Oxygen atoms can react with saturated hydrocarbons to form hydroxyl groups. It is stated that alcohols thus formed can be further oxidized, eventually producing CO and CO<sub>2</sub> products [34]. Abstraction of hydrogen by atomic oxygen is another possible way for polymer radical site generation.

Etching rates are enhanced when fluorinated gases are added to an oxygen plasma. Even a few percent of C<sub>2</sub>F<sub>6</sub> added to oxygen can bring about a large increase in the removal rate for many polymers [35]. The enhancement seems to be caused by two effects: fluorine atom reactions produce reactive sites on the polymer backbone, and small amounts of fluorine increase the concentration of atomic oxygen in an oxygen plasma. Atomic fluorine abstracts hydrogen from organic polymers, leaving unsaturated or radical sites. These sites are much more susceptible to oxygen than a saturated polymer chain. When oxygen attacks these sites, carbonyl groups are formed, and the polymer is "burned" into volatile oxidation products.

From the above discussion, it is clear that to enhance the etching of polymers in pure oxygen plasmas, plasma parameters should be modified to increase the dissociation of O<sub>2</sub> to atomic oxygen, to decrease recombinative losses of atomic oxygen and to increase the flux of O atoms from the plasma to the sample. Of course, simultaneous bombardment by energetic ions is known to enhance the etching of polymers

in oxygen plasmas. The plasma etch rate of polymers also increases with temperature.

### Plasma Etching and Plasma Polymerization

Plasma etching and plasma polymerization are two opposite processes which can take place in the same reactor under different reaction conditions. For example, for the etching of silicon and silicon oxide in  $\text{CF}_4$ , the addition of hydrogen to a  $\text{CF}_4$  discharge causes the etch rate of silicon to decrease whilst the silicon oxide etch rate remains fairly constant. This is evidently a way of selectively etching the oxide, by obtaining a favorable etch rate ratio between the two materials. Given that some hydrogen depresses the silicon etch rate, why not add so much that the etch rate drops to zero? The reason is that the silicon etch rate would actually become negative, i.e., we would start to deposit a coating on the silicon. The coating would be a polymer, and plasma polymerization occurs. The polymer is of the form  $(\text{CF}_2)_n$ , or a related form [35]. It is caused by the association of fluorocarbon radicals on surfaces or, if the pressure is high enough, in the gas phase. If we go too far, polymerization occurs and etching stops everywhere. The achievement of high etch rate ratios is therefore an exercise in trying to get as close to the onset of polymerization, or the polymer point as it is known,

without actually depositing polymers onto the wafer. Plasma polymerized coatings have all kinds of useful applications, but polymerization has an uneasy role in plasma etching.

The balance between etching and polymerization seems to be a very sensitive one which can be "pushed" either way. Ion bombardment appears to have a major effect, with increased bombardment pushing the balance towards etching. Indeed, one has the situation in reactive ion etching systems where etching is occurring on the cathode, and polymerization on the walls. Mauer and Carruthers [36] have made a study of how the various plasma process parameters control the onset of polymerization in the plasma etching of silicon and silicon oxide.

#### Glow Discharge Reactors

Surveys of glow discharge reactors show that in general there are three components (Figure 5): a power source, a coupling mechanism and a chamber which contains the plasma [37]. Power sources can be either DC or AC, and their applications depend on the particular experiment. In current practice, glow discharge processes are almost always driven by high frequency power supplies, usually in the megahertz range. Power coupling systems fall into three categories: resistive coupling, capacitive coupling and inductive coupling. The majority of plasma systems have been

capacitively coupled using parallel plates within or across the reactor volume. The inductively coupled system is often used in laboratory experiments. Reactor chambers can be divided into bell-jar systems and tubular-flow systems.

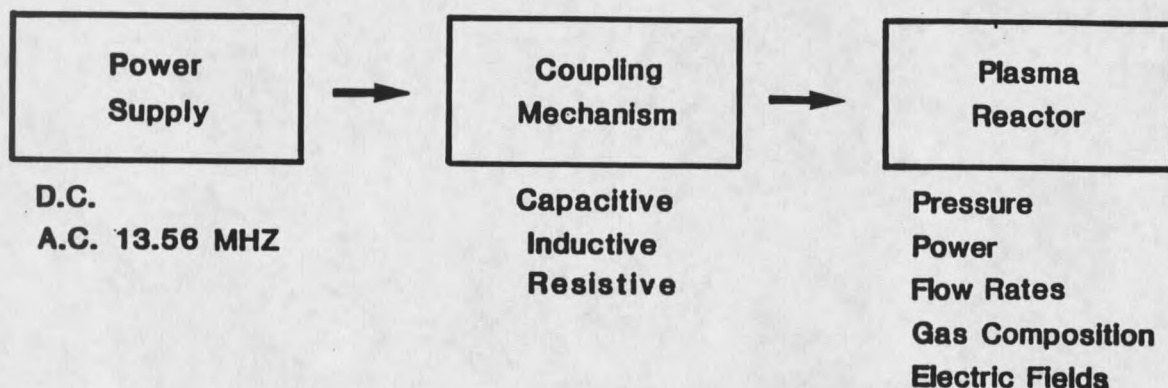


Figure 5. System components used in a glow discharge reactor

Glow discharges using DC power sources are resistively coupled, which means that the electrodes are in contact with the gas in the reactor [37]. This situation has several problems in organic plasmas where an insulating film is often deposited on the electrodes making them useless. Furthermore, internal metal electrodes normally act as good catalysts and can affect the plasma chemistry, as well as contaminate the deposited organic films because of sputtering of metal particles from the electrodes by energetic plasma ions. Positioning the electrodes outside of

the reactor circumvents these problems, but only AC excitation can be used in this case. The frequency used must be greater than a specific value above which the electrons in the plasma do not reach the opposite electrode but oscillate in the plasma eliminating the need for the electrodes to be in contact with the gas.

External electrodes exhibit some disadvantages when compared to internal ones. One of these is non-uniform glow which tends to concentrate in regions close to the external electrodes. This non-uniform glow is the result of limitations in the depth of penetration of the electromagnetic waves in the discharge media. Furthermore AC discharges are more difficult to characterize because of the varying fields [37].

The properties of the plasma can be controlled by several externally controlled variables which were discussed in the former section: the discharge power, the pressure, flow rates, gas composition of reactants and additional magnetic or electric fields, etc.

#### RF Reactors and Matching Networks

An AC frequency of 13.56 MHz is generally used in glow discharges because it is a frequency reserved for commercial rf generators by the Federal Communications Commission [38]. These discharges are generally referred to as radio

frequency (rf) glow discharges. At this frequency rf generators can radiate a certain amount of energy without interfering with communications. Unfortunately this isn't such a great help for rf glow discharge systems because the glow discharge has so many nonlinear effects that it generates many harmonics of the fundamental frequency, and the radiation requirements in the harmonic frequencies are far more stringent. For example, at the Allen Clark Research Center in Northampton, the converted machine with which the researchers powered an early rf sputtering system incapacitated the internal paging system [38].

Coupling of the rf power to the plasma reactor can be done either capacitively, where an electrode is placed outside of the reactor, or inductively where the reactor is placed inside a coil. It is a common practice to use a matching network between the rf generator and the glow discharge. The purpose of this network is to "tune out" reflected power which could damage the rf generator and inhibit ignition of the plasma and to efficiently couple the power to the discharge. Tuning is usually accomplished by matching the resistance and capacitance of the load so that the generator sees an impedance of 50 ohms. Matching networks are typically combinations of variable capacitors and inductors, and placement of a single screw of magnetic material within the rf field can affect performance of the system.

## Thin Film Analysis Techniques

### X-Ray Photoelectron Spectroscopy

The technique of X-ray photoelectron spectroscopy (XPS) is a relative newcomer to the field of surface analysis. In 1954, a high resolution electron spectrometer for low energy electrons produced by X-ray excitation was operated for the first time by the Swedish group headed by Siegbahn [39]. It was quickly recognized that the available precision in locating the photo-peaks provided a far more accurate means for studying atomic orbital energy systematics than those previously available, and the technique was first used for this purpose. It was soon discovered, however, that chemical shift effects occurred, showing that the chemical differences between atoms and their oxidation states were clearly distinguishable by XPS. Because of these readily observed and useful chemical effects, the Swedish group coined the name "Electron Spectroscopy for Chemical Analysis" to describe this technique. The corresponding acronym "ESCA" is widely used synonymously with the generic name "XPS". The advent of commercial manufacturing of surface analysis equipment in the early 1970s enabled the placement of equipment in laboratories throughout the world,

and XPS has matured into one of the most powerful and valuable methods of surface analysis currently available.

Surface analysis by XPS involves irradiating a solid in vacuum with monoenergetic soft x-rays and analyzing the emitted electrons by energy. Because the mean free path of electrons in solids is very small, the detected electrons originate from only the top few atomic layers, making XPS a unique surface-sensitive technique. A major advantage of the technique is that the photoelectron energy is dependent on the precise chemical configuration of the surface atoms and information about the binding environment (oxidation state, bonding atoms, etc.) can be obtained. XPS is amenable to virtually all vacuum-compatible samples since the incident x-rays do not normally cause surface damage. Hence XPS may be used to analyze surfaces of delicate powder materials, polymers and organic coatings. XPS can also provide quantitative determination of the approximate elemental surface composition (error <  $\pm 10\%$ ) and easily analyze nonconductive samples due to charge neutralization [39].

The disadvantages of XPS lie in the fact that it is essentially a broad area technique with only limited capability for small area analysis and the poor depth resolution in composition-depth profiling.

Principles of the Technique The basic XPS experiment is shown schematically in Figure 6 [40] for a free atom in

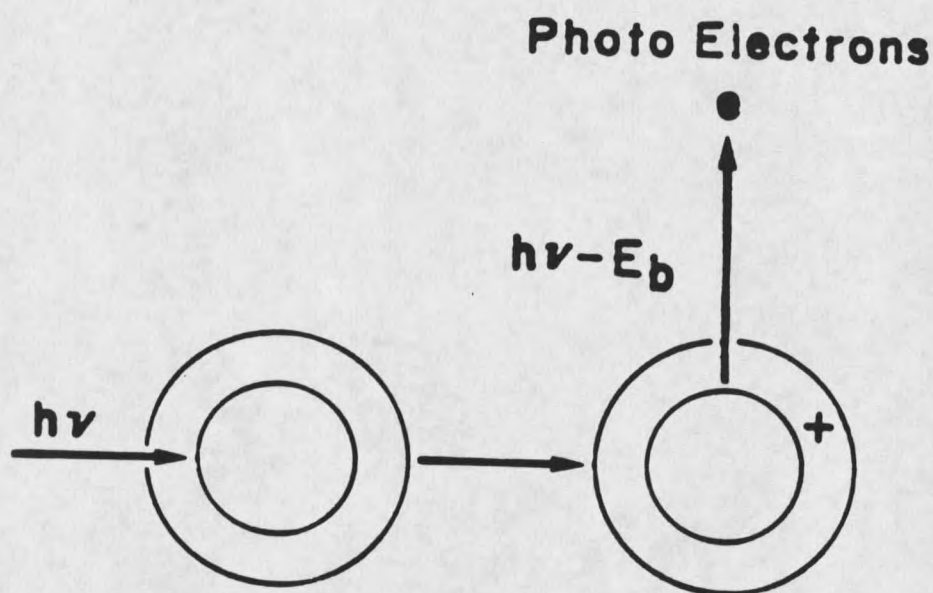


Figure 6. The physical basis of XPS

the gas phase. X-ray photons,  $h\nu$ , from a nearly monoenergetic beam are directed onto the sample. The photons are absorbed by sample atoms with each absorption event resulting in the prompt emission of an electron. Electrons from all the orbitals of the atom with a binding energy,  $E_b$ , less than the x-ray energy are excited, though not with equal probability. Thus, some peaks are more intense in the spectra than others. Since energy is conserved, the kinetic energy,  $KE$ , of the electron plus the energy required to remove it from its orbital to the spectrometer vacuum must equal the x-ray energy. Total transfer of the photon energy

to the electron is the essential element of photoemission which is the basis of XPS. If the x-ray energy is known and the kinetic energy is measured with the electron spectrometer, the binding energy of the electron in the atomic orbital can be obtained. In practical solid state experiments, a correction for the spectrometer work function,  $\phi_s$ , must also be applied, normally as part of the spectrometer calibration procedure. Thus, one obtains  $E_b = h\nu - KE - \phi_s$  [40].

Photoemission may be observed from solids, liquids and gases, in fact from any state of matter containing bound electrons, but it is the application of the photoelectric effect to solids that has aroused the most interest in recent years.

Since the atomic structure of each element in the periodic table is distinct from all the others, measurement of the positions of one or more of the electron lines allows the ready identification of an element present at a sample surface. Each element has a unique elemental spectrum, and the spectral peaks from a mixture of elements are approximately the sum of the elemental peaks from the individual constituents. The intensity of the signal observed is, of course, a function of the amount of material present. Thus, quantitative data can be obtained from the peak heights or areas, and identification of

chemical states often can be made from the exact positions and separations of the peaks, as well as from certain spectral contours.

In addition to the photoelectrons emitted in the photoemission, irradiation of a solid by x-rays can also result to emission of Auger electrons [41]. The Auger effect is the de-excitation of an ionized atom by a non-radiative process. In the Auger process, an outer electron falls into the inner orbital vacancy, and a second electron is emitted, carrying off the excess energy. The Auger electron possesses kinetic energy equal to the difference between the energy of the initial ion and the double-charged final ion. Of course, the energies of the electrons emitted cannot exceed the energy of the ionizing photons. A characteristic of Auger electron is that their energy is independent of irradiation energy.

Instrumentation A schematic drawing of a contemporary XPS instrument is shown in Figure 7 [42]. The functions of the spectrometer are to produce intense x-ray radiation, to irradiate the sample to photoeject core electrons, to introduce the ejected electrons into an energy analyzer, to detect the energy-analyzed electrons, and to provide a suitable output of signal intensity as a function of electron binding energy. Thus, the primary components that make up the XPS instrument are ultra-high vacuum chamber, x-

ray source, electron energy analyzer and detector, and data collection system.

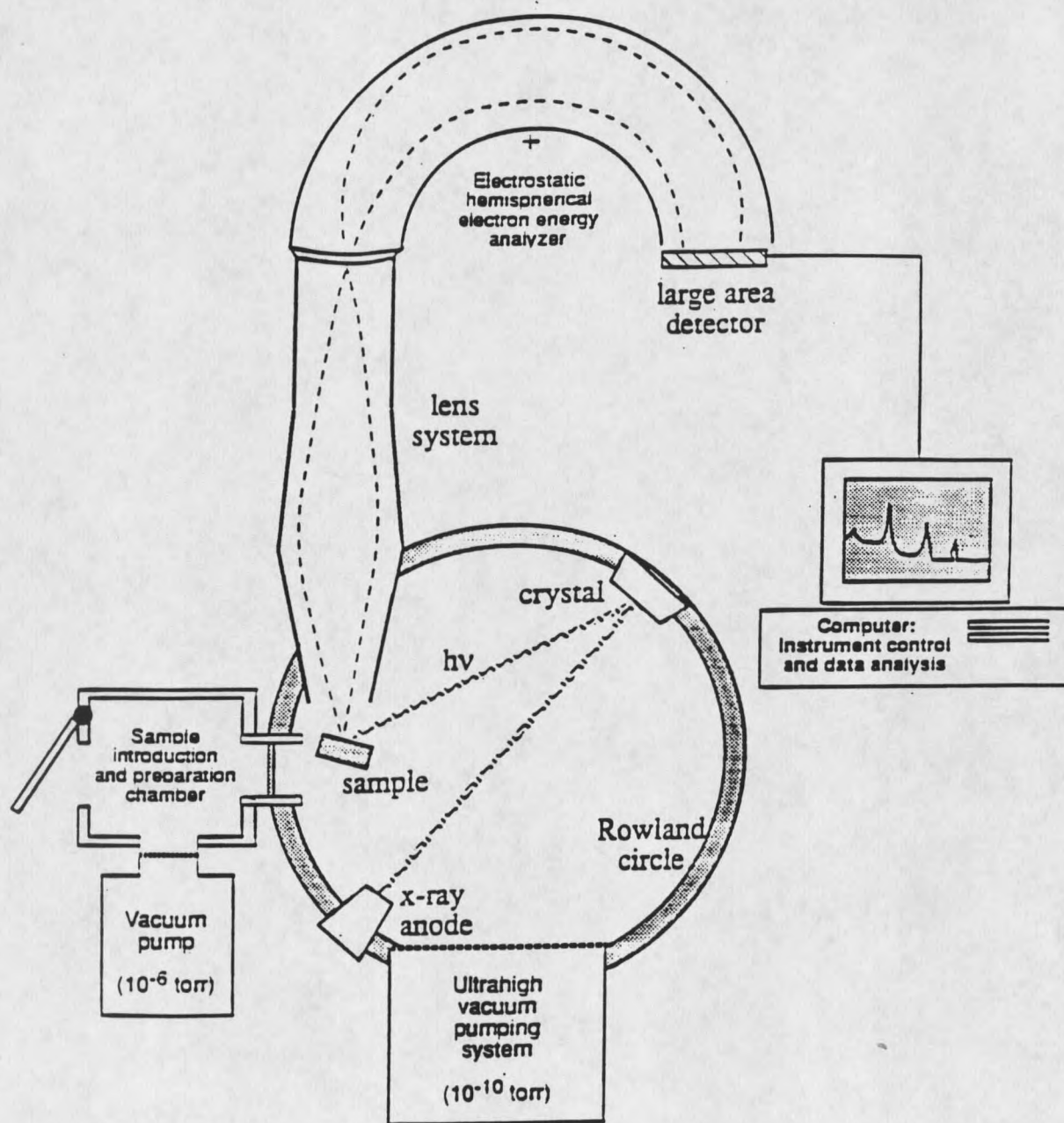


Figure 7. Schematic diagram of an XPS instrument

The commercial availability of reliable ultra-high vacuum technology in the late sixties was a critical step for the development of surface analysis techniques. Even under conventional high vacuum, surfaces are exposed to constant interaction with atoms and molecules in the residual vacuum, so that monolayers of contamination can form in the course of a measurement. Vacuum system also allows the emitted photoelectrons to travel from the sample through the energy analyzer to the detector without colliding with gas phase particles. Another reason to use high vacuum chamber in XPS is that many of the constituent parts, such as x-ray, electron analyzers and detectors will operate only under high vacuum conditions.

The necessary characteristics of an x-ray source suitable for XPS are that the x-ray energy should be sufficiently high to excite core-level electrons of all elements, the x-ray spectrum should be relatively "clean", with very few satellites or other peaks (i.e. low atomic number anode material), the characteristic x-ray linewidth should be narrow in comparison to the intrinsic core-level linewidths and chemical shifts we wish to study, and the material must be suitable for the construction of an anode [39]. Most commercial XPS instruments are fitted with aluminum and/or magnesium anodes, which when bombarded by high energy electrons, emit  $AlK_{\alpha}$  (1486.6 eV) and/or  $MgK_{\alpha}$

(1253.6 eV) x-rays. The x-rays generated pass through a thin aluminum window separating the high voltage anodes and spectrometer chambers, and then the sample surface is uniformly irradiated with a low flux of x-rays.

The electron energy analyzer is the most crucial part of any XPS instrument. The function of the energy analyzer is to measure the number of photoejected electrons as a function of their energy and to disperse them across a detector or detector array. The most common type of energy analyzer used is the spherical sector electrostatic analyzer (SSA). The SSA does not suffer from the specimen position dependence of energy and resolution which is a major drawback of its main rival, the cylindrical mirror analyzer (CMA). Since the electrons arrive at the analyzer exit with a range of energies, the multichannel detector array is the most efficient means of detection to count the number of electrons leaving the analyzer at each energy [42].

As an integral part of the XPS system, powerful workstation with softwares will deliver complete surface analysis, including controlling instrument operation, automatic peak fitting and quantitation, depth profiling, chemical state imaging, etc. In general, as the speed and power of computer systems increase, so do the capabilities for XPS data acquisition and analysis.

In addition to the basic requirements discussed above, most modern XPS spectrometers will also be equipped with

some additional facilities, such as charge neutralizer to obtain high-quality spectra from insulating materials, a controlled inert gas ion source for ion sputtering, and sample manipulators, etc. A more detailed discussion of instrumentation can be found elsewhere [43,44].

### Scanning Electron Microscopy

In our rapidly expanding technology, scientists and engineers are often required to observe and correctly explain phenomena occurring on a micrometer and submicrometer scale. The scanning electron microscopy (SEM) is a relatively new and powerful instrument which permits the characterization of heterogeneous materials and surfaces on such a fine scale. Among the major types of information obtained are compositional information of both a qualitative and quantitative nature, and topographic information contained in images obtained at relatively high resolution. The SEM, with its large depth of field and easily interpreted images of samples that often require little or no sample preparation for viewing, is capable of providing significant information about rough samples at magnifications ranging from 10X to 100,000X [45]. This range overlaps considerably with the optical microscope at the low end, and with the electron microscopy at the high end. A magnification of 100,000X with a spatial resolution better

than 100 Å can be obtained with SEM, whereas for optical microscopes, these figures are 1,000X and 10,000 Å, respectively. SEM can give a depth of field of 2-4 μm at 10,000X magnification and 0.2-0.4 mm at 100X magnification which are much deeper than those of optical microscopes.

The major drawbacks of SEM are that a conducting sample is needed, and hydrated samples cannot be observed since the experiment is conducted in a high vacuum system. The first problem can be overcome by gold or carbon sputtering of the sample or using a low-energy incident beam to help eliminate problems of surface charging. The second one can be avoided by using a cryostage or a field-emission SEM.

The development of the scanning electron microscopy began in 1935 with the work of Max Knoll at the Technical university in Berlin [46]. He placed specimens into a modified cathode ray tube and scanned the specimens with an electron beam of a diameter between 0.1 and 1 mm. In 1938, Manfred von Ardenne, working in his private laboratory in Berlin, published an important theoretical paper that clearly explained the principles of SEM. In fact, von Ardenne added scan coils to a transmission electron microscope and in so doing produced what amounts to the first scanning transmission electron microscope. In 1942, V.K. Zworykin, J. Hiller, and R.L. Snyder in the RCA Laboratories in the United States developed the first

scanning electron microscope that could examine bulk specimens. The modern SEM was developed by Sir Charles W. Oatley and his students at Cambridge University in England from 1948 to 1961. In the early 1960s, it became apparent that the SEM was a valuable instrument that was ripe for commercial production. This led to the first commercial production of an SEM by Cambridge Instrument Company in 1965. The instrument was an immediate success and won the Queen's Award for Technology for that year. Today, the SEM became one of the most versatile instruments available for the examination and analysis of the microstructural characteristics of solid objects.

Principles of the Technique In SEM, the area to be examined is irradiated with an energetically well defined, finely focused electron beam, which may be static, or swept in a raster across the surface of the specimen. The types of signals (shown in Figure 8) which are produced when the focused electron beam impinges on a specimen surface include secondary electrons, backscattered electrons, characteristic x-rays, Auger electrons, and photons of various energies [47]. They are obtained from specific emission volumes within the sample and are used to measure many characteristics of the sample (composition, surface topography, crystallography, etc.).

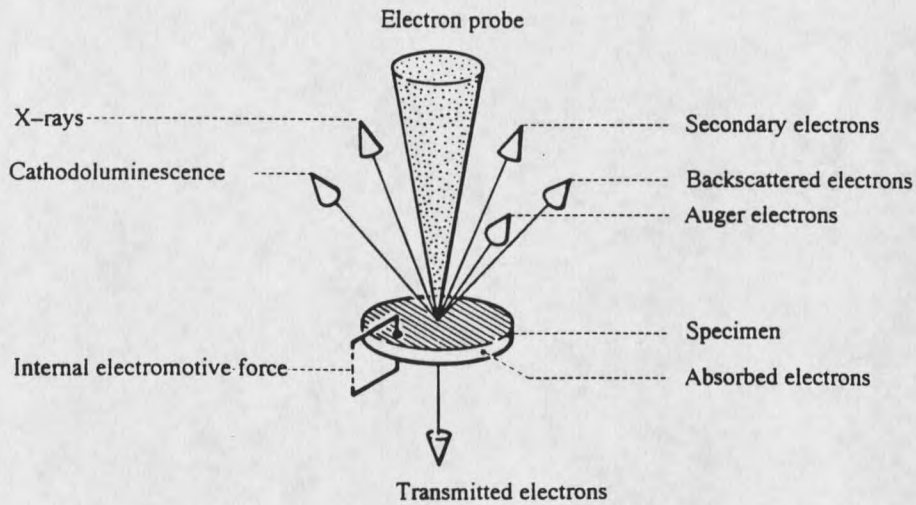


Figure 8. Signals from specimen in an SEM instrument

The secondary electron imaging works on the principle that this electron beam generates a "splash" of electrons with kinetic energies much lower than the primary incident electrons, called secondary electrons. Because of their low energies and low penetration depth, the detection of secondary electrons as a function of primary beam position makes it possible to attain high magnification and high resolution for imaging the areas of interest [48].

The backscattered electron detector detects high energy electrons which backscatter quasi-elastically off the sample. This imaging detector operates in two modes: topographical, which yields a topographic image of the sample surface; and compositional, which distinguishes between areas of relative low and high average atomic weights. This is because higher-density areas of the sample

produce increased back-scattering signals and hence appear brighter in a micrograph. This technique is extremely useful for locating areas with concentrations of heavy elements not necessarily visible to the secondary electron detector.

The cathodoluminescence (CL) detector detects luminescence in the visible light range produced by the sample from excitation produced by the electron beam. The luminescence is highly dependent on trace element abundances in solid substrates which makes this technique invaluable to the geological and semi-conductor communities. CL is complementary to backscattered electron imaging, which discriminates between different phases as a function of the mean atomic number (density); CL has the added capacity of distinguishing between different generations or domains of the same material (equal density) based on small variations in trace element content [49].

The energy-dispersive x-ray detector detects x-rays from the sample excited by the highly focused, high-energy primary electron beam penetrating into the sample. When the high-energy electrons interact with the atoms of material in this "interaction volume", typically several microns in diameter, they generate characteristic x-rays which are fingerprints of the individual atoms encountered. These x-rays can penetrate through the material, allowing them to escape and be detected by x-ray detector. Because the intensity of the individual x-ray is related to the quantity

of the "parent atom" in the interaction volume, quantitative elemental analysis can be obtained from the sample with the aid of the powerful computer and software analysis capabilities. The software also enable one to collect elemental maps of the sample as well as digitized secondary and backscattered electron images and perform other more sophisticated analyses.

Instrumentation The basic components of an SEM instrument are the vacuum system, the electron gun, the lens system, the electron collector and cathode ray tubes (CRT's), and the electronics associated with them. Figure 9 gives a schematic drawing of an SEM instrument [50].

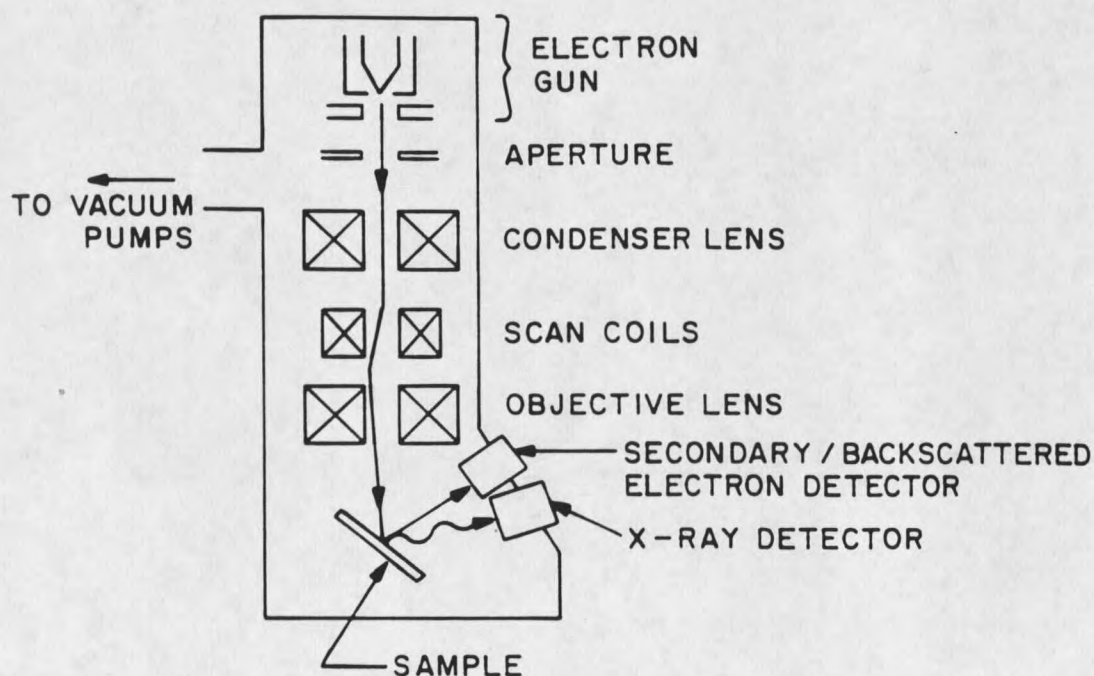


Figure 9. Schematic drawing of an SEM instrument.

The operation of SEM requires that the electron beam has unimpeded passage down the column, through the lenses and apertures, to collide with the specimen. It is not possible to maintain a coherent electron beam down the column if a significant number of gas molecules are present; the collisions of the electrons with the gas molecules result in a diffuse electron beam that is unusable. In addition, a poor vacuum results in a large number of gas molecules in the area of the electron-emitting cathode which may cause failure of the cathode.

The electron gun is the source of the electron beam. Electrons are drawn from a negative cathode and accelerated to an energy of 2 to 40 KeV toward an anode at ground potential. Almost all electron microscopes use one of three types of electron guns: (1) electron gun with thermionic emission from a tungsten cathode, (2) electron gun with thermionic emission from a lanthanum hexaboride ( $\text{LaB}_6$ ) cathode, or (3) electron gun with field emission from a tungsten cathode [51].

The function of lenses is to bend electrons so that they are deflected in a predictable way from their original paths. Lense systems determine the size and intensity of the electron beam and focus the electron beam on the sample surface. Scanning coils move the focused electron beam over the specimen in a raster pattern of lines.

Detectors used in SEM accept radiation from the specimen and convert the radiation to an electrical signal that, after amplification, is used to modulate the gray-level intensities on a cathode ray tube, producing an image of the specimen. SEM can use a large part of the electromagnetic spectrum (infrared, visible, ultraviolet, and x-rays), as well as electrons (Auger, secondary, backscattered, and conducted) to form an image, providing a detector system is available to convert the radiation into an electrical signal.

## CHAPTER 3

## EXPERIMENTAL, MATERIALS AND METHODS

Reaction System

In the present experiments surface modification of E-glass fiber strands and fabric by plasma etching and polymerization are studied using an instrument designed and constructed "in house". The construction of the reactor system is a part of this study. A schematic diagram of the reaction system which has been designed and built is given in Figure 10. The main parts of the system are: gas lines and controllers, the plasma reactor, the rf generator and matching network, pressure controllers, and traps and pumps.

Gas Lines and Controllers

The gas used for plasma etching is CP grade oxygen. CP grade Argon gas is used to purge the line after oxygen etching. Plasma polymerization monomers are CP grade (minimum purity 99.5%) ethylene and methane gases. All these gases are obtained from General Distributing Co. and used without additional purification.

Gas flow into the reactor is measured by mass flow meters. A combination of mass flow controllers (MKS 1259050SV), A four-channel readout and power supply unit (MKS 247C) and shutoff valves (Kurt J. Lesker SS-4BKT) are used for the two feed lines. The mass flow controller allows for the selection of flow rates and the ratio of the flow rates between the two feed lines. Shutoff valves are used to isolate the reactor from the gas feed lines. A third gas feed line is also available with a shutoff valve. It is used primarily for Argon gas to purge the line after oxygen etching.

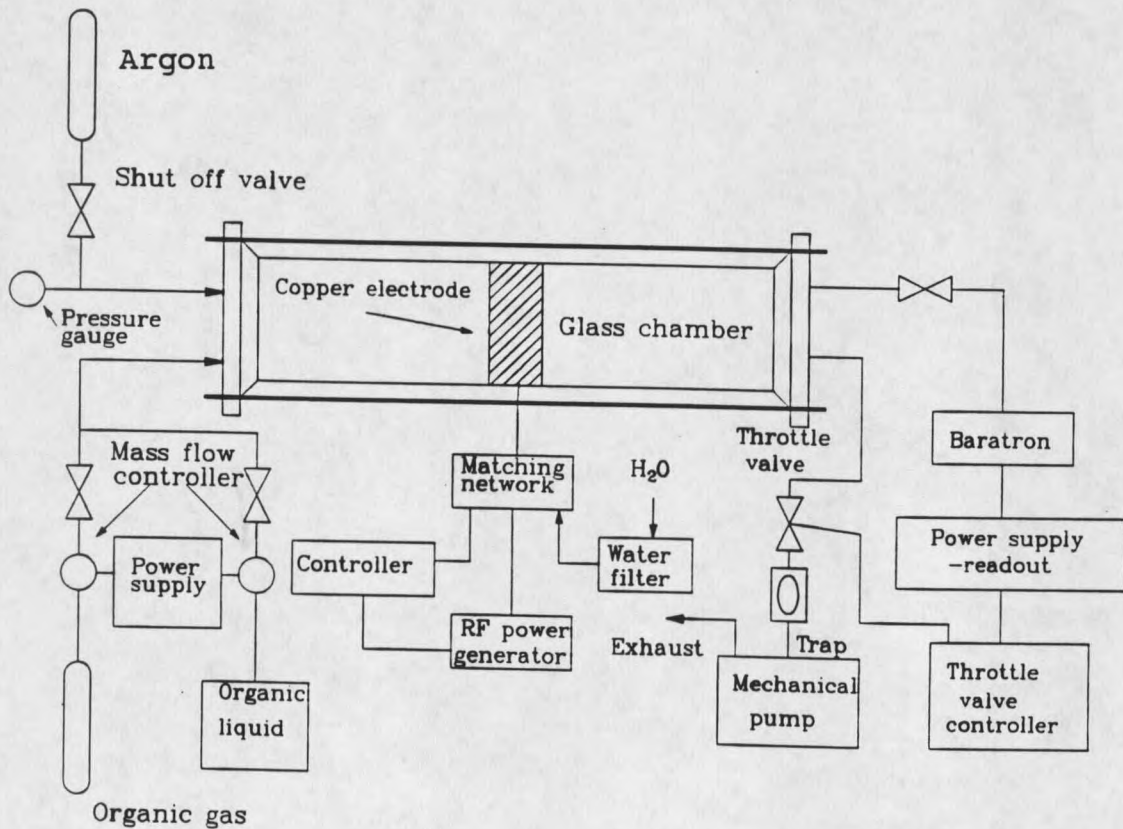


Figure 10. Schematic diagram of the reaction system

### Plasma Reactor

The plasma reactor is a Pyrex glass cylinder 24.1 in. long, 4.0 in. in inside diameter, and 4.6 in. in outside diameter, with a volume of about 5 liters. Both sides of the cylinder are rubber O-ring sealed (made "in house") to stainless steel Kurt J. Lesker ASA flanges. One flange incorporates three ports. Two of them are used for gas feedthroughs and the third one is used for pressure gauges (KJL-205). The other flange has two ports which are connected to a pressure transducer (Baratron MKS 127A001D) via a shutoff valve and a pumping line.

The glass chamber and the flanges are fixed by four steel rods separated evenly around the cylinder. The chamber can reach a vacuum of 5 mtorr when there is no gas feeding into the chamber.

### RF Generator and Matching Network

A rf power generator (RF-5S) and a matching network (AM-5) from RF Power Products Inc. are used to generate plasmas in the reactor. Power is coupled to the reactor inductively by a 1/4 in. copper coil which is wrapped eight turns around the glass cylinder.

The generator is a unique microprocessor based rf power supply designed to provide the user with a flexible

set of options for control. The supply provides a pure, stable power source from 0 to 500 Watts. With rf discharge on, forward and reflected power can be read from the vacuum fluorescent display on the generator. The matching network has a capacitor to handle the loading and a fixed coil and series capacitor to handle the tuning. A minimum flow of 5 G.P.H. of water is provided to the network to reduce the temperature of the series coil when the rf discharge is on.

#### Pressure Controllers

The reactor pressure is measured by an MKS Baratron vacuum gauge. The readings are in terms of absolute pressures and the gauge has a range of 0.0001-1 torr. The gauge is connected to an MKS PDR1C power supply and digital readout unit. The system pressure is automatically regulated by an MKS throttle valve (MKS 253A20401). The throttle valve is a butterfly valve and is placed on the pumping line after the reactor. Pressure is adjusted by varying the valve opening which in turn varies the pumping speed. The throttle valve is powered and controlled by an MKS type 152 exhaust valve controller linked to the pressure transducer.

#### Traps and Pumps

Pumping on the reactor can be performed by a pumping line which incorporates a throttle valve, a liquid nitrogen

trap, a shutoff valve, a micromaze trap (Kurt J. Lesker MMA-077-2QF), and a mechanical pump (Leybold LH-91245-1).

The mechanical pump is a dual-stage pump and has a pumping speed of 4 m<sup>3</sup>/h. It can reach a vacuum of 10<sup>-4</sup> torr when operating at perfect conditions. The pump is designed to provide vibration-free operation and is equipped with an anti-suckback valve to prevent oil from being sucked back into the vacuum chamber should the motor be stopped inadvertently. The pump is operated with HE-200 pump oil.

A liquid nitrogen trap purchased from Chem Glass is placed between the pump and the chamber to prevent oil backstreaming into the chamber and to condense polymerized residues. The trapping action of the micromaze trap results from its high-surface absorbent. It will provide for excellent elimination of hydrocarbons and/or water vapor backstreaming into the vacuum system.

### Materials

E-glass fiber strands and fabric cloth are used as the substrates and coated in the experiments. E-glass continuous roving fiber strands of type 102A-AA-56 were purchased from Owens Corning. The fiber strands are wrapped around a 7 in. long polycarbonate holder and placed under the electrode coil which is wrapped outside of the glass chamber. Type D155 unidirectional E-glass cloth was obtained from Knytex.

It is in the form of strands containing several hundred fibers each, stitched together with organic yarns. The fabric cloth is cut to about 7.5 X 8.0 in. (length X width) pieces and placed on the same holder in the same place of the reactor.

Both of the fiber strands and fabric cloth have manufacturer silane coupling agents (shown in Table 2) on them and need to be cleaned off before plasma coating.

### Experimental Procedure

#### Sample Preparation

Two methods are used to clean the fiber strands and fabric cloth and to remove the silane coupling agents. One is to put the fiber strand in the base bath containing KOH, ethanol and water for about 9 hrs, then clean it with distilled water and put it in an acid solution containing concentrated sulfuric acid with Nochromix for another 9 hrs. The sample is then cleaned once more with distilled water and air-dried. This method can only be used to clean fiber strands, however, because the organic yarn in the fabric cloth will be dissolved in the base bath and acid solution.

The other method is to use oxygen etch to remove the sizing. It is suitable for cleaning both the fiber strands and the cloth and takes less than one hour, much faster than

the solution cleaning. After the oxygen etch, the system is purged with Argon gas for about 20 minutes to remove the oxygen free radicals before introducing monomer gases. One drawback of this method is that the cloth will shrink in width from 8 in. to about 7.5 in. after etching. This makes it more difficult to coat the cloth since the fiber strands become tighter and plasma radicals are hard to get into the middle of the strands.

#### Plasma Polymerization

Before each experiment, reactor walls and flanges are wiped clean with methanol-dampened tissue to remove deposited polymers.

After placing the sample without the manufacturer sizing in the reactor, initial pumpdown is done through the pumping line for about 20 minutes. When a vacuum better than 20 mtorr is reached, a monomer gas (either ethylene or methane) is introduced into the reactor chamber and kept at a constant flow rate which can be between the ranges of 5 sccm and 10 sccm. The pressure in the system depends on the monomer used and the flow rate, usually around 200 mtorr. When the set pressure in the chamber becomes stable, the rf discharge is on and plasmas are generated. In the experiments, the rf powers vary from 20 W to 200 W, and reaction times vary from 5 minutes to 60 minutes.

Plasma treated surfaces have a substantial amount of living free radicals which may react with air oxygen or other molecules to alter the surface properties. Therefore, the post treatment is to leave the fibers in a partial vacuum with monomer gases for about 20 minutes. Then the monomer gases are stopped and the system is pumped down to a pressure of about 5 mtorr which takes 5 to 10 minutes. The chamber is then filled with air to atmospheric pressure, and the sample is taken out.

#### Analytical Methods

In this study, changes in the surface properties of the fibers are characterized by XPS and SEM. Consistency in sampling is maintained by taking the samples from similar locations on fiber strands or fabric cloth placed at similar positions of the holder.

#### X-Ray Photoelectron Spectroscopy

XPS analysis is conducted with a PHI 5600ci small-spot XPS system in the Imaging and Chemical Analysis Laboratory (ICAL) at Montana State University. A monochromatic aluminum 2 mm source operated at 300 W or 350 W is used as the x-ray source. An aperture setting of 4 corresponding to an 800  $\mu\text{m}$  spot size of analysis is used.

Charge compensation is achieved using an electron flood gun since glass fibers are nonconductive samples. Pressure in the introduction chamber and analysis chamber is maintained at about  $10^{-7}$  torr and  $10^{-9}$  torr, respectively. The system has a typical spatial resolution of 200  $\mu\text{m}$  and 30  $\mu\text{m}$  at best. The survey spectra of all the samples are usually taken at 93.9 eV pass energy, and the elemental binding energy curves are taken at pass energy of 58.7 eV to get better resolutions.

#### Scanning Electron Microscopy

The SEM analysis is carried out with a JEOL electron microscopy with a JSM-6100 scanning attachment in the ICAL laboratory at Montana State University. The samples for SEM analysis are mounted on sample holders with both-sided conductive tapes. The samples are first sputter-coated with gold/palladium to eliminate the surface charging problems of insulating materials. The electron gun source is  $\text{LaB}_6$  and the current is 3.0 A. Images are taken at 8 KeV primary beam energies and at 750X - 15,000X magnifications. Pictures are taken using Polaroid 665 instant films. The system has a lateral resolution of 40  $\text{\AA}$ . The pressure in the analysis chamber will reach  $10^{-7}$  torr after pumping the system for 10 to 20 minutes and is maintained at this pressure during analysis.

## CHAPTER 4

## RESULTS AND DISCUSSION

In this study, a radio frequency plasma reactor has been constructed for the experiments. E-glass fiber strands and fabric cloth are first etched by oxygen plasma or cleaned by base/acid solutions to remove the silane coupling agents. Then a low temperature rf discharge is used to coat the fiber strands or fabric using ethylene or methane monomers. XPS and SEM are used routinely during the study to estimate the changes on the surface of the fibers. The static strength and the fatigue resistance of fiber stands and fabric cloth of interest are tested by Jinhua Bian at Montana State University.

Analytical Results

In this research, the XPS is used to determine which elements are on the fiber surface (except hydrogen) and to estimate the surface concentration of each element. A quantitative comparison of fiber surface composition is made by measuring the peak area above background, correcting for

elemental sensitivities and normalizing. The SEM is used to examine the texture and imaging of the fiber surface.

### Solution Cleaning of Fiber Strands

As mentioned before, base bath and acid solution can be used to remove the silane coupling agents on the fiber strands. The cleaning time varies from 4 hrs to 36 hrs and the cleaned fibers are analyzed by XPS and SEM.

XPS Analysis The XPS analysis of as-received strands and different effects of base/acid cleaning are shown in Table 3. Atomic concentrations are calculated from the peak areas adjusted for differences in individual element cross-sections and normalized to 100 percent of C, O and Si. The spectrum is displayed as a plot of the number of electrons versus electron binding energy in a fixed energy interval.

From the table we can see that the best cleaning results are obtained by putting fiber strands in base bath and acid solutions for 9 hrs, respectively. Therefore, fiber strands were cleaned under this condition before plasma coating. After cleaning in this manner, the C content which is from the silane coupling agent and air contamination reduces from 76% to about 20%, and the results are reproducible. Oxygen and silicon contents increase significantly after cleaning, which is what we expect, since

they are the major components of glass fibers. The ratio of O to Si is a little higher than 2 : 1 which is the ratio of SiO<sub>2</sub>. This is because glass fibers also have other oxide components, such as CaO, Al<sub>2</sub>O<sub>3</sub>, MgO and B<sub>2</sub>O<sub>3</sub>, etc.

The survey spectra from XPS analysis before and after fiber strands cleaned by base/acid for 9 hrs, respectively, are shown in Figures 11 and 12. We can see the Ca and Al peaks after cleaning which are from glass fiber itself, but other glass fiber contents, like Na, Mg, B are still not detectable. This is because of their small concentrations in glass fibers and less sensitivity in the XPS.

Table 3. Elemental Surface Concentration (%) Obtained by XPS Analysis of Uncleaned and Base/Acid Cleaned Strands

	C1s	O1s	Si2p
fiber strands as received	76.50	20.49	3.00
	78.54	19.96	1.50
fiber strands cleaned by base/acid for about 4 hrs, respectively	22.11	54.93	22.96
fiber strands cleaned by base/acid for about 7 hrs, respectively	26.70	51.97	21.33
fiber strands cleaned by base/acid for about 9 hrs, respectively	14.67	60.41	24.92
	17.06	58.85	24.09
	26.83	51.48	21.70
	25.05	52.44	22.51
	28.55	49.15	22.31
	26.21	51.93	21.87
fiber strands cleaned by base/acid for about 13 hrs, respectively	22.55	54.19	23.26
fiber strands cleaned by base/acid for about 24 hrs, respectively	26.82	50.71	22.47
	41.72	41.53	16.75
fiber strands cleaned by base/acid for about 36 hrs, respectively	36.27	44.48	19.25
	35.84	45.48	18.68

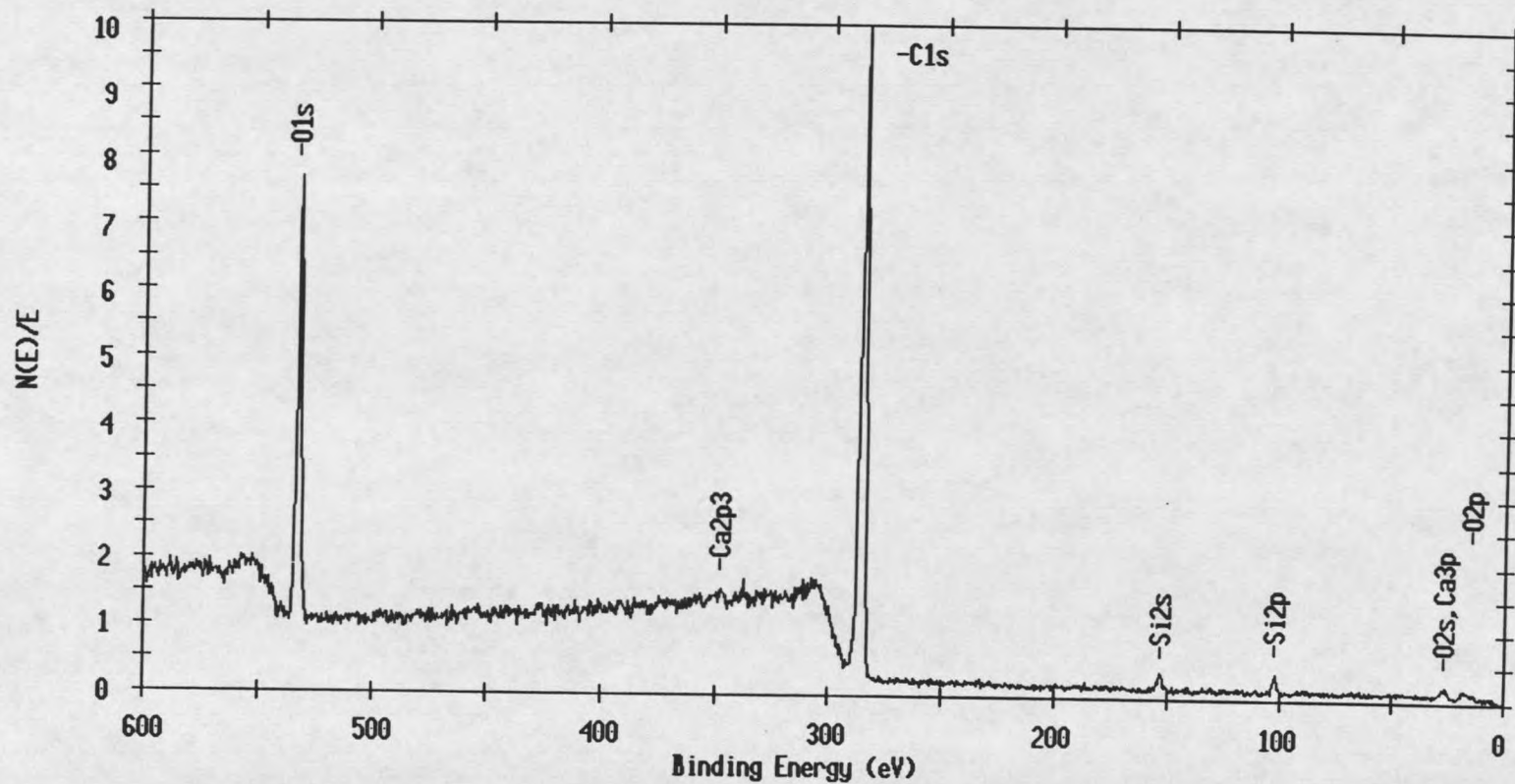


Figure 11. XPS survey spectra of uncleaned fiber strands

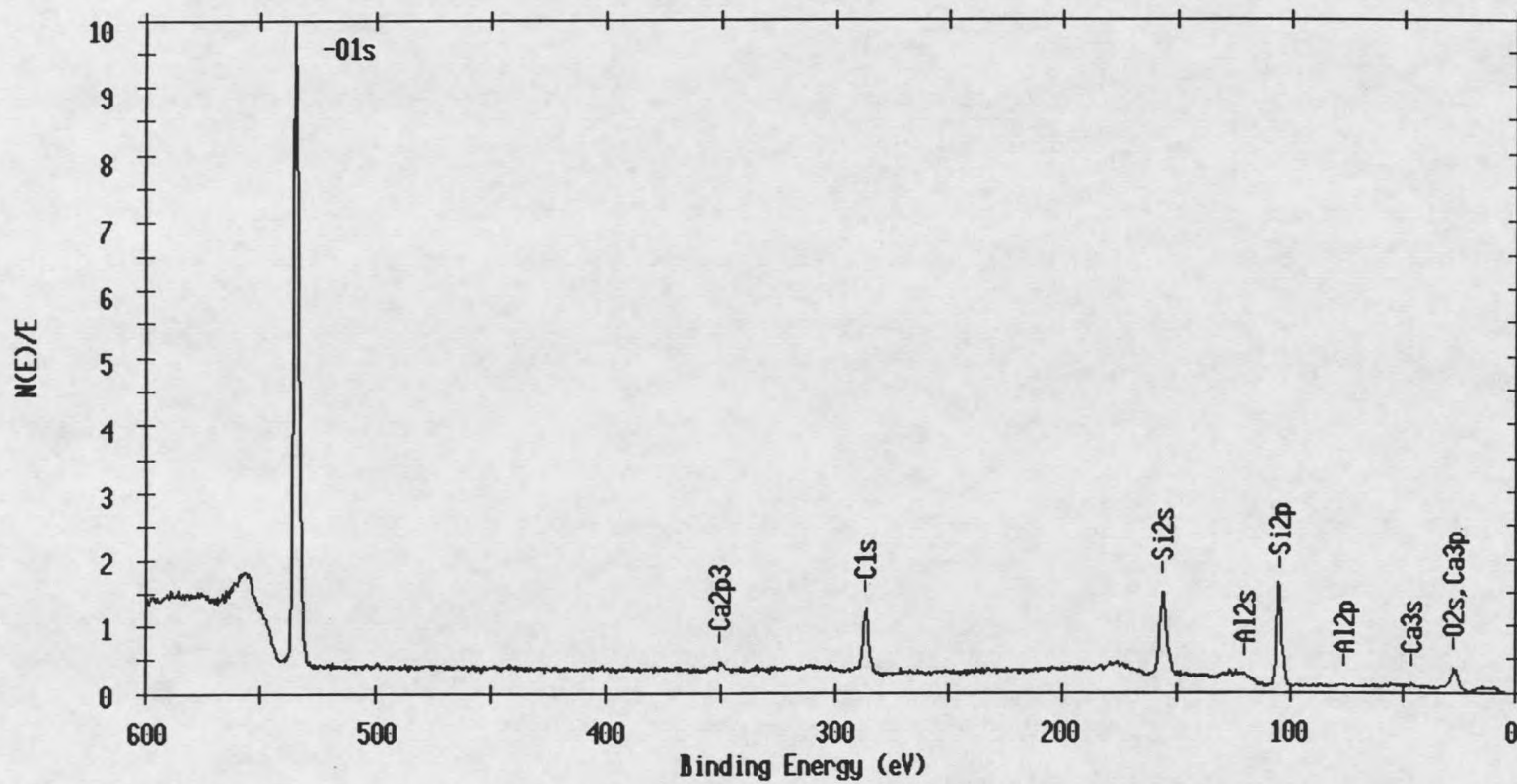


Figure 12. XPS survey spectra of fiber strands cleaned by base/acid solutions for 9 hrs, respectively

SEM Analysis Electron microscopy clearly reveals the changes on the fiber surfaces after they are cleaned by the base/acid solutions. Typical SEM data are shown in Fig. 13.

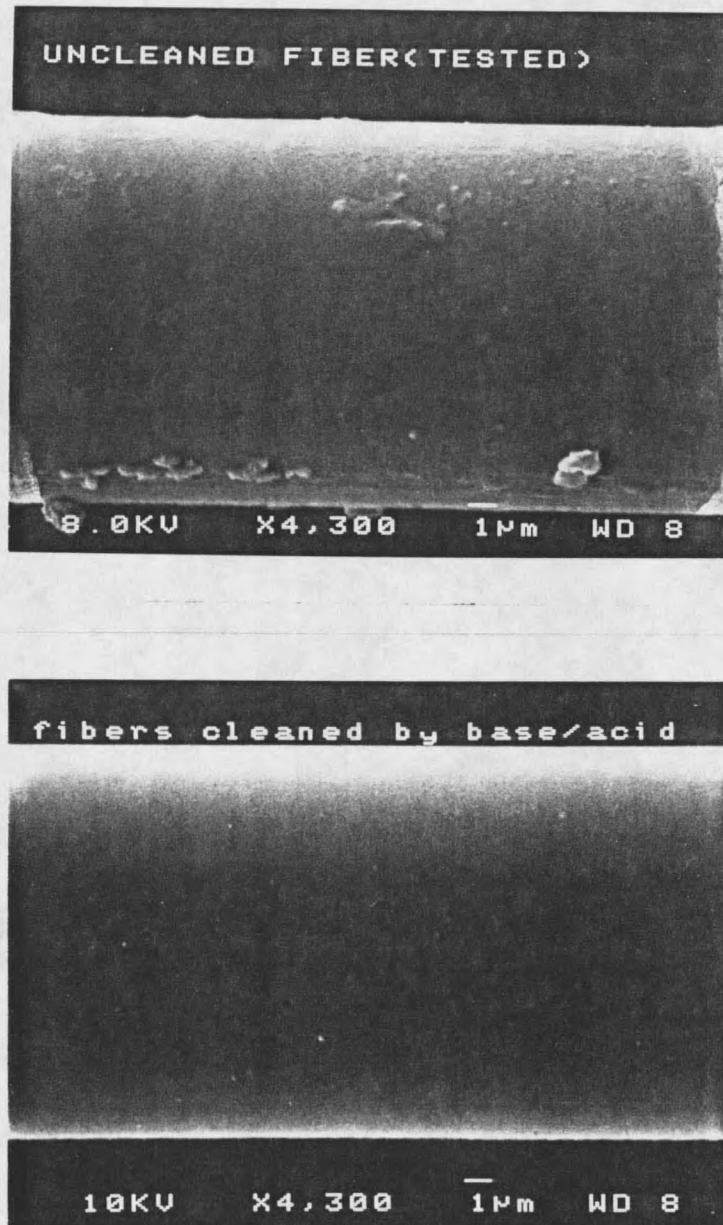


Figure 13. SEM micrographs of glass fibers as received (top), and as cleaned by base/acid solutions for 9 hrs, respectively (bottom)

From the SEM micrograph we can measure the diameter of a single fiber in the fiber strands to be about 13  $\mu\text{m}$ . Examination at high magnification (4,300X) shows the individual fibers in the as-received fiber strand to be quite variable in surface texture. Some surface areas are relatively smooth while others are largely covered by numerous randomly oriented particle-like structures as seen in Figure 13 (top). This is not unexpected since fiber strands used in the experiments are supplied with a matrix compatible sizing. The particles could also be dust from the air.

Fiber strands cleaned by base/acid show much smoother surfaces than as-received fibers. As shown in Figure 13 (bottom), the single fiber has an essentially clean surface, with some tiny irregularities on it which could be the contaminants from air or left-over impurities. The contamination could also come from the base/acid solutions since they have been reused many times to clean all kinds of samples.

#### Oxygen Etch of Fiber Strands

In this project, the manufacturer sizing on the fiber strands can also be etched in an oxygen or Argon plasma. Since Argon plasma has less etching ability than oxygen plasma under the same reaction conditions, oxygen plasma is

chosen to clean the fiber surfaces. Bulk properties of fiber strands are unchanged because the attack by atomic oxygen is limited to the surface of the strands. Possibly the plasma does not completely remove the sizing deep in the tow of fibers, but when these tows are wound on the holder they are flattened to allow more penetration of the plasma.

XPS analysis The XPS measurements of sized fibers and oxygen plasma etched fibers show that the plasma greatly changed the surface compositions of the fibers. The results of fiber strands etched at different conditions are shown in Table 4. Usually two or three samples are taken from different strands at different positions of sample holder, and the range of compositions are obtained by choosing the lowest and highest results from the XPS measurements of three different spots for each sample.

In these experiments, the input power is the primary variable examined for the plasma etching process. The oxygen plasma appeared a light blue to the eye. The C content after etching usually becomes lower at higher input power when all the other reaction parameters remain the same, which shows that we can get better etching results at higher power in a certain range of discharge power. But when the input power reaches a certain level, further increase of the power will not increase the etching rate any more. As shown in Table 4, when the input power is increased to 100 w or 120 w at 5

sccm and 0.24 torr for 30 min., the C content after etching seems to remain the same as that in 80 w. Therefore, 80 w input power is chosen to etch fibers before plasma coating since the temperature in the reactor will become higher at higher power. The etch of fiber strands is not really uniform although the majority of fibers are etched. This is because the strand has 200-300 fibers in it and the plasma could not penetrate evenly deep in the tow of fibers.

Table 4. Elemental Surface Concentration (%) Obtained by XPS Analysis of Oxygen Plasma Etched Fiber Strands

oxygen	C1s	O1s	Si2p	Ca2p	Al2p
3sccm, 0.18torr, 30min., 20w	21.2-	48.1-	20.1-	1.6-	1.8-
	28.5	53.9	21.2	2.0	2.7
50w	23.1-	52.1-	17.9-	1.7-	2.25-
	24.8	52.9	20.9	2.1	2.31
80w	21.4-	54.6-	18.4-	1.4-	2.3-
	21.6	55.6	20.1	2.1	2.4
5sccm, 0.22torr, 30min., 20w	17.3-	44.4-	17.8-	1.4-	1.7-
	34.2	59.6	18.6	2.2	2.5
50w	20.2-	50.6-	18.8-	1.7-	2.1-
	24.7	54.7	20.7	1.9	2.6
80w	11.7-	45.5-	20.0-	1.4-	1.6-
	31.0	62.0	21.5	2.0	2.9
5sccm, 0.24torr, 30min., 20w	18.5-	53.1-	18.4-	1.7-	2.7-
	24.1	57.0	19.9	2.0	2.8
50w	15.6-	57.1-	19.6-	2.1-	2.6-
	17.8	58.1	21.1	2.4	2.9
80w	17.1-	54.3-	19.3-	1.6-	2.0-
	22.1	58.6	20.5	1.9	2.3
100w	13.1-	53.5-	19.2-	1.9-	2.2-
	22.6	62.3	20.5	2.0	2.7
120w	14.7-	51.3-	18.7-	1.7-	2.4-
	25.7	60.0	21.6	2.0	2.7
100w	13.5-	58.2-	20.7-	2.15-	2.5-
	15.8	60.6	20.8	2.16	2.6
120w	10.5-	44.2-	21.1-	1.1-	1.6-
	31.9	62.4	22.7	1.8	2.7
120w	13.2-	56.3-	21.7-	1.6-	2.2-
	18.2	60.3	21.9	1.8	2.4

The XPS survey spectra of fiber strands etched at 5 sccm, 0.24 torr and 80 w for 30 min. is shown in Figure 14. The Ca and Al peaks are much clearer and higher than those in the spectra of base/acid cleaned fiber strands. Sometimes the Na peak can also be seen in the spectra of etched fiber strands and its atomic concentration is about 0.5%.

The XPS C1s and O1s binding energy curves for oxygen plasma etched fiber strands are shown in Figures 15 and 16. The binding energy of the symmetrical O1s peak is identical to the binding energy of the O1s in SiO<sub>2</sub> (533 eV). In the C1s binding energy curve, there is some hint of a peak shifted to higher binding energy except the normal C1s peak in the form of hydrocarbon functional group. The higher binding energy peak can be the functional group of C bonded to O. Since strong oxidizing agents such as ozone, atomic oxygen and singlet molecular oxygen are known to be present in oxygen plasma system and these free radicals may react with molecules in the air [52], it is not surprising that surface oxidation occurs.

SEM Analysis The SEM micrographs of fiber strands etched by oxygen plasma at 5 sccm, 0.24 torr and 80 w for 30 min. are shown in Figure 17. Generally speaking, the oxygen etched fiber surfaces are not as clean and smooth as those washed by base and acid solutions. Surface roughening occurs due to oxygen plasma etching.

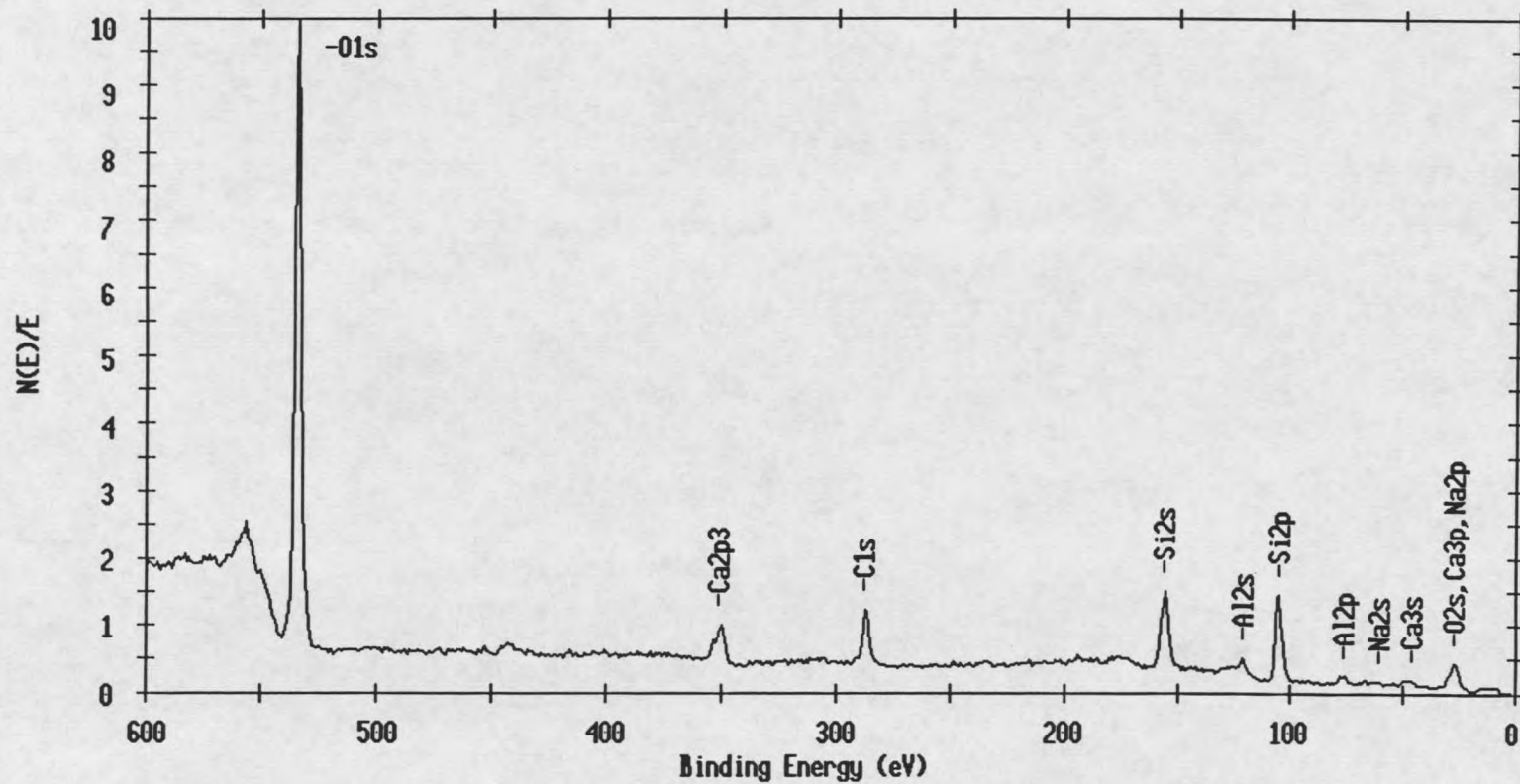


Figure 14. XPS survey spectra of oxygen plasma etched fiber strands at 5 sccm, 0.24 torr and 80 w for 30 min.

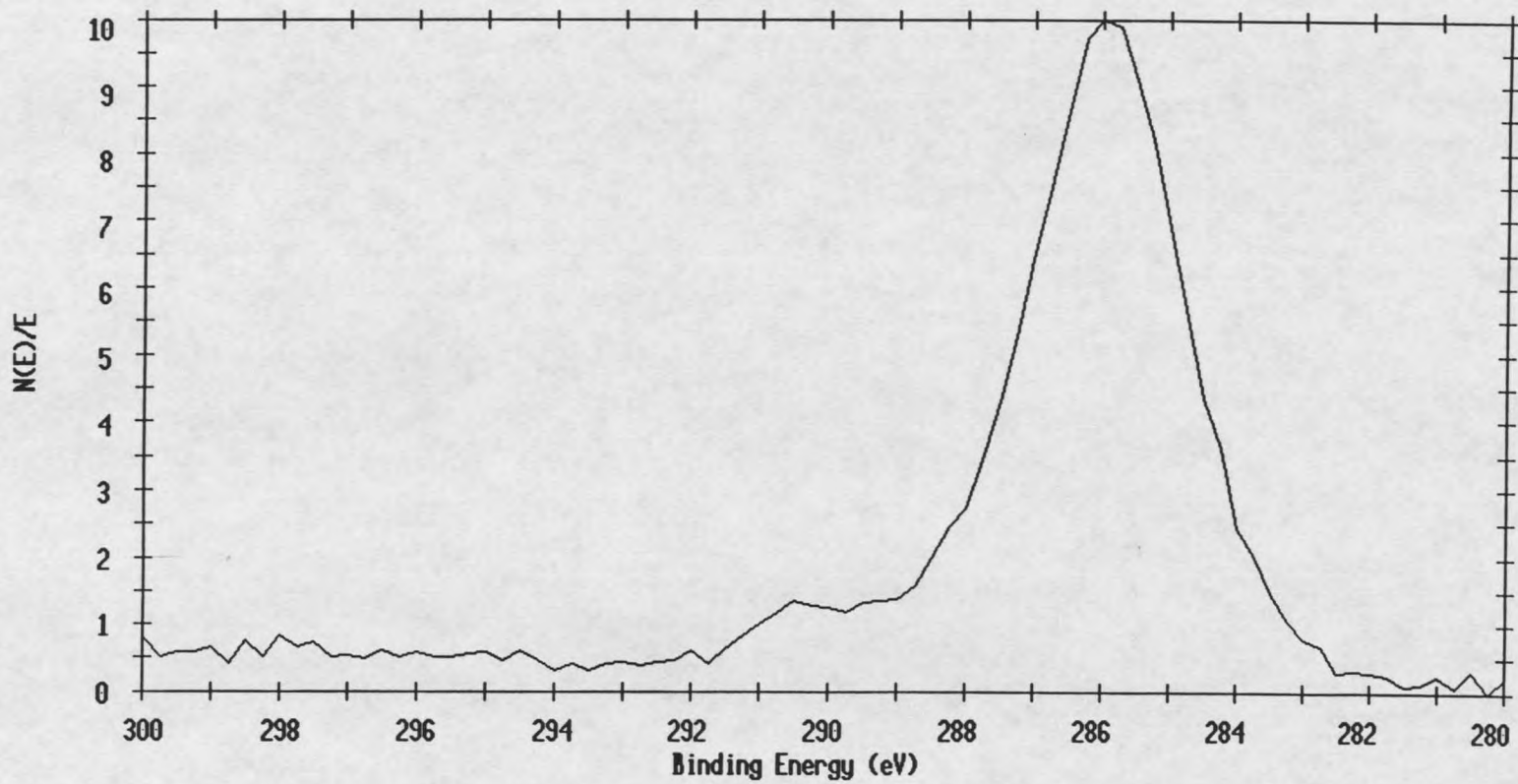


Figure 15. XPS C1s binding energy curve for oxygen plasma etched fiber strands

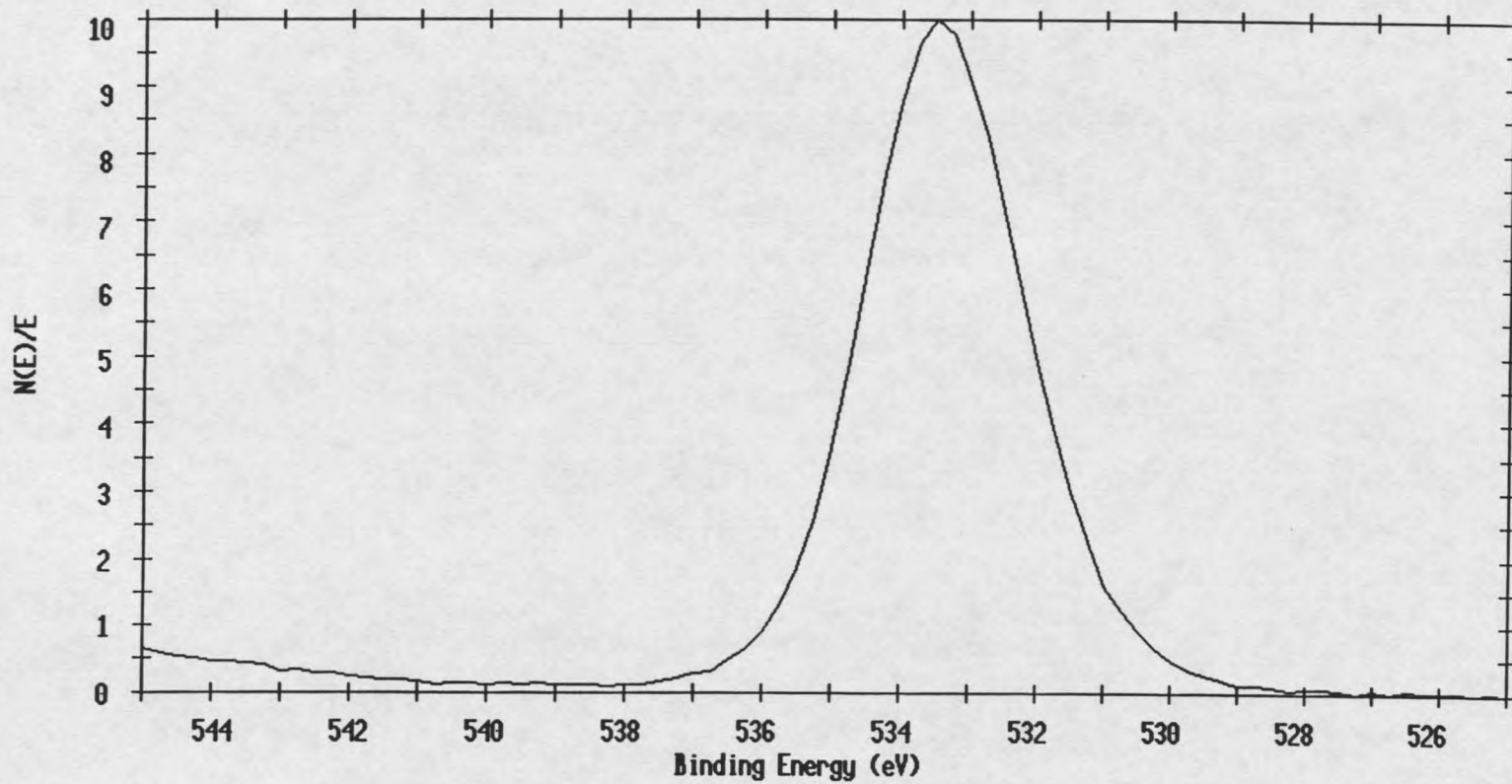


Figure 16. XPS O1s binding energy curve for oxygen plasma etched fiber strands

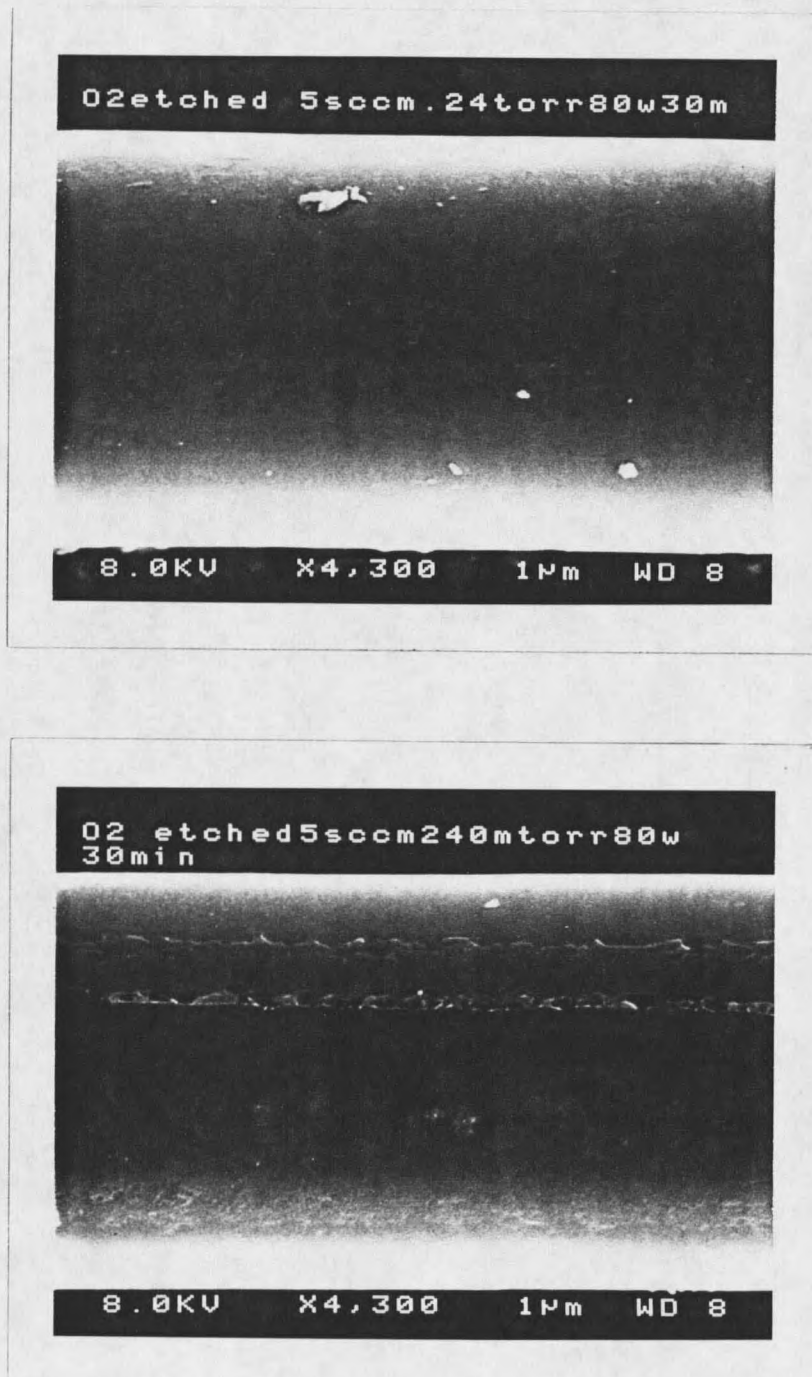


Figure 17. SEM micrographs of the different spots of oxygen plasma etched fiber strands at 5 sccm, 0.24 torr and 80 w for 30 min.

The SEM images in Figure 17 clearly reveals the existence of surface modifications arising from oxygen plasma etching. Most areas of oxygen etched fiber surfaces are essentially smooth, with some particles on them, as what is shown in Figure 17 (top). But some areas of treated fiber surfaces are very rough, as shown in the bottom image of Figure 17, having long irregular strips. These can be the silane coupling agents which are not etched by oxygen plasma or due to the surface oxidation of glass fibers.

#### Fiber Strands Coated by Ethylene Monomer

After fiber strands cleaned by base/acid solutions or etched by oxygen plasma to remove silane coupling agents, they are coated by plasma polymerization of ethylene monomer. Slight yellowing of fibers is observed after the coating.

In the plasma polymerization, the chemical structure of ethylene monomer is sufficiently altered that no repeat unit will be recognizable in the structure of the product. This is illustrated by the structure of an ethylene plasma polymer film formed in a capacitively coupled rf reactor, shown in Figure 18, as deduced from infrared and NMR data [53]. The broken bonds shown in this structure are crosslink points and connect to other portions of the film. It was found that the degree of crosslinking in rigid films of

plasma polymerized ethylene is in the range of 6 to 16 chain carbons between crosslink [54]. Although no repeat unit is obvious in Figure 18, the plasma polymer is a hydrocarbon as is the monomer. There has been no wholesale elimination of hydrogen in the transition of monomer to plasma polymer.

XPS Analysis The XPS analysis of fiber strands coated by ethylene plasma shows no differences in whether they are cleaned by base/acid solutions or oxygen plasma, and the results of coated fibers are shown in Table 5. The discharge power and reaction time are the two main parameters examined in these experiments, although ethylene flow rate and system pressure are also variables in the processes.

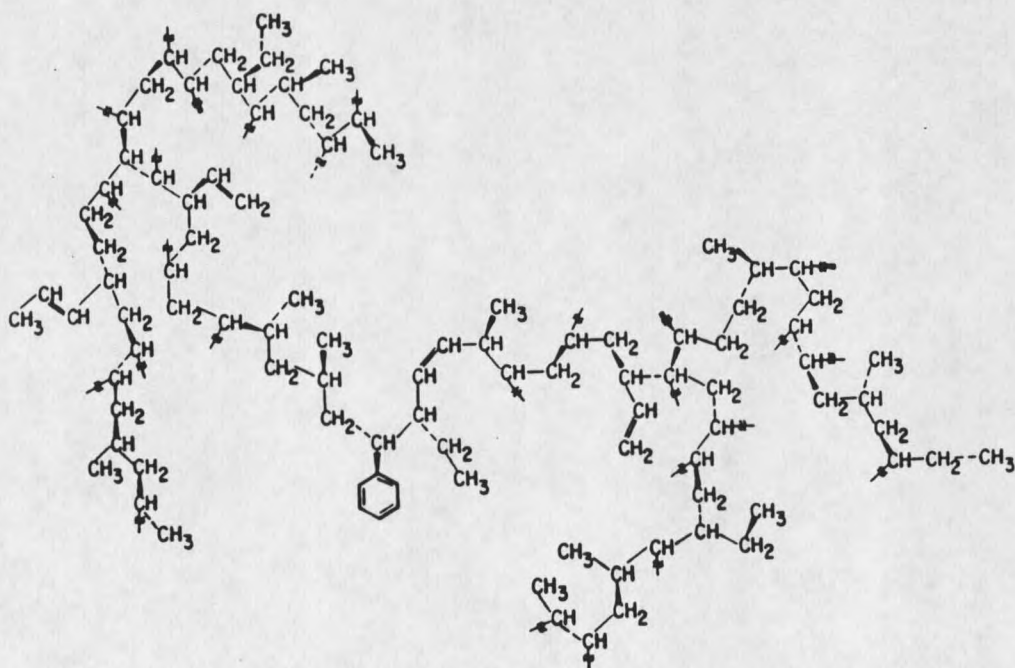


Figure 18. Structure deduced on the basis of crosslink density calculations and functional group concentrations for an ethylene plasma polymer

Table 5. Elemental Surface Concentration (%) Obtained by XPS Analysis of Ethylene Plasma Coated Fiber Strands

ethylene	C1s	O1s	Si2p
5sccm, 0.08torr, 15min, 20w	88.99-92.76	5.99-8.68	1.25-2.33
40w	74.66-82.30	12.38-18.12	5.32-7.21
60w	79.46-92.52	5.42-16.47	1.85-4.07
80w	75.70-90.78	6.94-17.21	2.28-7.09
5sccm, 0.17torr, 15min, 20w	84.93-91.68	7.09-10.84	1.23-4.24
40w	96.17-97.47	2.39-3.24	0.14-0.59
60w	85.34-95.24 93.88-97.02	3.82-10.31 2.96-5.74	0.68-4.35 0.35-0.38
5sccm, 0.18torr, 15min, 20w	88.08-90.51	7.44-10.51	0.72-2.32
40w	90.98-91.14	7.41-7.71	1.31-1.45
60w	91.85-95.42	4.06-6.46	0.51-1.69
120w	91.12-96.91	2.84-7.38	0.24-1.49
5sccm, 0.18torr, 5min, 20w	88.58-92.35	5.97-8.97	1.86-2.46
60w	90.67-93.04	5.45-6.64	1.51-2.69
10sccm, .27torr, 15min, 60w	88.13-95.06	4.78-10.03	0.16-1.84
200w	86.63-95.98	3.67-10.84	0.21-2.53
5sccm, 0.17torr, 60w, 10min	80.50-90.32	7.08-14.21	2.60-5.29
15min	85.34-95.24 93.88-97.02	3.82-10.31 2.96-5.74	0.68-4.35 0.35-0.38
20min	71.39-95.87	5.59-19.92	0.69-8.69

In the surface modification of glass fibers, the primary goal is to coat a uniform carbon film on the surface of glass fibers, which is, in XPS analysis, to get the highest C content and the lowest all the other contents. From Table 5 we can see that the surface concentration of C for ethylene plasma coated fiber strands can reach as high as 97% (except hydrogen), and the Si content can be reduced to nearly zero under some conditions. But the ratio of O/Si is much higher than 2 ( $\text{SiO}_2$ ), which shows the surface

oxidation of fiber strands after plasma exposure. Oxygen may have been in the plasma due to vacuum leaks or desorption from the reactor walls. Oxygen also readily combines with free radicals upon exposure to air, so some oxidation would be expected.

Ethylene plasma appears a purple light to the eye at a high discharge power, and the color becomes lighter when a lower discharge power is used. From the XPS analysis results, it can be seen that the surface composition of ethylene plasma treated strands is greatly changed. However, the composition basically remains the same after the discharge power is greater than 60 w when all the other parameters remain constant. It shows that the plasma deposition reaches equilibrium under these conditions. Examination of reaction time effects on plasma deposition also shows that the surface contents remain the same when deposition time is longer than 15 min. with all the other parameters remaining constant.

The XPS is also used to examine the degradation and stability of base/acid solution cleaned and then ethylene plasma treated fiber strands. The coatings are tightly bound and highly crosslinked. As shown in Table 6, they can not be washed off with acetone which is a part of the matrix to make composites, and the surface composition of treated fiber strands does not change after putting fibers in the air for one week. However, the plasma polymer coatings can

be washed off with methanol, since methanol is used to clean reactor walls after every experiment.

The uniformity of ethylene plasma polymerized films on strands is examined using XPS analysis and the results are shown in Table 7. The fiber strands were first cleaned by base/acid solutions. The two samples were taken from the treated strands at different positions of the sample holder under the same reaction conditions (5 sccm, 0.17 torr, 60 w and 15 min.). The surface concentrations were obtained at three different spots (at one edge, in the middle, at the other edge) for each sample. The results shows that the plasma can penetrate into the fiber strands and the coating is uniform for ethylene plasma treated fibers.

Table 6. The XPS Analysis Results to Examine the Degradation and Stability of Ethylene Plasma Treated Strands

ethylene	Cl <sub>s</sub>	O <sub>1s</sub>	Si <sub>2p</sub>
5sccm, 0.17torr, 60w, 10min.	90.05	7.34	2.60
after 1 week	89.63	7.98	2.39
5sccm, 0.17torr, 60w, 10min.	82.73-90.99	6.89-11.77	2.13-5.50
after putting fibers in acetone for 2 min.	78.75-91.39	6.77-15.27	1.84-5.98

Table 7. The XPS Analysis Results to Examine the Uniformity of Ethylene Plasma Coatings on Fiber Strands

ethylene, 5sccm, 0.17torr, 60w, 15min.	Cl <sub>s</sub>	O <sub>1s</sub>	Si <sub>2p</sub>
sample 1: at one edge	96.54	3.46	ND
in the middle	97.02	2.98	ND
at the other edge	95.38	4.62	ND
sample 2: at one edge	93.88	5.74	0.38
in the middle	96.91	3.09	ND
at the other edge	96.69	2.96	0.35

The XPS survey spectra of ethylene plasma coated strands and the Cls binding energy curve are shown in Figures 19 and 20, respectively. No other glass fiber components, such as Al, Ca, Mg and Na, are observed in the survey spectra except O and Si. The Cls binding energy curve shows a symmetrical peak at 285 eV corresponding to C-C and/or C-H bonds, with no evidence of significant degree of unsaturation.

SEM Analysis As mentioned before, the XPS analysis shows no difference between base/acid solution cleaned fiber strands and oxygen plasma etched strands, but they appear different in the SEM analysis. The SEM micrographs of fibers cleaned by base/acid solutions and then coated in ethylene plasma at 20 w and 60 w with constant flow rate, pressure and deposition time are shown in Figure 21, and SEM high magnification micrographs for 40 w power at different spots of fiber strands are shown in Figure 22. The SEM micrographs of fiber strands etched by oxygen plasma and then coated by ethylene monomers at 20 w and 60 w are shown in Figure 23.

The base/acid cleaned and then coated fibers have smooth surfaces with some particle-like structures on them, while the oxygen etched and then coated fibers have rough surfaces, and some areas have long irregular strips similar to those reported earlier in Figure 17 (bottom). The strips become less distinguishable and the surfaces are smoother at higher power as seen in Figure 23 (bottom).

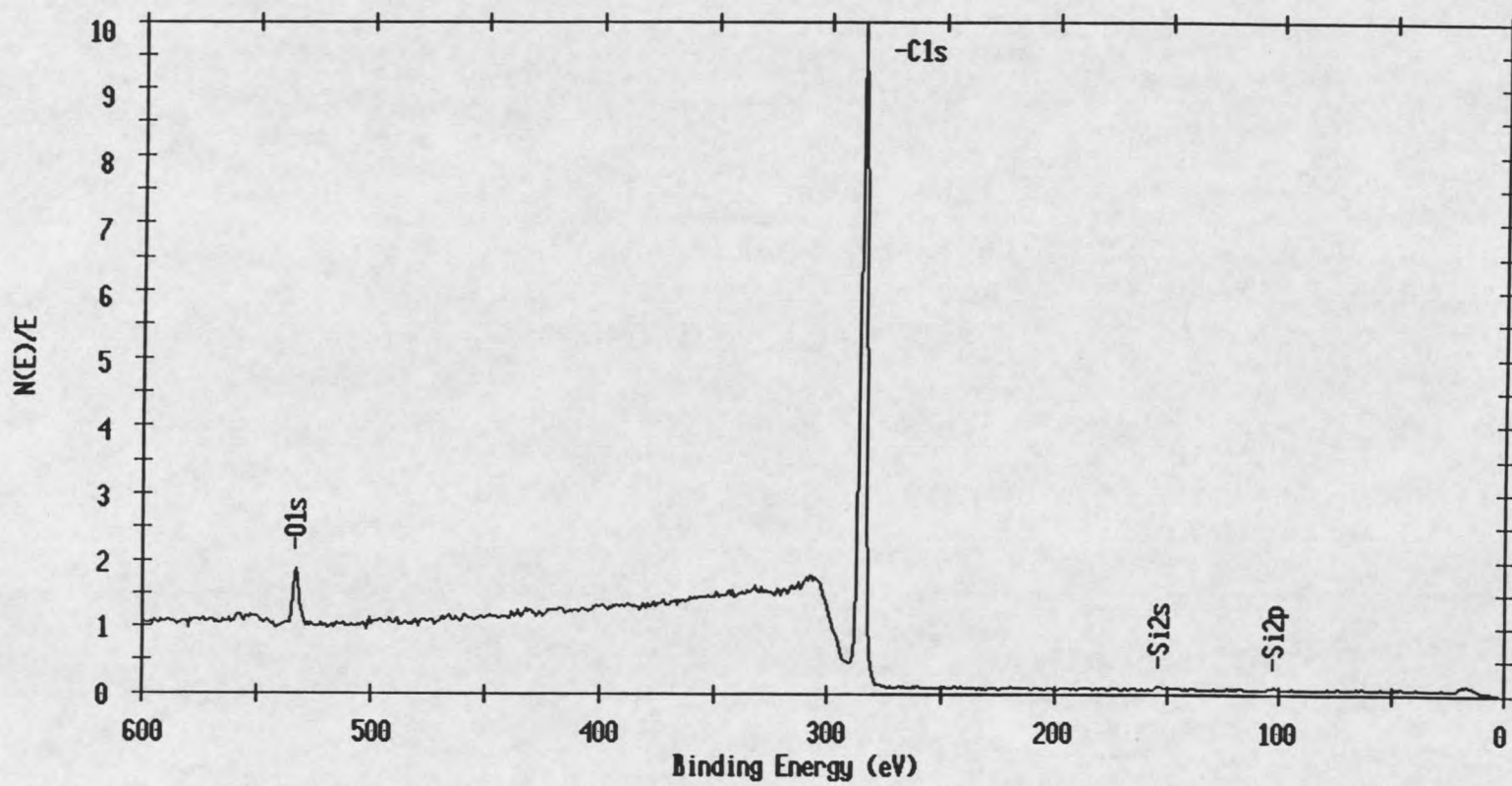


Figure 19. XPS survey spectra of fiber strands coated by ethylene monomer at 5 sccm, 0.18 torr and 60 w for 15 min.

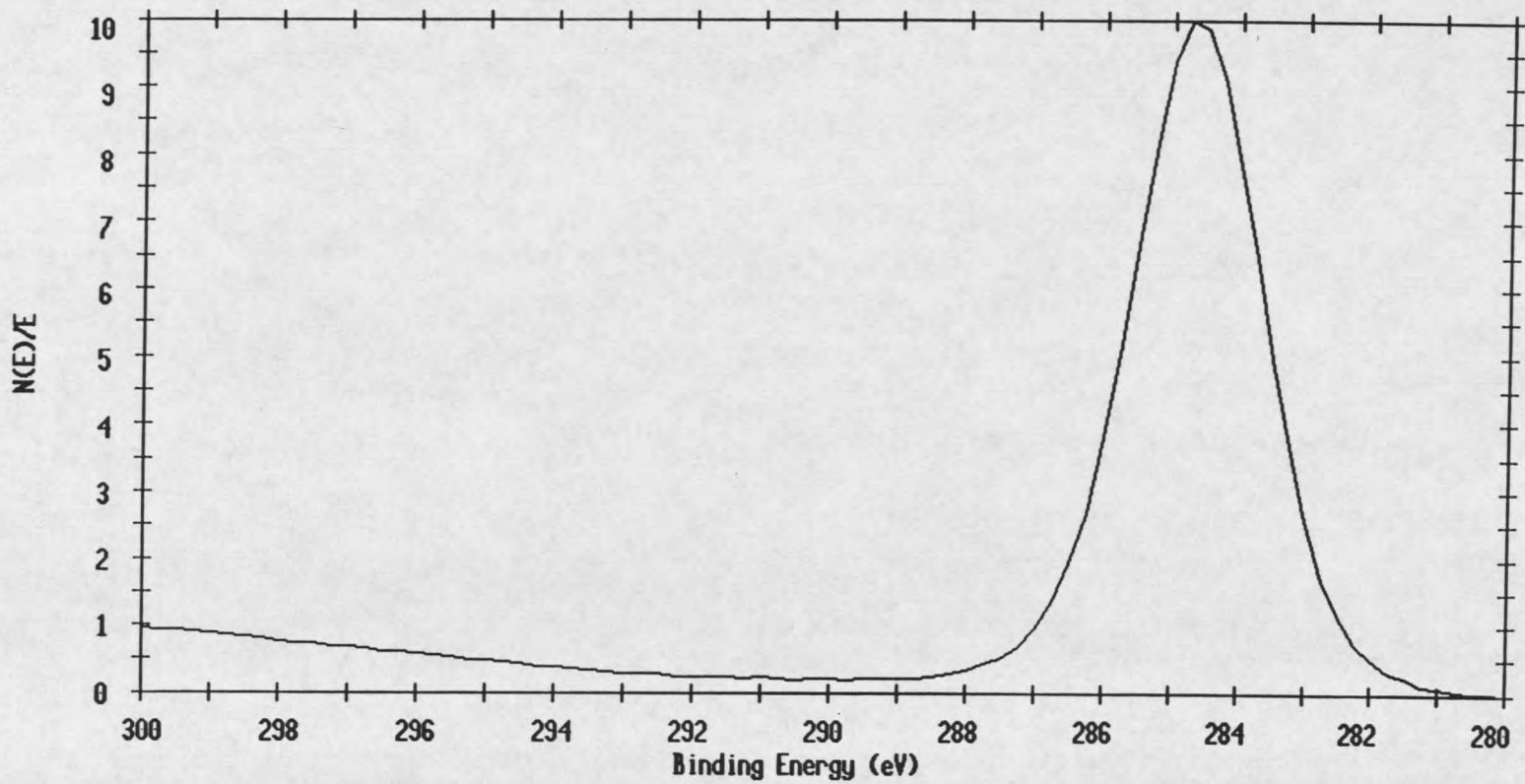


Figure 20. XPS Cls binding energy curve for fiber strands coated by ethylene monomer

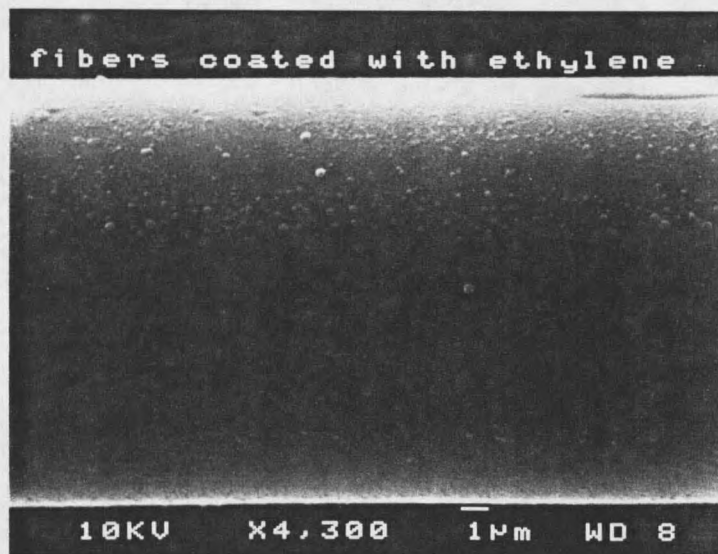


Figure 21. SEM micrographs of fiber strands cleaned by base/acid solutions and coated by ethylene monomer at 20 w (top) and 60 w (bottom)

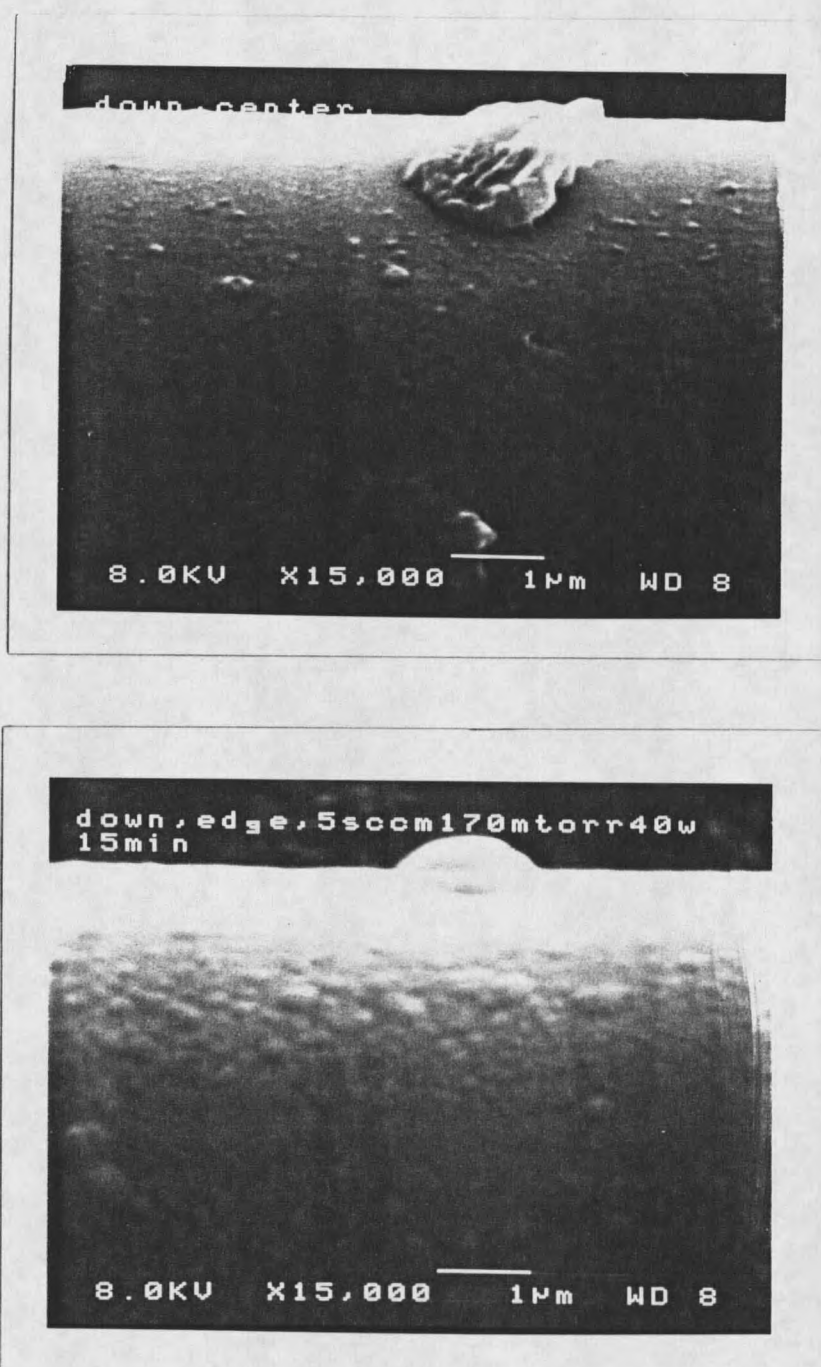


Figure 22. High magnification SEM micrographs of the different spots of fiber strands cleaned by base/acid solutions and coated by ethylene monomer at 40 w

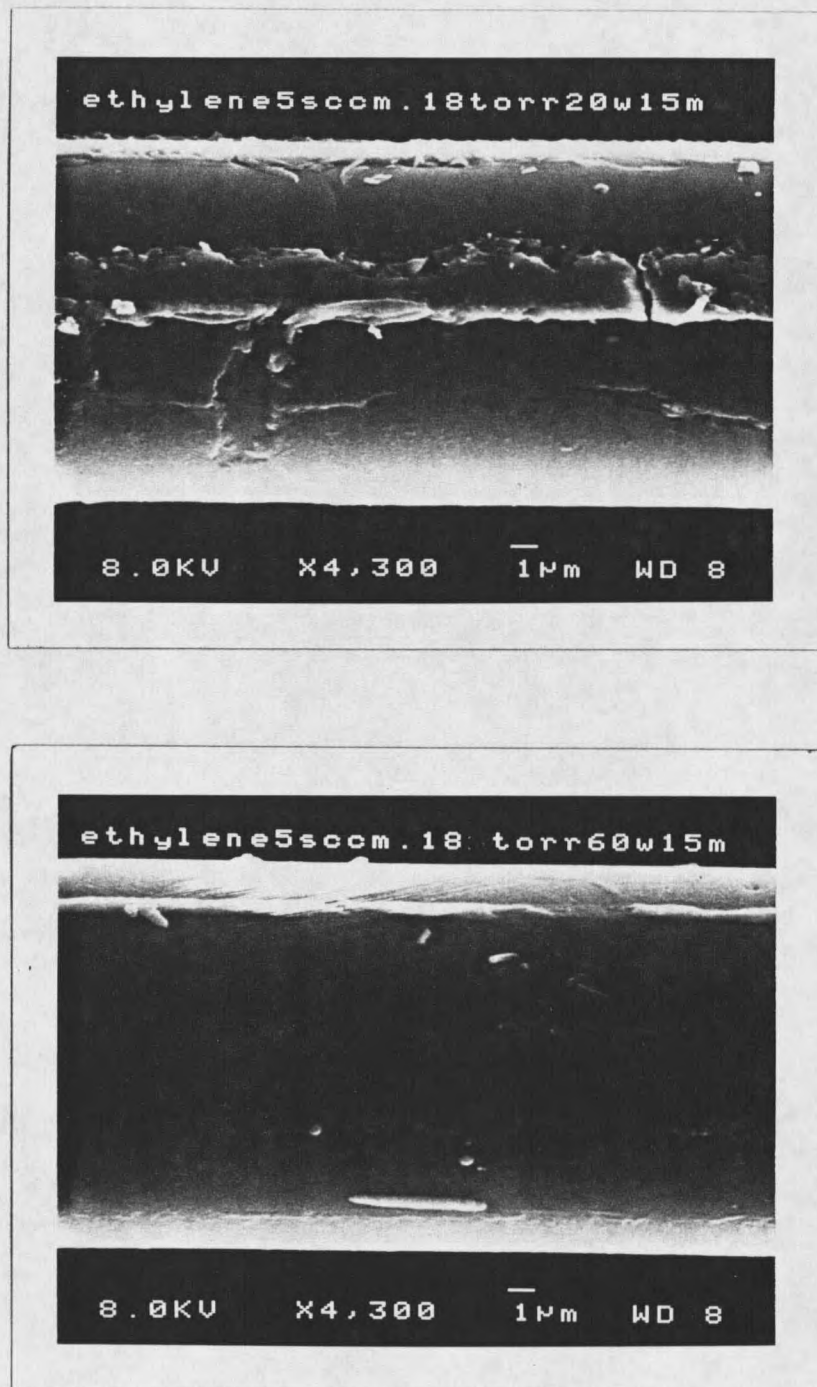


Figure 23. SEM micrographs of fiber strands etched by oxygen plasma and coated by ethylene monomer at 20 w (top) and 60 w (bottom)

Examination at high magnification (Figure 22) shows the film growth and surface changes after ethylene plasma treatment. In SEM analysis, when the coatings are thin and uniform, they can not be observed with the SEM except when the coatings have holes or bumps. In Figure 21 (top), the film peels from the substrate, and we have attributed this to hydrogen trapping in the film and at the film-substrate interface and building up a stress. Some areas of coatings have bumps on them, as seen in Figure 22 (bottom), and this is also because of  $H_2$  that is trapped in the film or absorbed in the fibers which diffuses to the film-substrate interface. The peeling condition is not a common feature, but it clearly shows the coatings on treated fibers.

#### Fiber Strands Coated by Methane monomer

XPS Analysis Methane is also used to generate the plasma and modify the surface of strands. The XPS analysis results for strands etched by oxygen plasma and then coated by methane monomer are shown in Table 8. Discharge power and deposition time are the two variables examined in these experiments with constant gas flow rate and system pressure. The color of methane plasma is also purple.

Unlike ethylene monomer, methane does not have an active double bond or functional group. Therefore, methane monomer is less polymerized and has a lower deposition rate

than ethylene under the same conditions. The XPS analysis results of methane and ethylene polymerized films on fiber strands are in agreement with this theory. Under the same reaction condition, methane plasma polymerized film has much lower C content and higher O and Si contents than ethylene polymerized film. Also, N content can be observed in the surface composition of methane plasma coated fibers (Table 8), while it can not be seen in ethylene plasma coated fibers. This is probably because that methane has nitrogen impurity in it since the same experimental procedures are used for both the methane and ethylene monomers.

In general, the amount of plasma radicals attached to the substrate increases with the discharge power and deposition time until reaching saturation. As seen in Table

Table 8. Elemental Surface Concentration (%) Obtained by XPS Analysis of Methane Plasma Coated Fiber Strands

methane	C1s	O1s	Si2p	N1s
5sccm, 0.22torr, 15min., 60w	72.62- 79.19	13.10- 18.67	2.62- 3.91	4.73- 5.09
100w	66.26- 86.89	9.30- 24.19	2.13- 7.03	1.30- 1.95
120w	82.09- 83.82	12.27- 12.39	3.80- 4.35	0.00- 0.83
5sccm, 0.22torr, 20min., 100w	92.45- 98.66	1.34- 6.23	1.00- 1.32	ND
120w	74.65- 86.19	9.68- 17.49	3.34- 6.08	0.79- 1.42
5sccm, 0.22torr, 30min., 80w	89.88- 92.21	4.74- 6.66	0.63- 1.33	1.80- 2.25
100w	92.63- 98.78	1.22- 5.35	0.21- 1.58	ND
120w	81.77- 88.77	6.49- 11.70	0.92- 2.53	3.82- 4.25

8, the C concentration reaches 98% at 100 w and 20 min., and remains the same when the reaction time extends to 30 minutes. The C concentration even decreases to about 86% when the discharge power increases to 120 w, which is because the etching effect becomes dominant at higher power.

Figure 24 shows the XPS survey spectra of methane plasma coated strands at 5 sccm, 0.22 torr and 100 w for 20 min., and the C1s binding energy curve is shown in Figure 25. The symmetrical C1s peak at 285 eV corresponds to C-C and/or C-H bonds, same as the C1s peak for ethylene plasma polymerized coatings except its shape is fatter, which suggests the surface charging in the XPS.

SEM Analysis Methane plasma polymerized film can be formed into an extremely tight network, because of the small building unit. The SEM images of strands etched by oxygen plasma and coated by methane monomer at 5 sccm, 0.22 torr and 100 w for 15 min. and 30 min. are given in Figure 26.

Observation of fibers coated for 15 min. at low magnification (750X) reveals numerous randomly oriented strip-like structures and particles on and within the fiber bundles (Figure 26, top). These elevated, rough regions seem to be ablated off and smoothed by the longer plasma treatment (Figure 26, bottom). This is because a raised feature should have lower stability and experience higher molecular and photon fluxes that will increase the ablation.

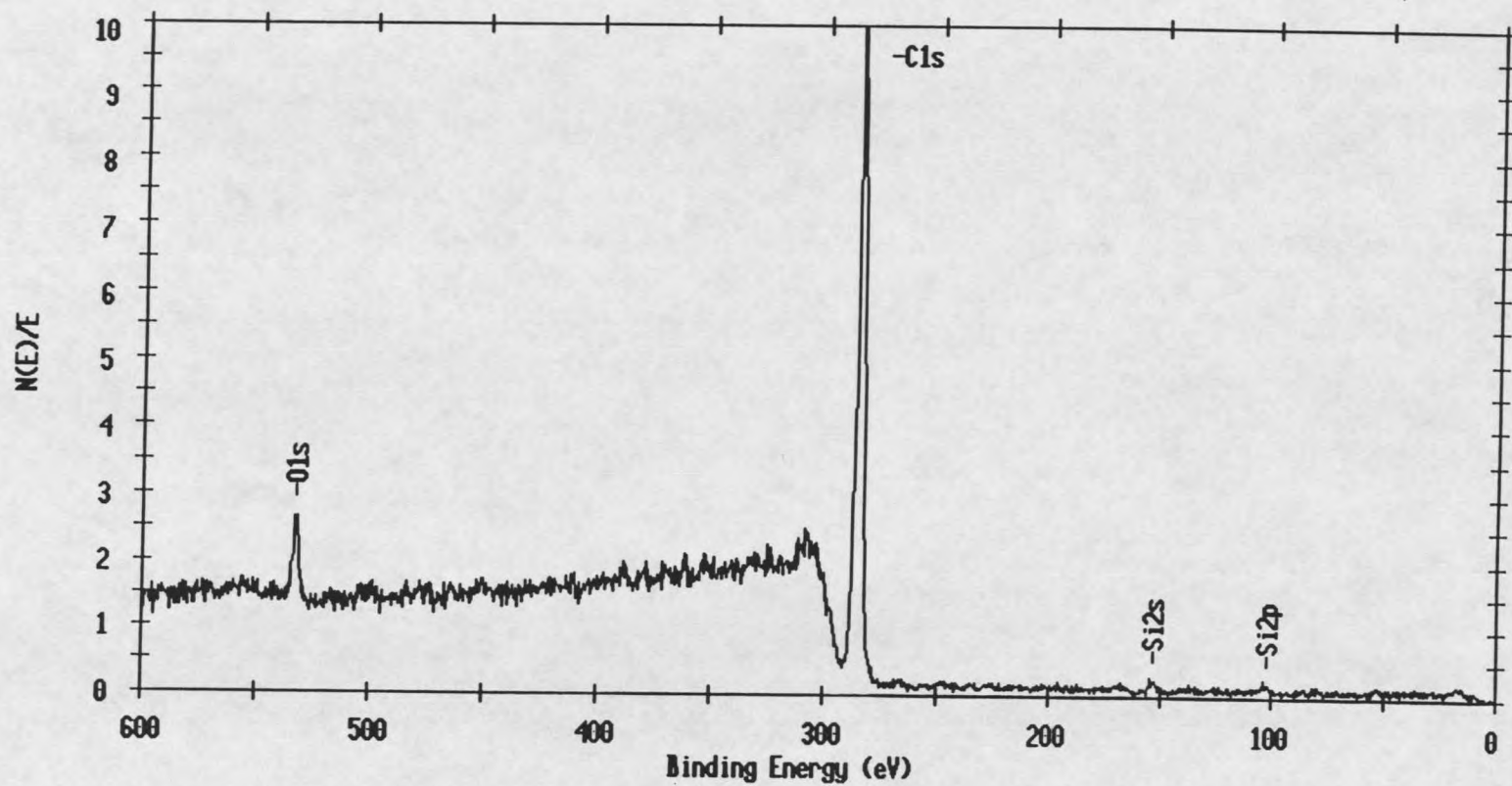


Figure 24. XPS survey spectra of fiber strands coated by methane monomer at 5 sccm, 0.22 torr and 100 w for 20 min.

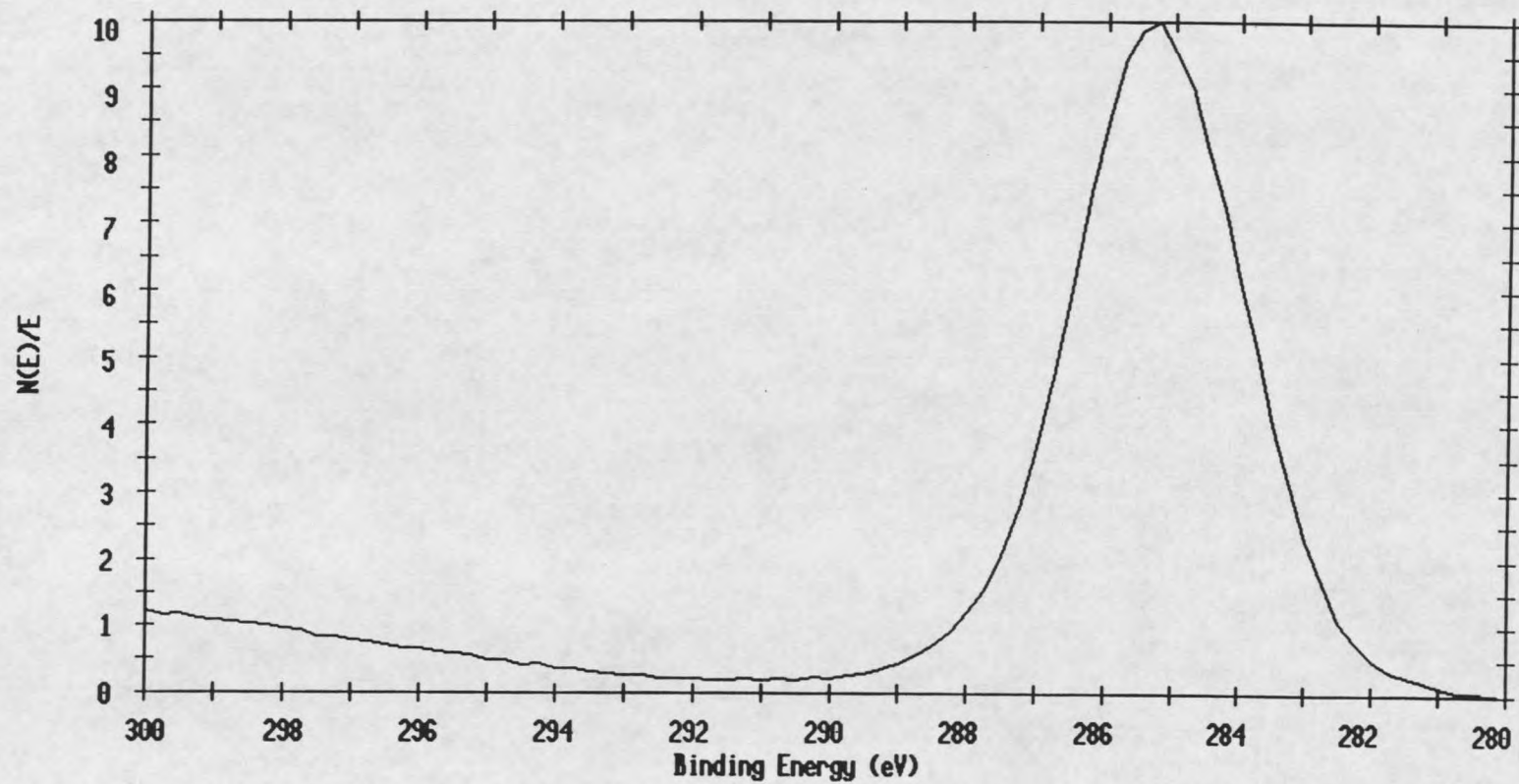


Figure 25. XPS Cls binding energy curve for fiber strands coated by methane monomer

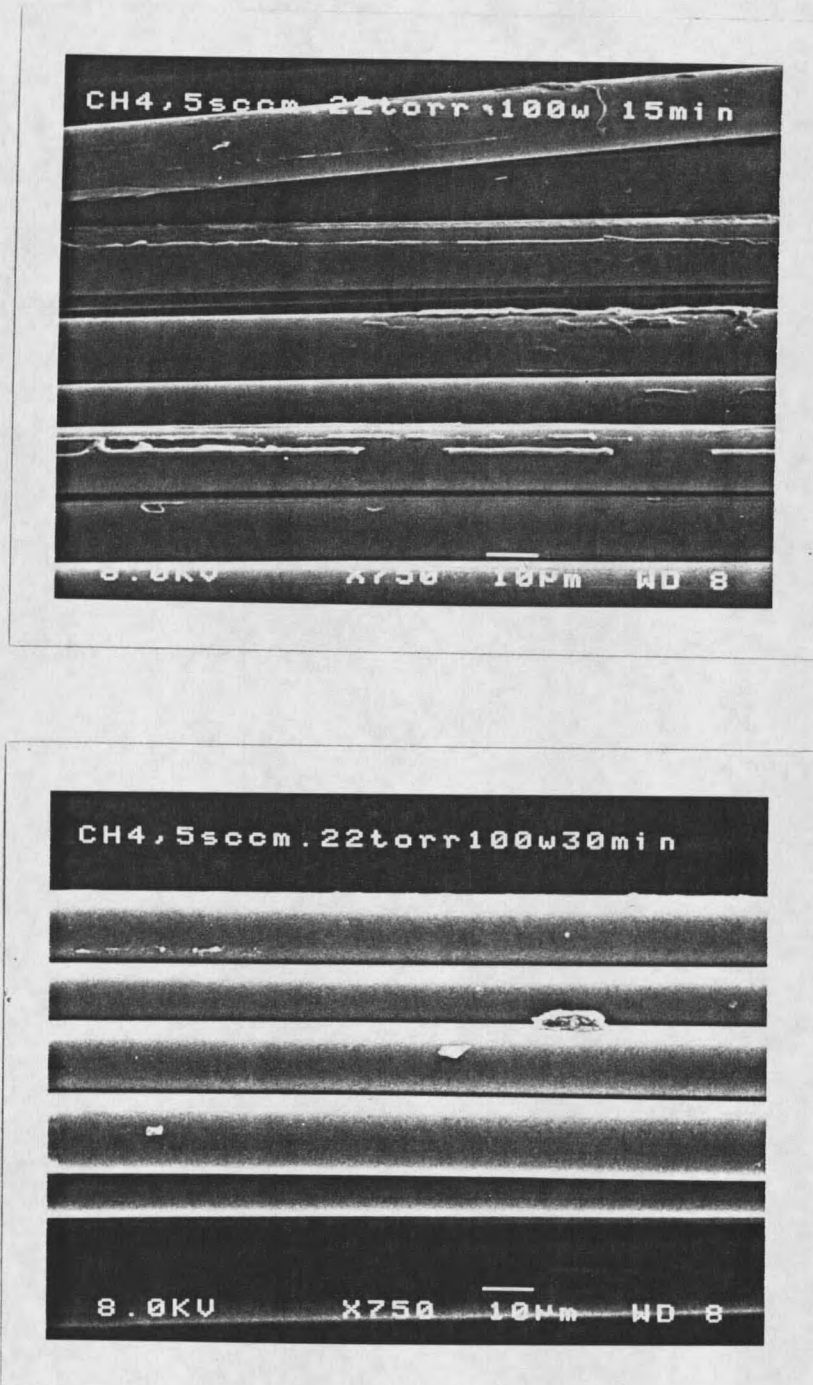


Figure 26. SEM micrographs of fiber strands etched by oxygen plasma and coated by methane monomer for 15 min. (top) and 30 min. (bottom)

### Oxygen Etch of Fabric Cloth

After the surface modification of fiber strands, experiments are carried out for bigger samples, 7.5 X 8 in. fabric cloth, the one that is directly used to make all kinds of composites. Since the fabric cloth has organic yarns which will be dissolved in base/acid solutions, it can only be cleaned by oxygen plasma etching.

XPS Analysis The XPS analysis results of as-received and oxygen plasma etched fabric cloth at various conditions are shown in Table 9. The discharge power, etching time and gas flow rate are the three variables examined in these experiments, although the system pressure also changes with the gas flow rate.

After oxygen plasma etching, the C concentration of the fiber surfaces decreases from about 72% to the lowest of 16% and the glass fiber contents, such as Si, Ca, Al, and sometimes Na can be detected in the XPS analysis. Therefore, we can assume the fabric cloth is free of silane coupling agents after etching, although the etching is not really uniform because of the tight fiber bundles. As seen in Table 9, it takes higher discharge power, longer etching time and greater gas flow rate for the fabric cloth to get the same etching results than the fiber strand does because the fabric has much more fibers in each bundle, with all the

strands stitched together by organic yarns, which makes it harder for the plasma to penetrate into the strands.

The reaction condition of 10 sccm, 0.36 torr, 120 w and 60 min. is chosen to etch the fabric before any coating, since higher power and greater gas flow rate will not get better etching results as shown in Table 9.

Table 9. Elemental Surface Concentration (%) Obtained by XPS Analysis of As-received and Oxygen Plasma Etched Fabric Cloth

oxygen	C1s	O1s	Si2p	Ca2p	Al2p
As-received fabric cloth	71.53- 73.25	22.39- 23.81	4.36- 4.65	ND	ND
5sccm, 0.24torr, 80w, 30min.	40.67- 51.70	34.65- 42.83	10.42- 15.57	0.84- 1.41	1.09- 2.06
5sccm, 0.24torr, 120w, 45min.	27.06- 36.90	42.03- 50.73	16.93- 18.09	1.57- 1.89	2.10- 3.20
10sccm, 0.36torr, 80w, 60min.	30.30- 34.18	45.55- 48.56	15.26- 15.88	1.82- 1.99	2.69- 3.00
10sccm, 0.36torr, 100w, 60min.	27.08- 33.13	46.53- 51.16	14.27- 16.79	1.76- 2.01	2.39- 2.83
10sccm, 0.36torr, 120w, 30min.	26.52- 37.73	44.44- 52.40	13.76- 16.28	1.61- 2.15	2.46- 2.80
45min.	23.16- 25.83	52.41- 54.63	16.32- 17.25	2.23- 2.36	3.09- 3.18
	18.05- 26.98	49.76- 58.00	17.52- 18.92	2.01- 2.60	2.94- 3.96
60min.	20.99- 28.29	48.74- 54.12	17.03- 18.76	2.06- 2.42	2.93- 3.48
	16.26- 26.53	50.35- 57.84	17.10- 19.87	2.07- 2.54	2.74- 3.54
10sccm, 0.36torr, 160w, 45min.	19.99- 28.55	49.46- 55.89	16.33- 18.72	1.86- 2.77	3.06- 3.64
15sccm, 0.46torr, 120w, 45min.	19.16- 28.79	48.19- 55.71	18.44- 18.79	1.92- 2.62	2.66- 3.72

The XPS survey spectra of oxygen etched fabric cloth at 10 sccm, 0.36 torr and 120 w for 60 min. is given in Figure 27, and the C1s and O1s binding energy curves are shown in figures 28 and 29, respectively. The survey spectra and elemental binding energy curves look like the same as those for oxygen etched fiber strands, with C1s curve having a small peak at higher binding energy region which shows the surface oxidation.

SEM Analysis The SEM images of uncleaned and oxygen plasma etched fabric cloth are given in Figure 30. The SEM analysis shows that the single fiber in the fabric has bigger diameter than the one in fiber strands. The diameters of fibers in the fabric are in the range of 15 - 20  $\mu\text{m}$ .

In Figure 30 (top), the big particle-like structures on the surface of uncleaned fabric can be silane coupling agents. However, most areas of the fabric surface are smoother. The surface texture of oxygen etched fabric is more variable than the surface of etched fiber strands. Some areas are relatively clean while others are largely covered by raised features as shown in Figure 30 (bottom). This is not unexpected since the fabric has much more fibers in it than the fiber strand does. The common features in oxygen etched fabric and fiber strand are that surface roughening occurs on both of them and they all have the strip-like structures on and within the fiber bundles.

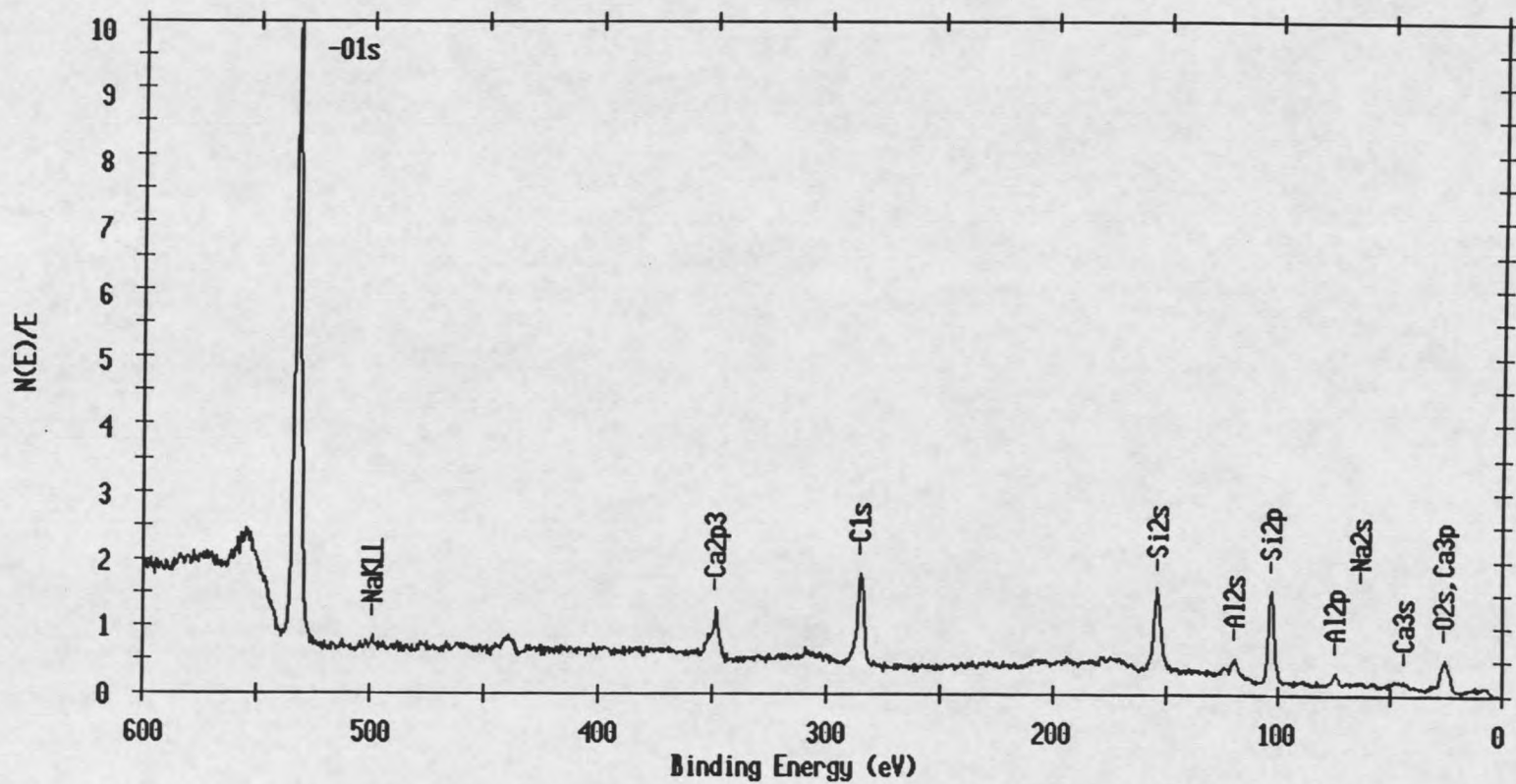


Figure 27. XPS survey spectra of oxygen plasma etched fabric cloth at 10sccm, 0.36 torr and 120 w for 60 min.

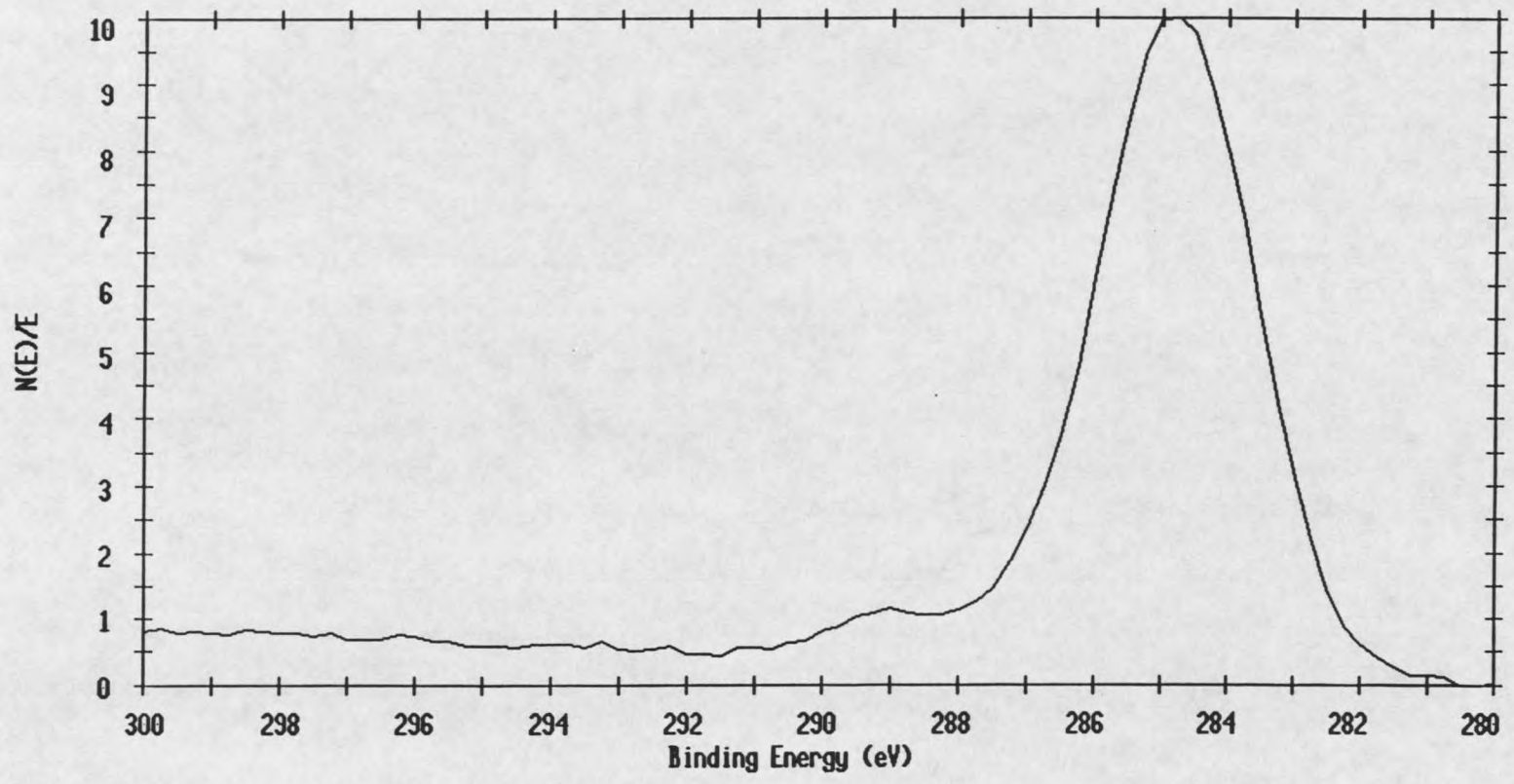


Figure 28. XPS Cls binding energy curve for oxygen plasma etched fabric cloth

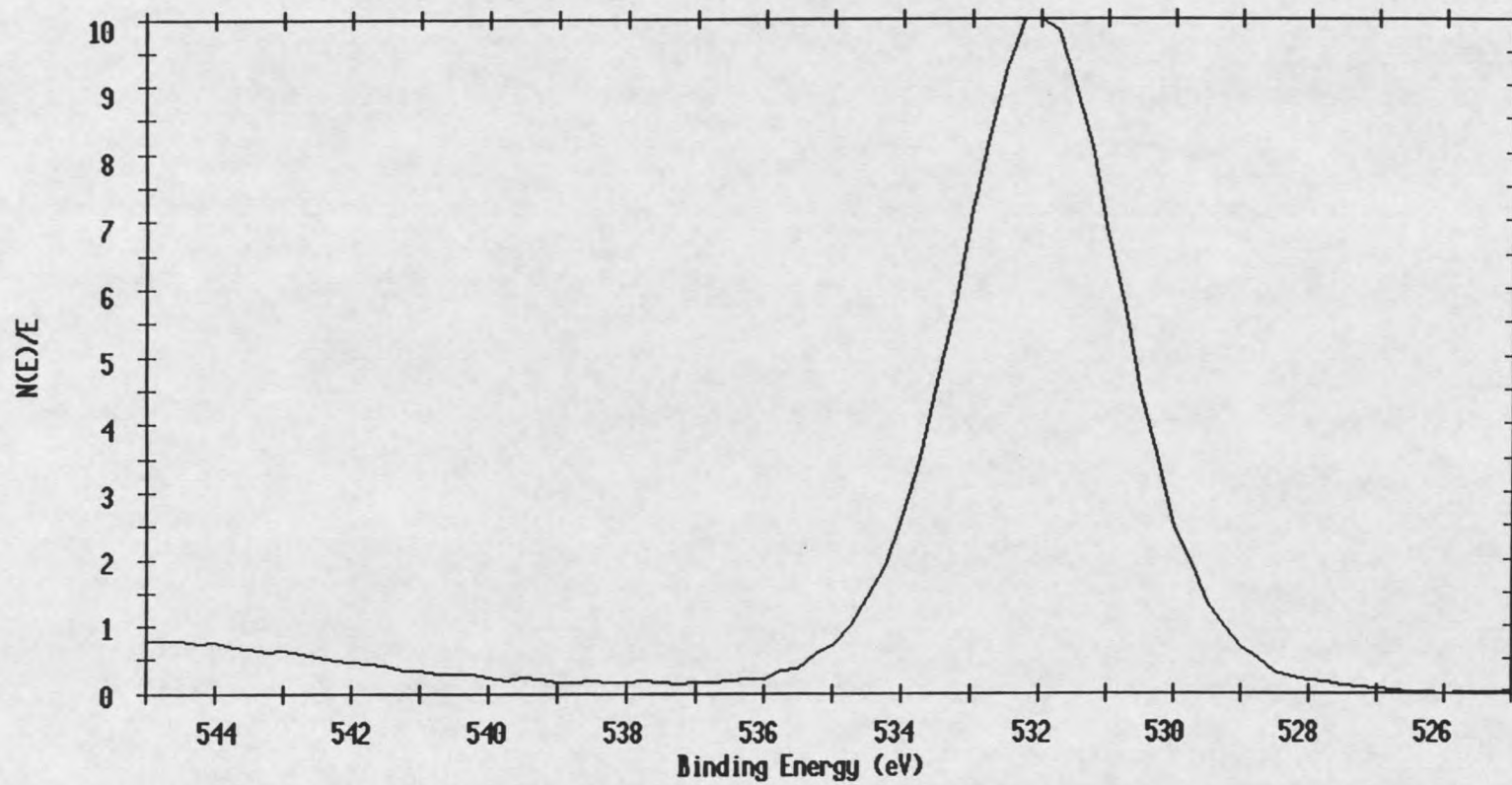


Figure 29. XPS O1s binding energy curve for oxygen plasma etched fabric cloth

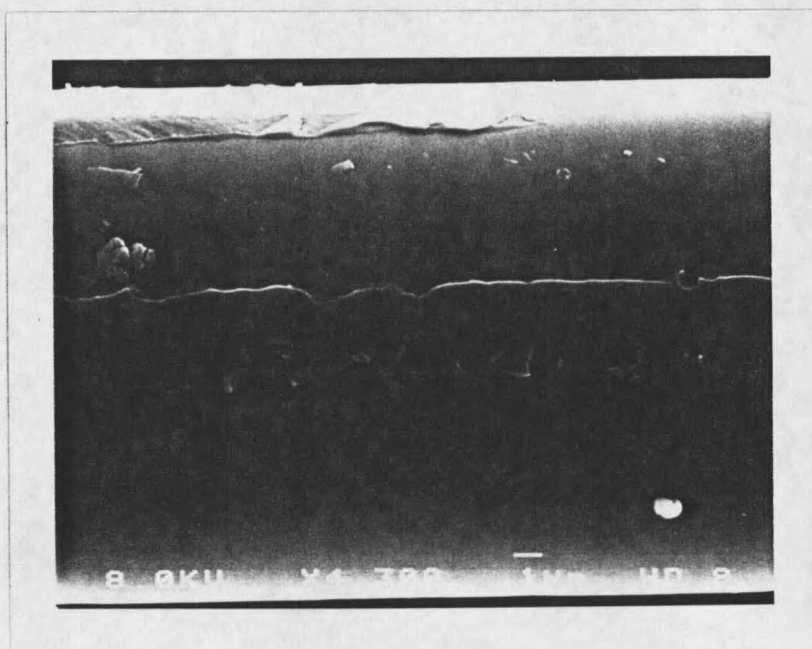
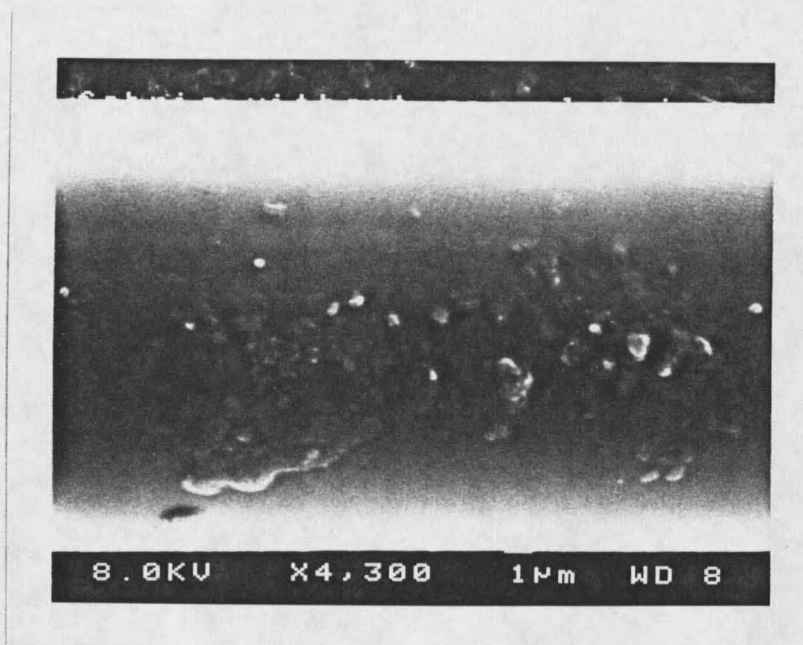


Figure 30. SEM micrographs of fabric cloth as received (top), and as etched by oxygen plasma at 10 sccm, 0.36 torr and 120 w for 60 min. (bottom)

### Fabric Cloth Coated by Ethylene Monomer

After the fabric is etched by oxygen plasma to clean the surface, ethylene monomer is introduced into the reactor to get the plasma polymerized films on the fabric. The experimental procedure is the same as that for fiber strand coatings. Figure 31 clearly shows the differences between as-received and ethylene plasma coated fabric. The untreated fabric cloth reflects the light the way that the glass does, while the treated fabric has coatings on it and slight yellowing of the fabric can be observed.

XPS Analysis The elemental surface concentration obtained by XPS analysis of ethylene plasma coated fabric at different conditions is shown in Table 10.

When 60 w discharge power is used to coat ethylene plasma polymerized films on fiber strands or fabric cloth, it only takes 15 min. for fiber strands to reach the 95% C surface concentration, while it takes 60 min. for the fabric to get the almost same results, as seen in Table 10. What is more, we can not see the glass fiber contents like Ca or Al on the surfaces of coated fiber strands, but both Ca and Al show up on the surfaces of coated fabric in XPS analysis results, which shows that there are some defects, such as holes and/or peeling situations, on the coated surfaces of the fabric.

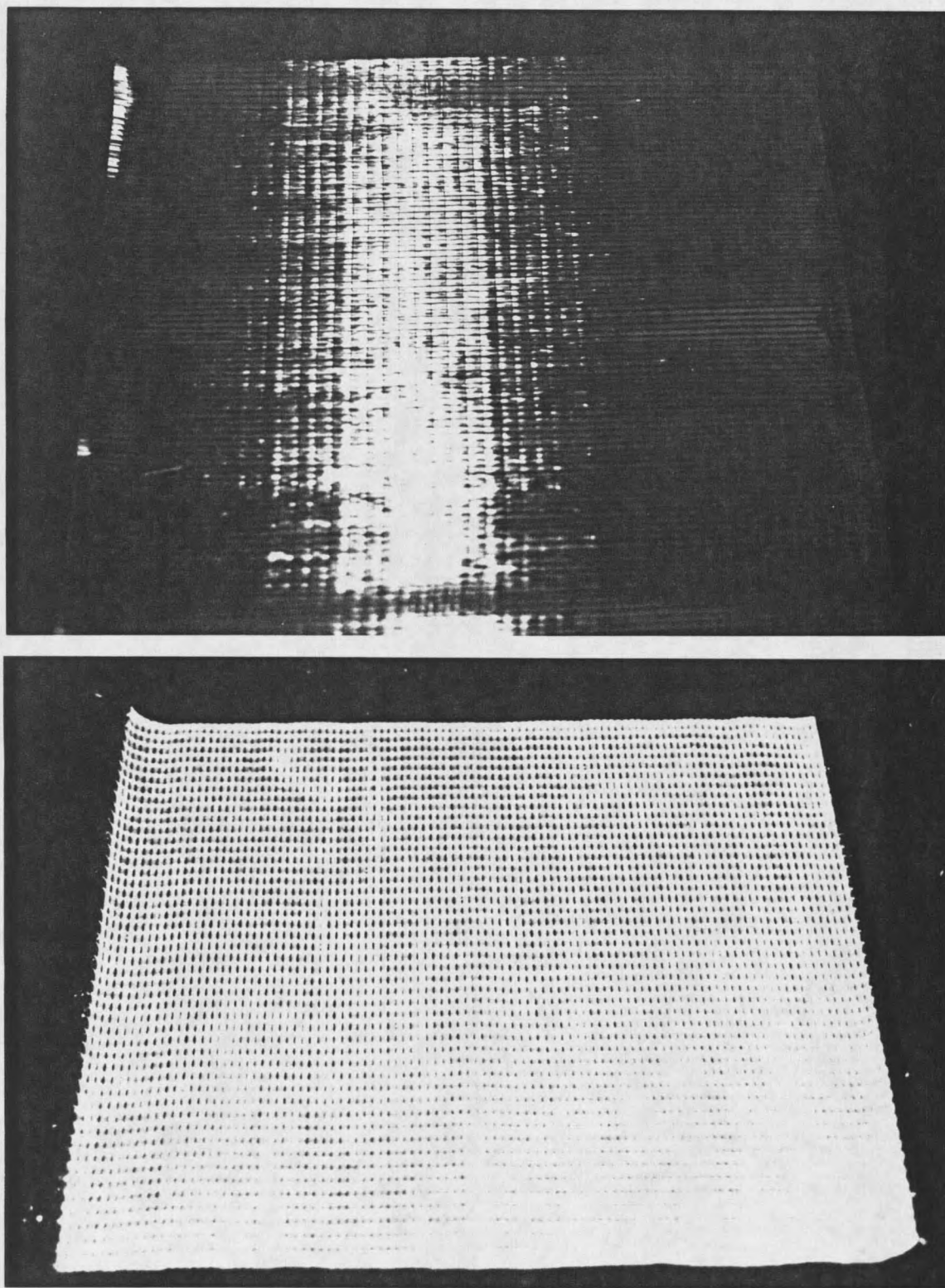


Figure 31. Pictures of as-received (top) and ethylene plasma treated fabric cloth (bottom)

Table 10. Elemental Surface Concentration (%) Obtained by XPS Analysis of Ethylene Plasma Coated Fabric

ethylene	C1s	O1s	Si2p	Ca2p	Al2p
5sccm, 0.18torr, 60w, 15min.	45.18- 76.70	15.81- 37.87	7.29- 13.29	0.41- 1.49	0.52- 2.17
30min.	56.13- 65.49	24.42- 29.32	8.07- 12.08	0.90- 1.21	1.11- 2.43
5sccm, 120w, 30min, 0.18torr	56.03- 78.00	15.74- 30.57	5.82- 10.54	0.32- 1.28	0.74- 1.58
0.27torr	46.23- 81.30	12.84- 37.70	4.81- 12.84	0.41- 1.27	0.61- 1.96
8sccm, 0.27torr, 120w, 30min	57.87- 81.91	12.27- 29.80	4.72- 9.48	0.46- 1.22	0.64- 1.63
10sccm, 0.27torr, 60w, 45min	62.92- 87.80	9.58- 25.33	2.23- 9.07	0.17- 0.97	0.22- 1.71
60min	63.45- 90.78	6.69- 25.16	2.42- 8.63	0.11- 0.96	0.90- 1.53
10sccm, .27torr, 120w, 15min	57.47- 75.78	16.37- 30.18	6.35- 10.46	0.58- 1.22	0.92- 1.95
30min	56.71- 85.74	10.57- 28.00	3.69- 12.22	0.52- 1.38	0.92- 1.69

As shown in Table 10, the coatings on the surfaces of the fabric are less uniform than those on the surfaces of fiber strands, especially for C surface concentration. For coated fabric cloth, the differences of C contents between the inside and outside of one fiber bundle is about 10%, but the differences for fiber bundles at different positions of coated fabric can be as great as 30%. Therefore, the nonuniformity not only comes from the thick fiber bundles in the fabric, but also from the nonuniform plasma conditions. The way to improve this situation can be to design a new

sample holder to get the uniform gas flow pattern in the reactor, or improve the electrode coil to generate uniform plasmas.

The XPS survey spectra of ethylene plasma coated fabric at 10 sccm, 0.27 torr and 120 w for 30 min. is given in Figure 32, and C1s binding energy curve is shown in Figure 33. The O1s peak in the survey spectra of coated fabric is much higher than that in the survey spectra of ethylene plasma coated fiber strands, which matches the XPS surface concentration analysis presented earlier. Another difference between the survey spectra of treated fiber strands and fabric is that Ca and Al peaks can be seen in the survey spectra of coated fabric cloth. The C1s binding energy curve for treated fabric looks like the same as that for ethylene plasma treated fiber strand, with the symmetrical peak at 285 eV.

SEM Analysis The SEM images of fabric treated by ethylene plasma at 10 sccm, 0.27 torr and 120 w for 30 min. are shown in Figure 34. In general, the surface of ethylene plasma coated fabric cloth is rougher than the surface of treated fiber strand, but they both have the strip-like structures on and within the fiber bundles. This is the problem that should be related to oxygen plasma etching, since fiber strands cleaned by base/acid solutions and then treated with plasmas do not have this kind of structures.

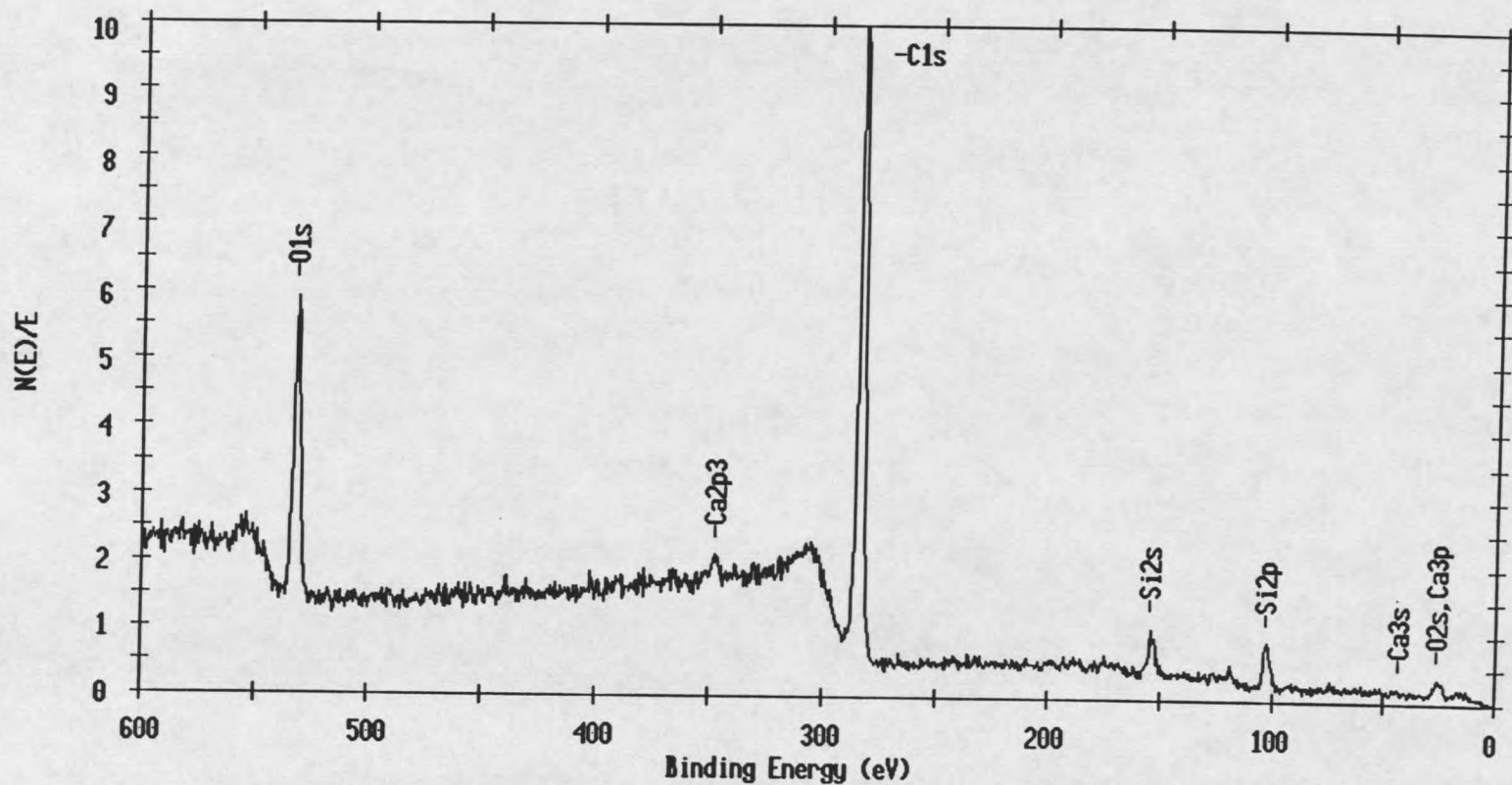


Figure 32. XPS survey spectra of fabric cloth coated by ethylene monomer at 10 sccm, 0.27 torr and 120 for 30 min.

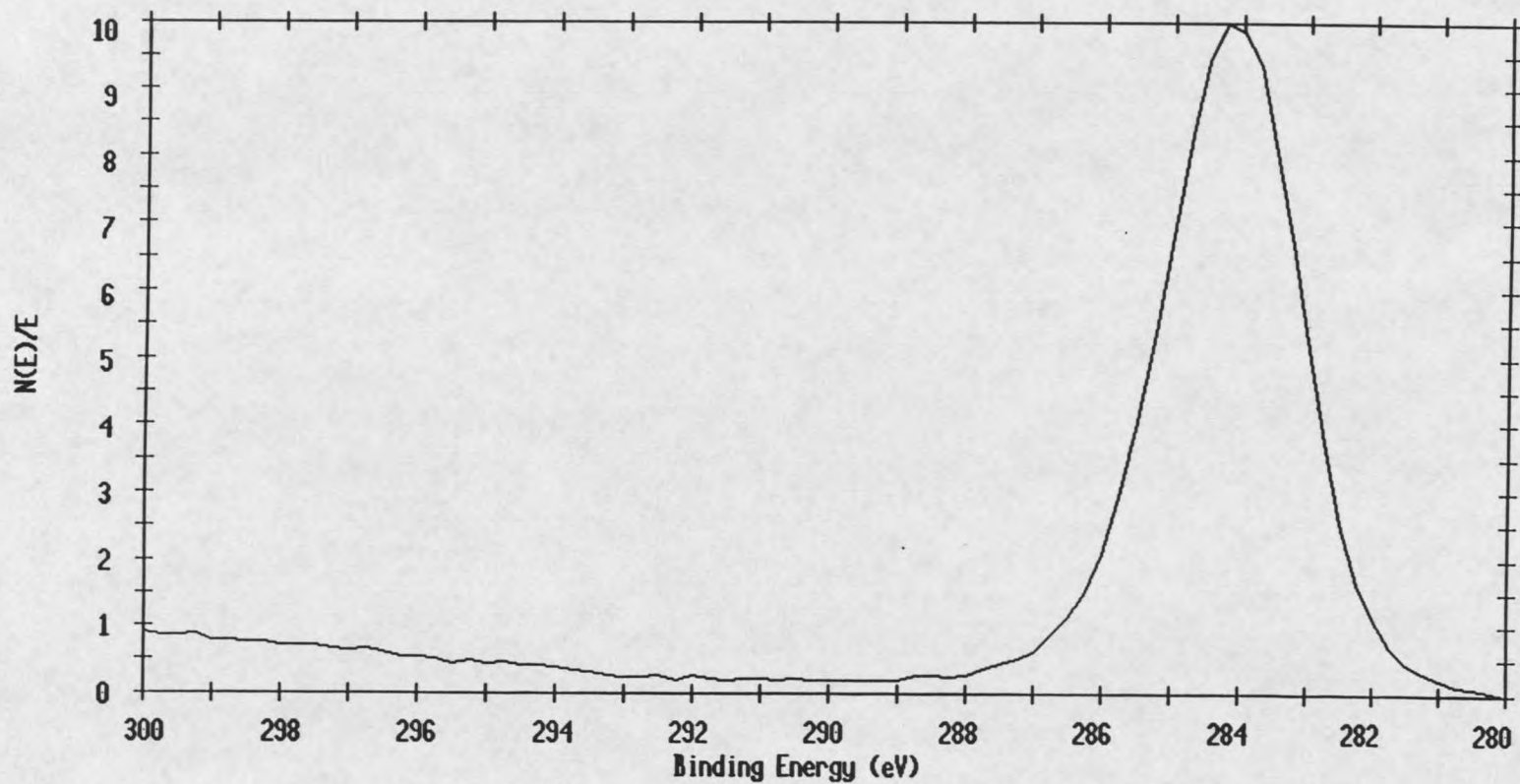


Figure 33. XPS Cls binding energy curve for ethylene plasma coated fabric cloth

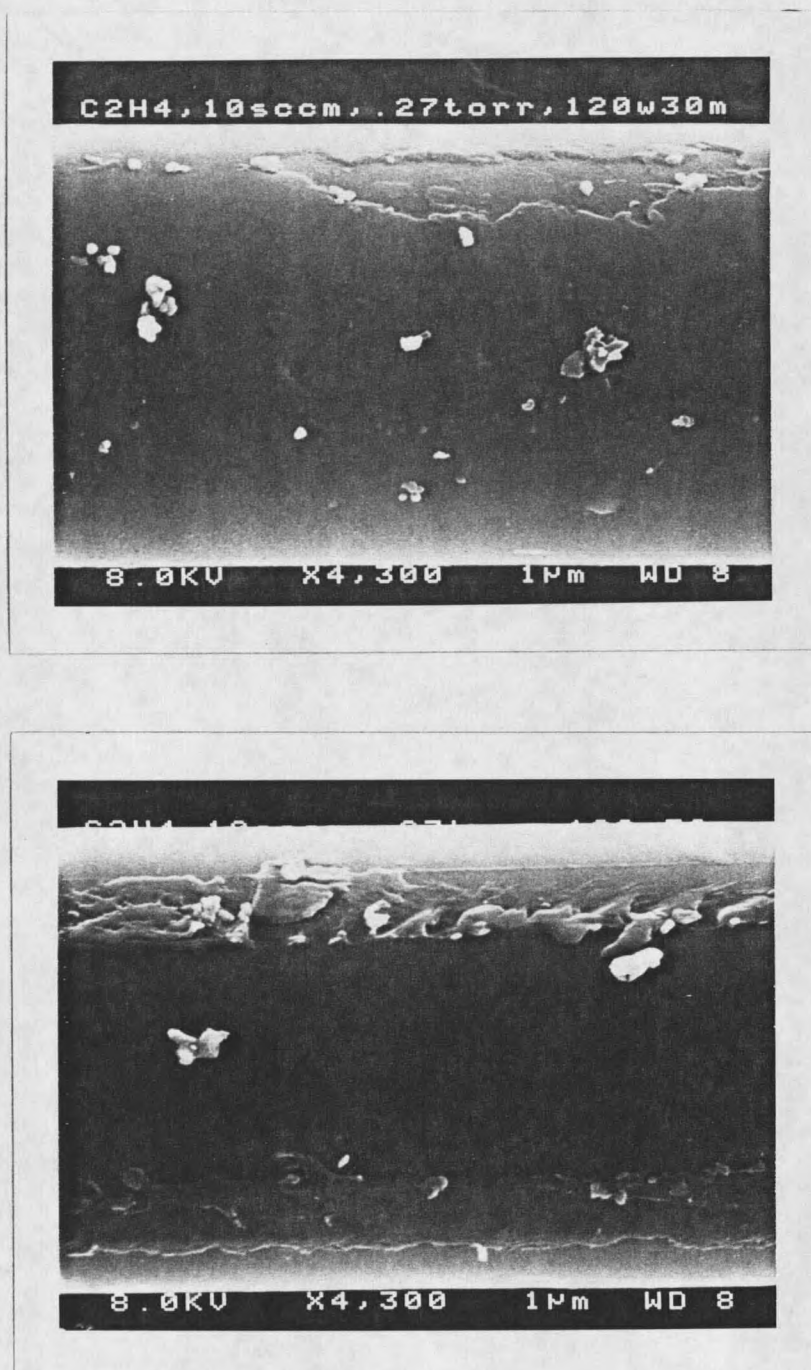


Figure 34. SEM micrographs of the different spots of fabric cloth coated by ethylene monomer at 10 sccm, 0.27 torr and 120 w for 30 min.

Although very thin and uniform coatings, such as the middle area in the bottom micrograph of Figure 34, can not be seen in the SEM analysis, but we can assume that there is a coating on it since the surface concentration has been greatly changed in the XPS analysis. In Figure 34 (top), there are some holes on the surface of treated fabric cloth which are the defects in this technique, but it also clearly shows the surface coating on the treated fabric cloth.

#### Mechanical Test Results

The mechanical tests for fiber strands etched by oxygen plasma and then treated by ethylene or methane monomers have been done by Jinhua Bian and the results are given in Table 11. The results show that both the static strength and fatigue resistance are decreased after the treatment. This is probably because the oxygen plasma etching not only removes the silane coupling agents, but also causes damages to the glass fibers. Therefore, the minimum discharge power and shortest etching time are recommended to clean the fiber surfaces without damaging the glass fibers.

Another factor that causes the decreasing in fatigue resistance of composites could be the poor bonding between the plasma polymerized coatings and the polyester matrix. The bonding strength test has been done for one treated strand and the result is shown in Jinhua Bian's thesis [55].

Table 11. The Static Strength and Fatigue Cycle Numbers Obtained by Mechanical Tests of As-Received and Plasma Treated Fiber Strands

	static strength (Lbs)	fatigue cycle numbers at 40% level
as-received fiber strands	69	900,000 1200,000 2500,000
ethylene, 5sccm, 0.18torr, 15min., 20w	47.92	28,732 33,106 36,549
60w	61	46,375 95,433 102,827
120w	52.25	9,520 11,872 21,332
ethylene, 10sccm, 0.27torr, 15min., 60w	48.63	23,693 28,458 29,578
200w	50.82	18,427 20,172 27,613
methane, 5sccm, 0.22torr, 30min., 100w	41.43	13,899 22,174 30,211

Since the plasma polymerization is an extremely complex process and the properties of plasma polymerized films can be greatly changed by the manipulation of plasma polymerization parameters, the surface modification at proper reaction conditions would probably improve the fatigue resistance of composites. Experiments have been done at system pressure lower than 50 mtorr for ethylene plasma treated fiber strands, and the mechanical test results will

be shown in Jinhua Bian's thesis [55]. The low pressure conditions would be helpful to get graphite-type coatings on glass fibers to improve the fatigue resistance of composites.

## CHAPTER 5

## CONCLUSIONS AND RECOMMENDATIONS

Conclusions

Surface modification of E-glass fiber strands and fabric cloth with plasma polymerization of ethylene and methane monomers was studied in this research. An inductively coupled radio frequency glow discharge reactor was designed and constructed "in house" for the experiments which is also a part of this study. Fiber strands were first cleaned by either base bath and acid solution or oxygen plasma to remove the silane coupling agents, then they were coated with ethylene and methane monomers in a low temperature rf glow discharge. A discharge power range of 20-200 w and a reaction time range of 5-20 minutes were spanned in the experiments for ethylene plasma coated fiber strands. For methane plasma coated fiber strands, these values were 60-120 w and 15-30 minutes. These values were 60-120 w and 15-60 minutes for ethylene plasma coated fabric cloth. The monomer flow rate and system pressure were not the primary variables examined in these experiments, but

they were changed in the range of 5-10 sccm and 0.08-0.27 torr, respectively. The characteristics of the coatings were analyzed by XPS and SEM techniques.

Plasma polymerization treatment of glass fibers proved to be an effective method for modifying the fiber surface properties. Plasma treatment enables the production of thin tightly bound and highly crosslinked films on the fiber surface. Also, plasma treatment can be used for etching of the manufacturer sizing. This method is flexible in allowing us to easily switch monomers used for coating fibers. However, this method is limited to the use of organic monomers which are in the gas phase or which can be easily vaporized.

The following conclusions were derived from the surface analysis results:

(1) The plasma exposure does not modify the bulk properties of the fibers.

(2) The best solution cleaning results to remove the silane coupling agents on the fiber surfaces were obtained by putting fiber strands in the base bath and acid solution for 9 hrs, respectively.

(3) Oxygen plasma etch can also be used to remove the silane coupling agents, and the best treatment conditions for fiber

strands were under 80 w of discharge power, at the oxygen flow rate of 5 sccm, at the system pressure of 0.24 torr, and a treatment time of 30 minutes. For oxygen etch of fabric cloth, these values were: 120 w, 10 sccm, 0.36 torr and 60 minutes.

(4) Ethylene plasma polymerization can be used to coat the fiber strands and fabric cloth. The best coatings were obtained under these conditions: 60 w, 5 sccm, 0.18 torr and 15 minutes for the fiber strand, and 60 w, 10 sccm, 0.27 torr and 60 minutes for fabric cloth.

(5) Methane plasma polymerization can also be used to coat the fiber strands. Methane monomer was less polymerized and methane plasma polymerization had a lower deposition rate than did ethylene monomer. The best treatment conditions were: 100 w, 5 sccm, 0.22 torr and 20 minutes.

(6) The C1s binding energy curves for oxygen plasma etched fiber strands and fabric cloth looked similar to each other, with a small peak shifted to a higher binding energy showing the surface oxidation.

(7) The C1s binding energy curves for fibers coated by ethylene and methane monomers had the same symmetrical shape, with the peaks at 285 eV indicating C-C and/or C-H

bonds. But the Cls peak for methane monomer coated fibers was fatter than that for ethylene monomer coated fibers.

(8) The fiber strands cleaned by base/acid solutions had relatively smooth surfaces, while oxygen plasma etched fiber strands had rougher surfaces. Surface roughening also occurred when fibers were treated with ethylene or methane plasmas.

#### Recommendations

Plasma polymerization is a complex process and not well understood. The individual steps or reactions that are involved in the process of polymer formation in a glow discharge are extremely complex and are highly dependent on the system. Therefore, interlaboratory comparison of results is generally not straightforward. In this research, the XPS and SEM techniques are used to analyze the surface of plasma treated glass fibers, but the results only show that the fiber surface changes greatly after the treatment. So far, there is no direct relationship between the surface analysis results and the mechanical properties. Therefore, more mechanical tests of treated fibers would help to get the direct results since the primary purpose of this research is to increase the fatigue resistance of glass fiber composites. The graphite type coatings on glass fibers would

be helpful to improve the fatigue resistance of composites and should be the goal for the further study.

In the experiments of ethylene plasma coated fabric cloth, surface analysis results revealed that there were great differences in the surface concentration of coated fibers at different positions of the fabric cloth. Thus, a new design of sample holder to get the uniform gas flow and plasma pattern in the reactor will possibly eliminate this problem.

In plasma polymerization of hydrocarbons, triple bond and/or aromatic structure, double bond and/or cyclic structure, and saturated structure are three functional groups that determine the polymer deposition rate and the properties of plasma polymers. Plasma polymerization of ethylene and methane monomers has been studied in this research. Investigation of plasma polymerization of acetylene or styrene monomer will supplement the data of this study.

## REFERENCES CITED

1. Yasuda, H., "Plasma for Modification of Polymers", *J. Macromol. Sci.-Chem.*, **A10(3)**, PP.383-420, 1976.
2. Yasuda, H., "Plasma Polymerization", Academic Press, Orlando, Florida, 1985.
3. Morosoff, N., in "Plasma Deposition, Treatment and Etching of Polymers", D'Agostino, R., ed., PP.1-94, Academic Press, 1990.
4. Pan, R.Q., M.S. Thesis, Montana State University, 1994.
5. Allred, R.E., Merrill E.W., and Roylance, D.K., "Surface Chemistry and Bonding of Plasma-Aminated Polyaramid Filaments", *Polym. Sci. Technol.*, **27**, PP.333-375, 1983.
6. Wertheimer, M.R. and Schreiber, H.P., *J. Appl. Polym. Sci.*, **26**, PP.2087, 1981.
7. Moshonov, A. and Avny, Y., *J. Appl. Polym. Sci.*, **25**, PP.771, 1980.
8. Pluddemann, E.P., "Interfaces in Polymer Matrix composites", Pluddemann, E.P., ed., PP.173-216, Academic Press, New York, 1974.
9. Riggs, D.M., Shuford, R.J., and Lewis, R.W., in "Handbook of Composites", Lubin, G., ed., PP.196-271, Van Nostrand Reinhold, New York, 1982.
10. Chou, Shen and Lin, Chi-Hung, "A Study of Plasma Treatment to the Surface of Carbon Fiber for Interfacial Adhesion to Epoxy Resin", *J. of the Chinese Inst. of Engineers*, **15(5)**, PP.617-624, 1992.
11. Hammer, G.E. and Drzal, L.T., "Graphite Fiber Surface Analysis by X-Ray Photoelectron Spectroscopy and Polar Dispersive Free Energy Analysis", *Appl. of Surface Sci.*, **4**, PP.340-355, 1980.
12. Benatar A. and Gutowski, T.G., "Effects of Moisture on Interface Modified Graphite Epoxy Composites", *Polym. Composites*, **7(2)**, PP.84-90, 1986.

13. Mettes, D.G., in "Handbook of Fiberglass and Advanced Plastics Composites", Lubin, G., ed., PP.143-181, Van Nostrand Reinhold, New York, 1969.
14. Agarwal, B.D. and Broutman, L.J., "Analysis and Performance of Fiber Composites", PP.13-53, John Wiley & Sons, 1990.
15. Dow Corning Corporation, "A Guide to Dow Corning Silane Coupling Agents", PP.1-13, Midland, Michigan, 1990.
16. Yasuda, H.K., in "Plasma Polymerization", Shen, M. and Bell, A.T., eds, PP.37-52, American Chemical Society Symposium Series 108, 1979.
17. Ferreiro, L.M., Ph.D. Thesis, University of Minnesota, 1987.
18. Chapman B., "Glow Discharge Process", PP.21-48, John Wiley & Sons, 1980.
19. Thornton, J.A., "Plasma-Assisted Deposition Process: Theory, Mechanisms and Applications", *Thin Solid Films*, **107**, PP.3-19, 1983.
20. Yasuda, H., in "Thin Film Processes", Vossen, J.L. and Kern, W., eds., PP.361-398, Academic Press, New York, NY, 1978.
21. Claude, R., Moisan, M., Wertheimer, M., and Zakrzewski, Z., *Appl. Phys. Lett.*, **50(25)**, PP.1797, 1987.
22. Yeh, Y.S., Shyy, I.N., and Yasuda, H., "Influence of Reactor Design Factor on the Deposition Rate in Plasma Polymerization", *J. Appl. Polym. Sci.*, Appl. Polym. Symposium, **42**, PP.1-93, 1988.
23. Canepa, P., Castello, G., Munari, S., and Nicchia, S., *Rad. Phys. Chem.*, **15**, PP.485, 1980.
24. Yasuda, H. and Hirotsu, T., *J. Polym. Sci.*, Polym. Chem. Ed., **16**, PP.313, 1978.
25. Boenig, H. V., "Fundamentals of Plasma Chemistry and Technology", PP.355-412, Technomic Publ. Co., 1988.
26. D'Agostino, R. and Fracassi, F., "The Influence of Plasma Parameters on Polymerization Kinetics and the Structure of Deposited Films", *J. Appl. Polym. Sci.*, Appl. Poly. Symposium, **46**, PP.17-32, 1990.

27. D'Agostino, R., Favia, P., and Fracassi, F., "The Effect of Power on the Plasma-Assisted Deposition of Fluorinated Monomers", *J. Polym. Sci., Part A: Polym. Chem.*, **28**, PP.3387-3402, 1990.
28. Yasuda, H. and Hirotsu, T., "Critical Evaluation of Conditions of Plasma Polymerization", *J. Polym. Sci., Polym. Chem. Ed.*, **16**, PP.743-759, 1978.
29. Chapman, B., "Glow Discharge Processes", PP.297-349, John Wiley&Sons, 1980.
30. Irving, S.M., "A Plasma Oxidation Process for Removing Photoresist Films", *Solid State Technol.*, **14(6)**, PP.47, 1971.
31. Flamm, D.L., in "Plasma Etching: An Introduction", Manos, D.M. and Flamm, D.L., eds., PP.92-183, Academic Press, 1989.
32. Cook, J.M. and Benson, B.W., *J. Electrochem. Soc.*, **130**, PP.2459, 1983.
33. Egitto, F.D., Vukanovic, V., and Taylor, G.N., in "Plasma Deposition, Treatment, and Etching of Polymers", D'Agostino, R., ed., PP.321-422, Academic Press, 1990.
34. Suhr, H., "Application of Nonequilibrium Plasmas in Organic Chemistry", *Plasma Chem. and Plasma Process*, **3(1)**, PP.1-61, 1983.
35. Taylor, G.N. and Wolf, T.M., *Polym. Eng. and Sci.*, **20**, PP.1086, 1980.
36. Mauer, J.L. and Carruthers, R.A., "Selective Etching of SiO<sub>2</sub> with a CF<sub>4</sub>/H<sub>2</sub> Plasma", Proc. 21st Electron. MaHs. Conf., Boulder, Colorado, 1979.
37. Havens, M.R., Biolsi, M.E., and Mayhan, K.G., "Survey of Low Temperature rf Plasma Polymerization and Processing", *J. Vac. Sci. Technol.*, **13(2)**, PP.575-584, 1976.
38. Chapman, B., "Glow Discharge Processes", PP.139-175, John Wiley&Sons, 1980.
39. Christie, A.B., in "Methods of Surface Analysis", Walls, J.M., ed., PP.127-168, Cambridge university Press, 1989.
40. Riggs, W.M. and Parker, M.J., in "Methods of Surface Analysis", Czanderna, A.W., ed., PP.103-158, Elsevier Scientific Publishing Company, 1975.

41. Moulder, J.F., Stickle, W.F., Sobol, P.E., and Bomben, K.D., "Handbook of X-Ray Photoelectron Spectroscopy", Chastain, J., ed., PP.1-15, Perkin-Elmer Corporation, Minnesota, 1992.
42. Ratner, B.D. and Castner, D.G., in "Surface Analysis: Techniques and Applications", Vickerman, J.C. and Reed, N.M., eds., PP.151-218, John Wiley&Sons, Chichester, UK, 1992.
43. Carlson, T.A., "Photoelectron and Auger Spectroscopy", Plenum Press, New York, 1975.
44. Sevier, K.D., "Low Energy Electron Spectrometry", Wiley Interscience, New York, 1972.
45. Heywood, V.H., in "Scanning Electron Microscopy", Heywood, V.H., ed., PP.1-16, Academic Press, 1971.
46. Goldstein, J.I., Newbury, D.E., Echlin, P., Joy, D.C., Fiori, C., and Lifshin E., "Scanning Electron Microscopy and X-Ray Microanalysis", PP.1-18, Plenum Press, New York, 1981.
47. "Instructions: JSM-6100 Scanning Microscope", JEOL.
48. Reimer, L., "Scanning Electron Microscopy", Hawkes, P.W., ed., PP.1-12, Springer-Verlag, 1985.
49. Goldstein, J.I., Yakowitz, H., and Newburg D.E., in "Practical Scanning Electron Microscopy", Goldstein, J.I. and Yakowitz, H., eds., PP.1-20, Plenum Press, New York, 1975.
50. Marcus, R.B., in "VLSI Technology", Sze, S.M., ed., PP.507-550, McGraw-Hill, New York, 1983.
51. Lee, R.E., "Scanning Electron Microscopy and X-Ray Microanalysis", PP.1-15, P T R Prentice-Hall, Inc., Englewood Cliffs, New Jersey, 1993.
52. Millard, M.M., "Analysis of Surface Oxidized Wool Fiber by X-Ray Electron Spectrometry", Analytical Chemistry, 44(4), PP.828-829, 1972.
53. Tibbitt, J.M., Shen, M., and Bell, A.T., "Structural Characterization of Plasma-Polymerized Hydrocarbons", *J. Macromol. Sci.-Chem.*, **A10(8)**, PP.1623-1648, 1976.
54. Tibbitt, J.M., Bell, A.T., and Shen, M., "Effects of Reaction Conditions on the Structure of Plasma Polymerized Ethylene", *J. Macromol. Sci.-Chem.*, **A11(1)**,

PP.139-148, 1977.

55. Bian, J.H., M.S. Thesis, Montana State University, 1996.

MONTANA STATE UNIVERSITY LIBRARIES



3 1762 10230665 9